

TABLE OF CONTENTS

CHAPTER 1: INTRODUCTION	1
CHAPTER 2: SITE, INSTRUMENTATION, DATA, AND METHODOLOGY	5
2.1 Haukeliseter Site	5
2.2 Climate at Haukeliseter	6
2.3 Instruments	7
2.3.1 Double Fence Snow Gauge	9
2.3.2 MRR - Micro Rain Radar	10
2.3.3 PIP - Precipitation Imaging Package	12
2.3.4 MASC - Multi-Angular Snowfall Camera	12
2.4 Optimal Estimation Retrieval Algorithm	13
2.4.1 Snowfall Retrieval Scheme	14
2.4.2 Environmental Masks for the Optimal Estimation Retrieval	18
2.5 Operational Weather Forecast Model	19
2.5.1 MetCoOP Ensemble Prediction System - MEPS	19
2.5.2 Meso-NH and the ICE3 Scheme	20
2.5.3 Adjustment of ICE3 Inside AROME-MetCoOp	23
2.6 Computing Snowfall Quantities	23
2.6.1 Layer Thickness in MEPS	23
2.6.2 Snow Water Content	24
2.6.3 Snow Water Path	24
2.7 Statistical Methods for Analysing Data	24
2.7.1 Ensemble Mean and Coefficient of Variation	25
2.7.2 Mean Error and Mean Absolute Error	25
2.7.3 Percent Difference and Average Difference	25
CHAPTER 3: ANALYSIS OF THE CHRISTMAS STORM 2016	26
3.1 Extreme Weather	27
3.2 Dynamic Tropopause Map	28
3.3 Thickness, Sea Level Pressure, Total Precipitable Water, and Wind at 250 hPa	28
3.4 Integrated Vapour Transport	31
3.5 Observations at the Weather Mast	33
3.6 Large Scale Circulation	34
CHAPTER 4: SNOW OBSERVATIONS AND MEPS FORECASTS FOR HAUKELISETER	41
4.1 The Christmas Storm 2016	41
4.1.1 Meteorology Comparison	41

4.2	Snowfall	57
4.2.1	Sensitivity of the Optimal Estimation Retrieval	58
4.2.2	Comparison of Surface Observations	60
4.2.3	Comparison of Surface Observations and MEPS	62
4.2.4	Comparison of Snow Water Content in the Vertical	71
4.2.5	Discussion	84
CHAPTER 5: SUMMARY AND OUTLOOK		88
5.1	Outlook	90
LIST OF ABBREVIATIONS		92
REFERENCES		95
APPENDIX A: FORWARD MODEL		103
A.1	Scattering Model	103
APPENDIX B: FORECASTED SNOW WATER CONTENT		105
B.1	Hourly Averages Ensemble Member Zero and One	105
B.2	Vertical Snow Water Content - All Ensemble Members	108

CHAPTER 4: SNOW OBSERVATIONS AND MEPS FORECASTS FOR HAUKELISETER

In this chapter the results of the snow surface observations, and the regional mesoscale forecast model at Haukeliseter are presented. On the basis of the methodology described in Chapter 2 it should be evaluated if the regional mesoscale forecast model MEPS predicts the same synoptic patterns as observed at the measurement site. Also, snow water content forecasted by MEPS is being compared with the retrieved vertical SWC at Haukeliseter.

This study will give a first insight into comparing model observed with forecasts snowfall, for one particular extreme event, the 2016 Christmas storm.

4.1 THE CHRISTMAS STORM 2016

It has been shown earlier that two low pressure systems affect Norway around Christmas 2016. This section will investigate meteorological quantities at Haukeliseter during the Christmas storm 2016.

4.1.1 METEOROLOGY COMPARISON

A comparison between the surface observations at Haukeliseter and the ECMWF analysis of the dynamic tropopause and geopotential thickness maps show that frontal transitions occurred on three days during the 2016 Christmas storm, 23, 25, and 26 December 2016 (Section 3.6), which shows up in the measurements and MEPS ensemble forecasts (Figure 4.1.1).

Figure 4.1.1 displays the observations and model initialisation quantities for sea level pressure, 2 m air temperature, 10 m wind, and precipitation on 21 to 27 December 2016 for the Haukeliseter measurement site.

During all days the MEPS forecast seems to predict similar sea level pressure, 2 m air temperature, and 10 m wind direction as is observed. Overestimations are simulated for wind speed (Figure 4.1.1d, i, n, s, x, ac) and surface precipitation amount (Figure 4.1.1e, j, o, t, y, and ad.)

include R-coefficient Figure 4.1.2 presents the correlation of sea level pressure, 2 m air temperature, 10 m wind, and surface precipitation amount between the observations and the 48 h MEPS ensemble forecast. The relation for Haukeliseter observations and the MEPS forecast members is indicated with the regression calculated for each day. The scatter plots in Figure 4.1.2 show a good correlation for sea level pressure and 2 m air temperature. Sea level pressure has the best

correlation of all variables. The MEPS forecast imply a disagreement with southerly observed winds in Figure 4.1.2e, between 21 and 23 December 2016. A good agreement is seen for wind direction in Figure 4.1.2f for 24 to 26 December 2016. Wind speed is overestimated throughout the event and will be further investigated in Section 4.2.5 (Figure 4.1.2g, h). Surface precipitation amount agrees better between 21 to 23 December 2016 (Figure 4.1.2i) than during 24 and 26 December 2016 (j). Figure 4.1.2i suggests a better correlation below 20 mm, for 21 to 23 December 2016 than above. A detailed discussion about the precipitation overestimation at the surface is given in Section 4.2.3. On 23 and 26 December 2016, pressure decreases and increases, as well as temperature increases, and wind changes are present. Since these changes show up in the surface observations it is assumed that frontal boundaries passed through Haukelieseter. As described in Section 3.6 the ECMWF dynamic tropopause analysis (Figure 3.6.1j) shows more ridging at the DT level on 23 December 2016, than on the previous days. Warm air is advected closer over to Southern Norway (Figure 3.6.1j). The low-pressure system approaches in the course of the day south-east of Iceland and hence stronger west to south west wind are associated with the cyclone (Figure 3.6.1l). The MEPS forecast, initialised on 23 December 2016 at 0 UTC in Figure 4.1.1k estimates the sea level pressure observations and shows the decrease in pressure after 12 UTC due to the shift of the occluded front with a constant pressure after the transition. Since warmer air is more advected to the north and the DT in Figure 3.6.1j shows a warm low-pressure core, an increase in temperature is observed and predicted at the measurement site (Figure 4.1.1l). The 25 December 2016 shows an increase of temperature between 15 UTC and 17 UTC leading to the assumption of a warm air evolution in Figure 4.1.1v. The overall weather situation, described in Section 3.6, showed that a warm front as well as cold front influenced Norway, on 25 December 2016. Since pressure and wind do not indicate a change related to frontal development, it is assumed that only the warm air section between the warm and cold front is shown in the surface measurements at Haukeliseter (Figure 4.1.1v). **Include L, H in the surface pressure images**

As the cyclone is advected to the north-east, closer into the Norwegian Sea, a wind change is seen in the ECMWF analysis (Figure 3.6.1l). First west wind and later south-west wind is associated with the low-pressure system. The MEPS forecast and observations in Figure 4.1.1m and n indicate a wind change from west to south with a slight decrease in wind speed.

On 23 December 2016, the evolution of the occlusion is also observed by an increase in precipitation. Before 18 UTC the surface accumulation shows light precipitation (Figure 4.1.1o). During the passage of the occlusion, the observed surface accumulation increases which is associated to continuous, heavy precipitation shown in Figure 4.1.1o.

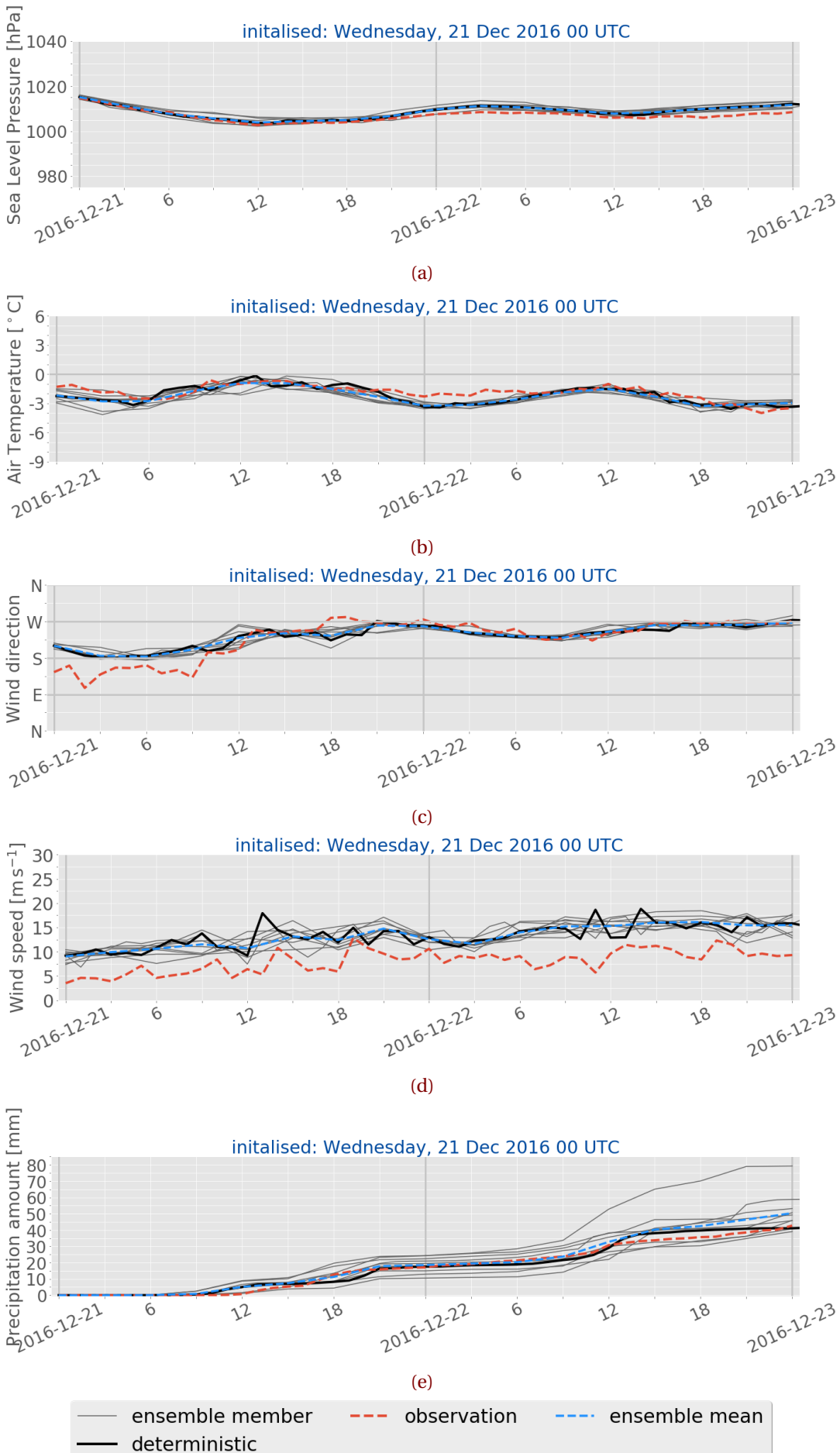
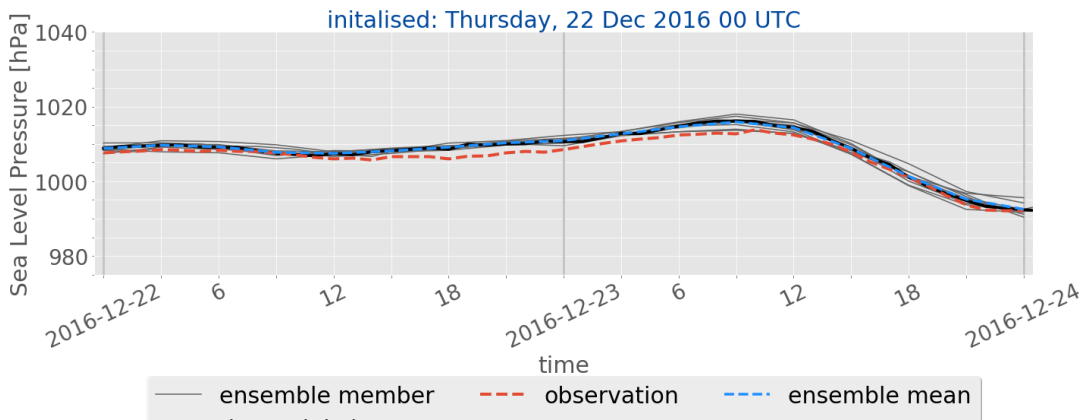
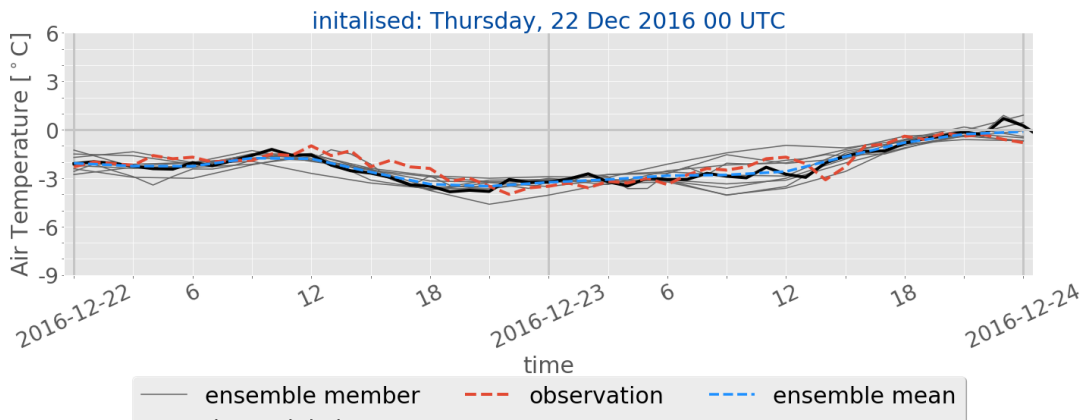


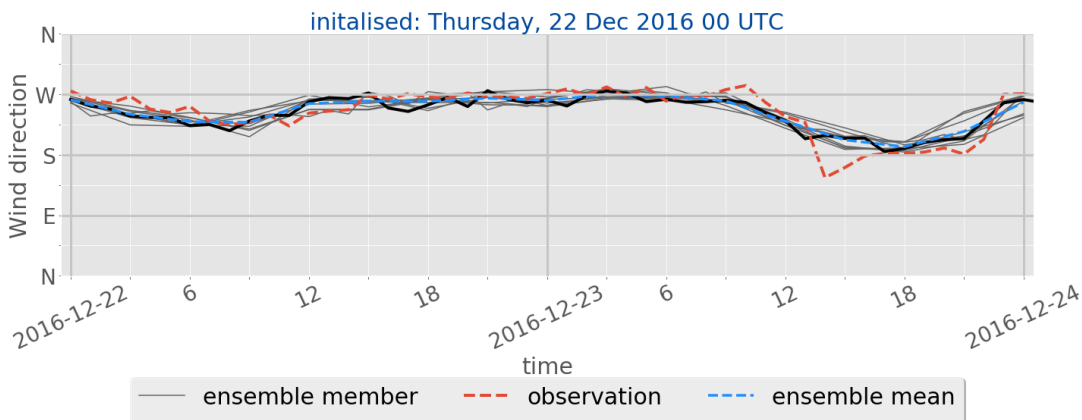
Figure 4.1.1: 48h surface observations and MEPS ensemble forecasts initialised on 21 December 2016 at 0 UTC. Line representation according to the label. Upper to low panel: sea level pressure, 2 m air temperature, 10 m wind direction and speed, and precipitation amount. *Continued on next page.*



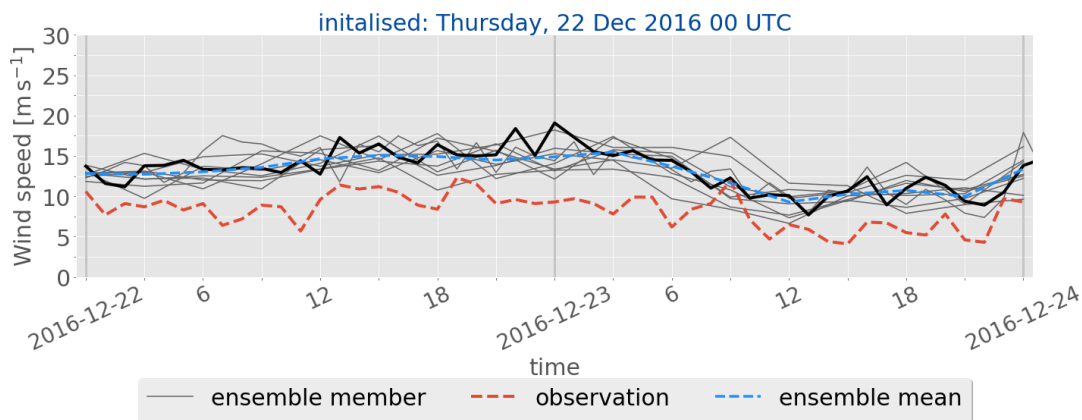
(f)



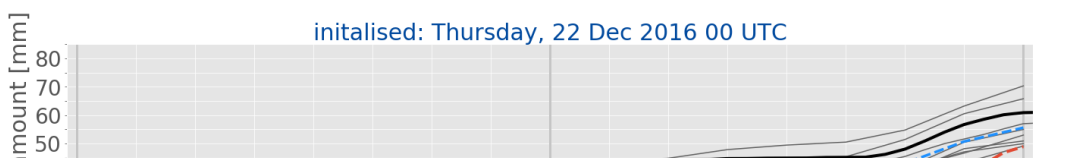
(g)



(h)



(i)



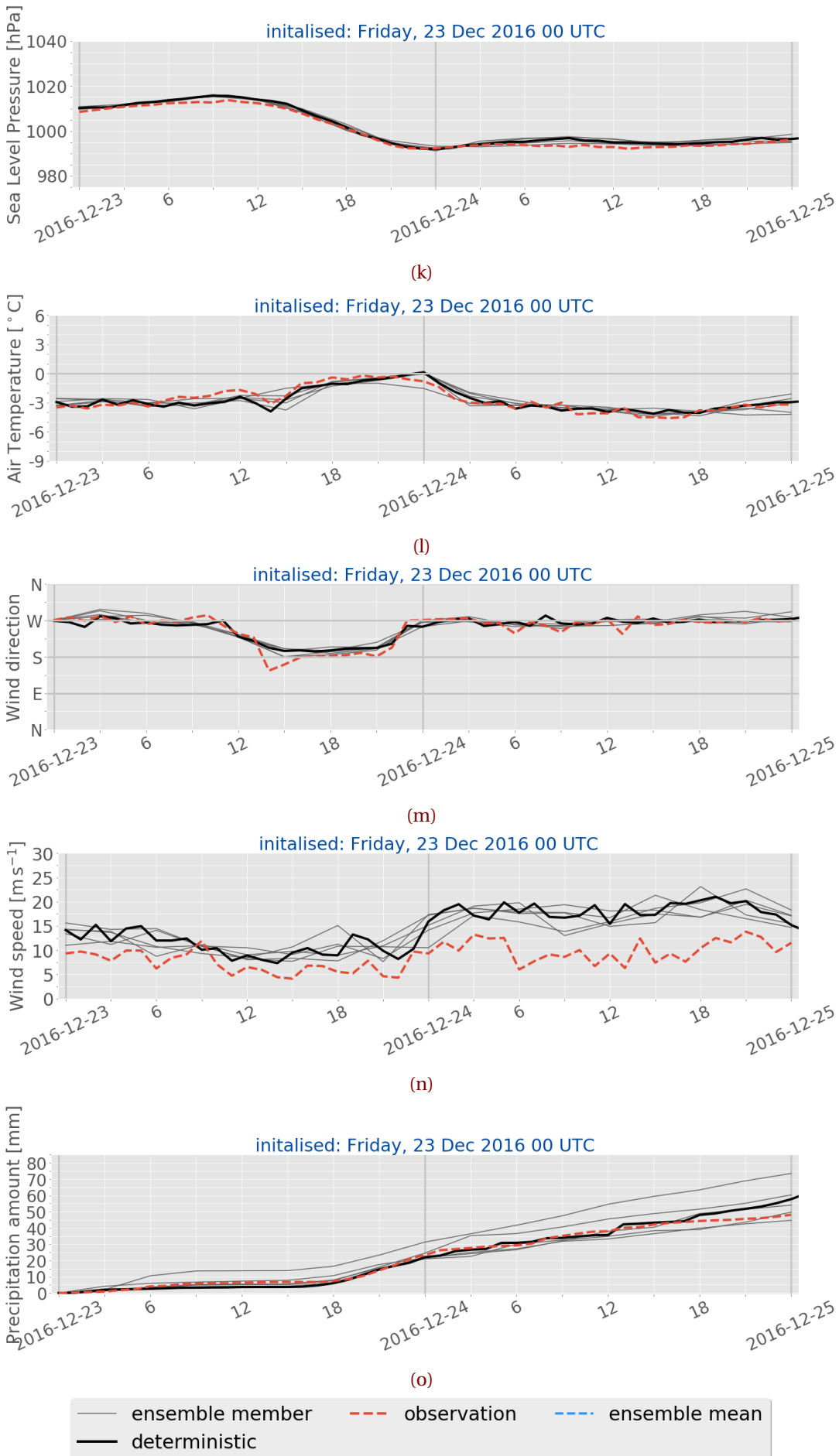
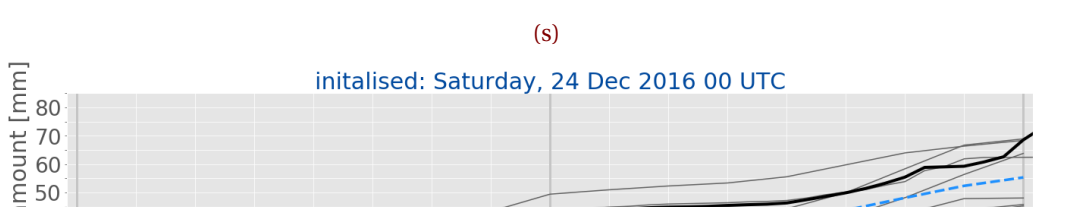
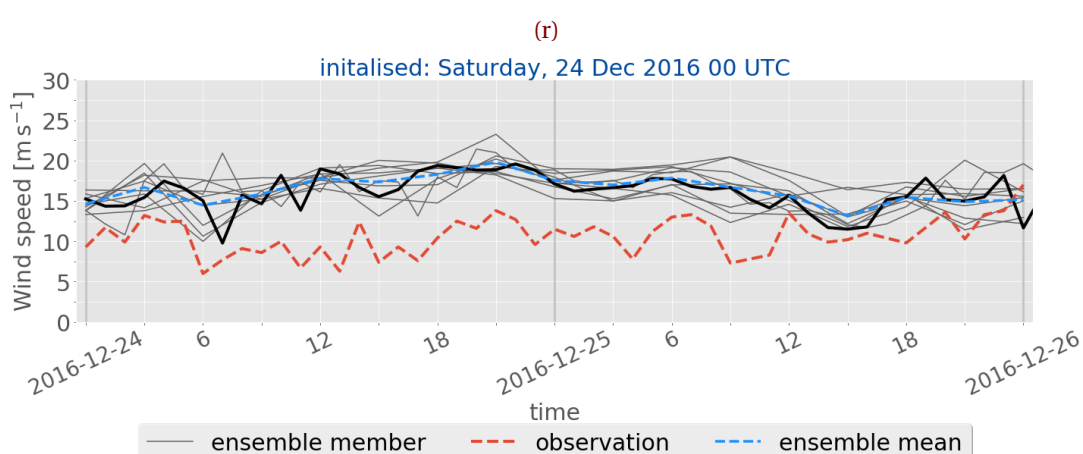
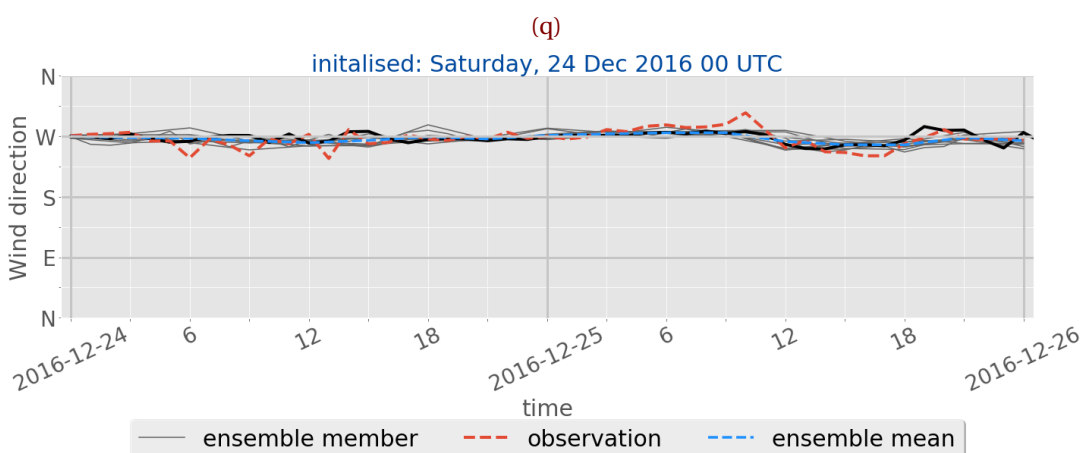
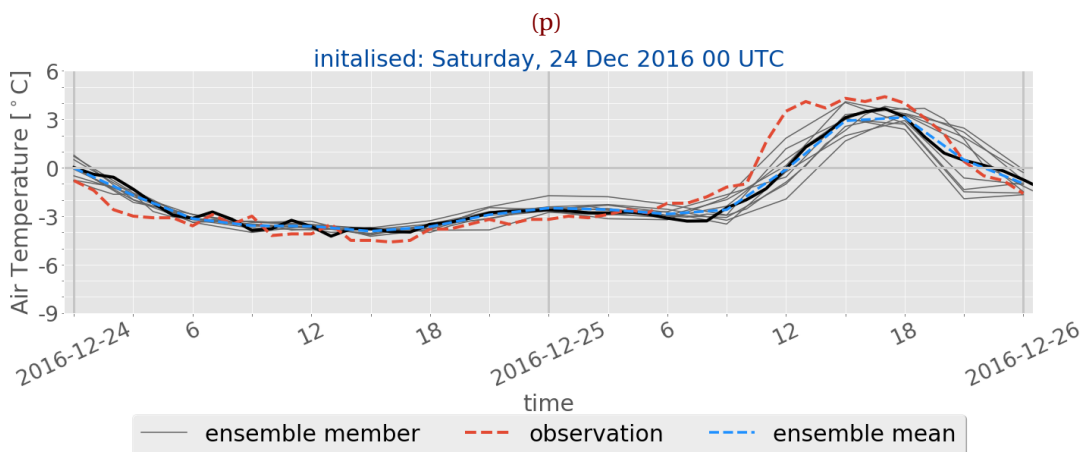
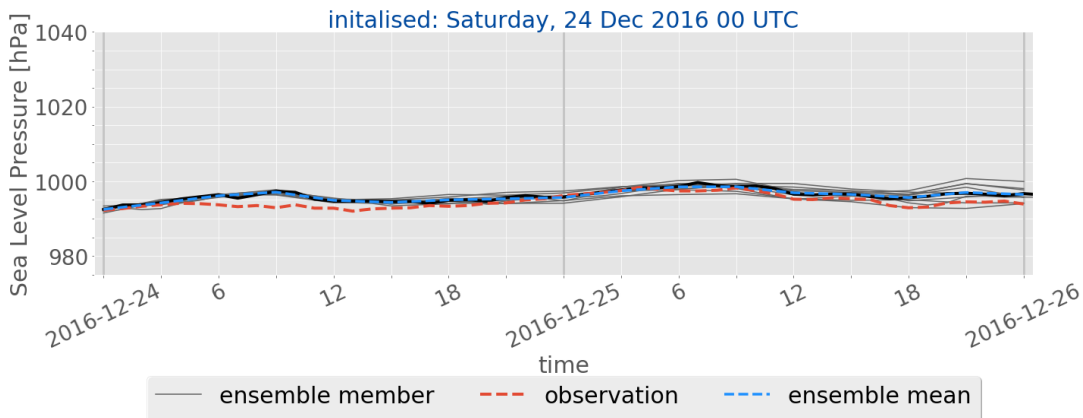


Figure 4.1.1: (Continued from previous page.) Initialisation on 23 December 2016 at 0 UTC.



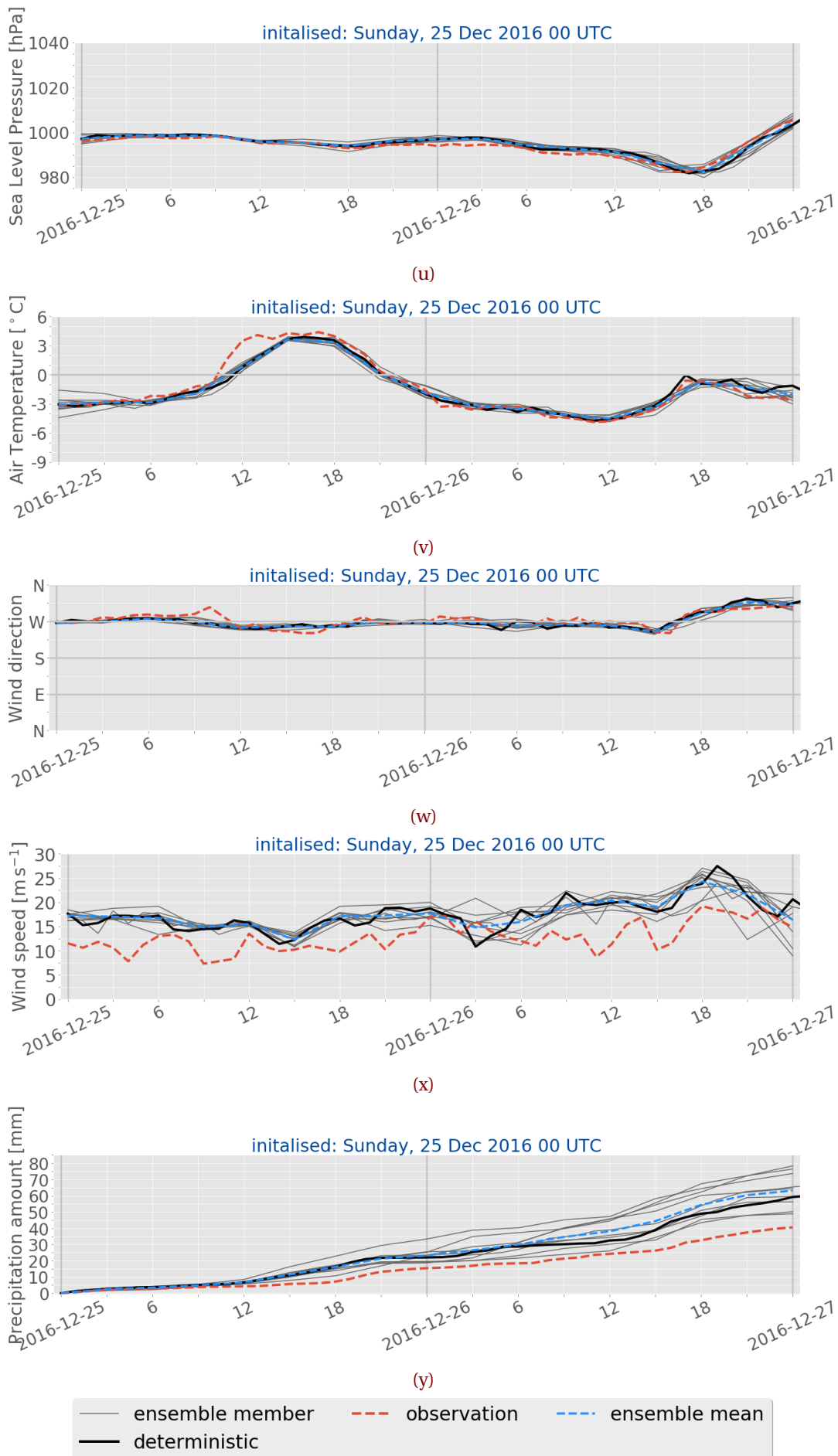


Figure 4.1.1: (Continued from previous page.) Initialisation on 25 December 2016 at 0 UTC.

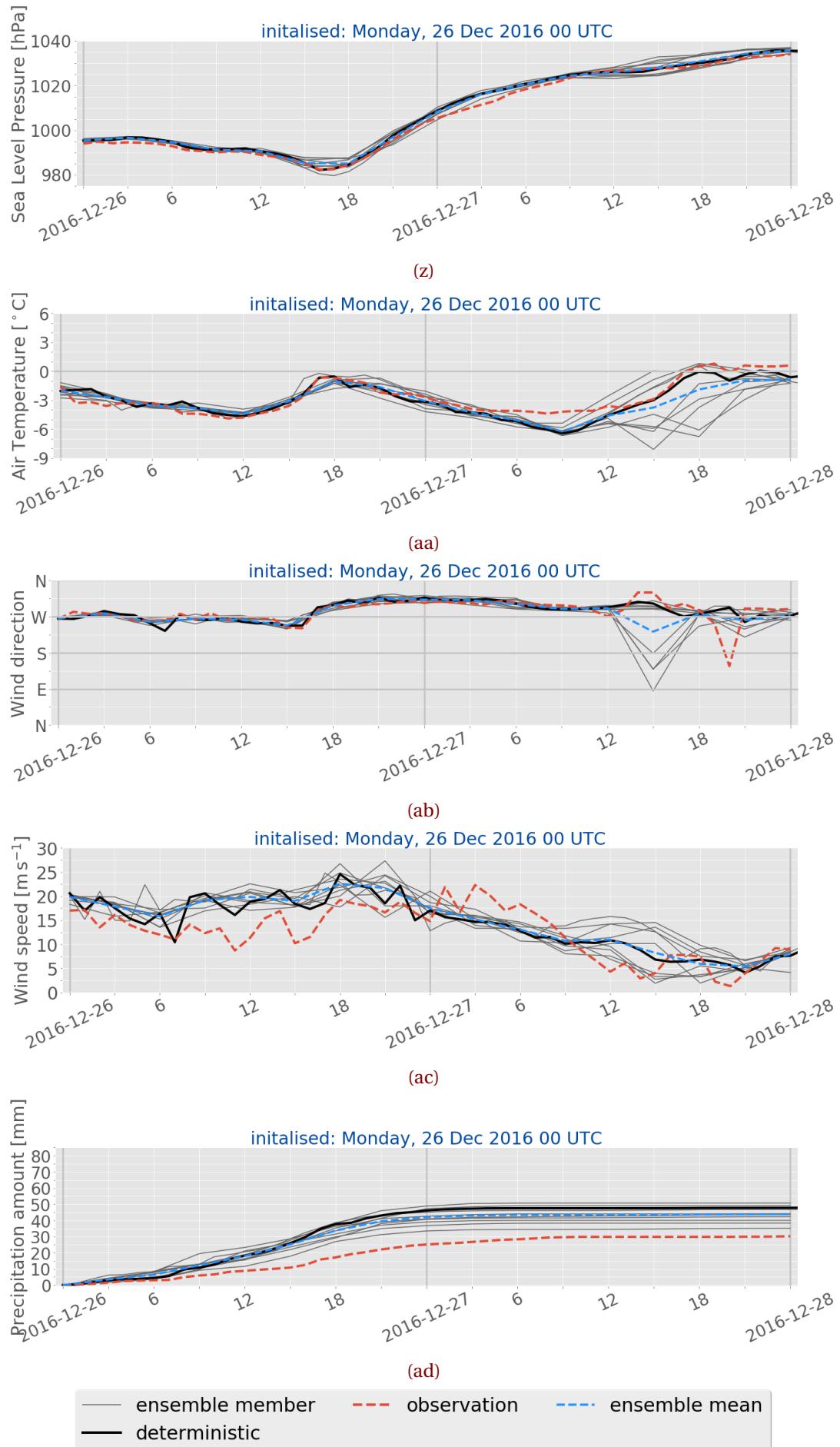


Figure 4.1.1: (Continued from previous page.) Initialisation on 26 December 2016 at 0 UTC.

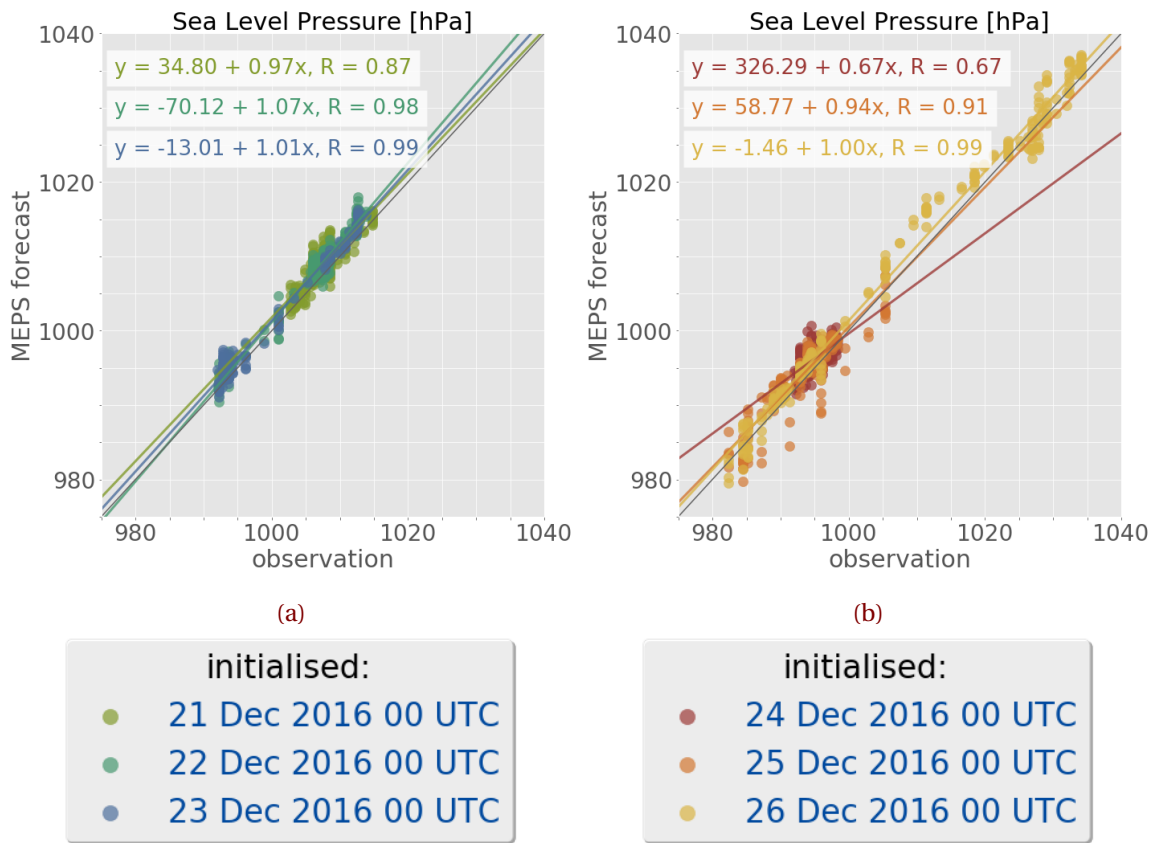


Figure 4.1.2: Scatter plots for surface observations and ensemble forecasts initialised for 21 to 23 December 2016 (left column, a, c, e, g, i) and for 24 to 26 December 2016 (right column, b, d, f, h, j). The 48 h scatter values indicate each day, showing the 1 h and 3 h forecasts respectively for 48 h. *Continued on next page.*

Similar patterns as on 23 December 2016 were seen for the evolution of the occluded front on 26 December 2016 in the ECMWF analysis Figure 3.6.1w and 3.6.1y. In this case the low-pressure system was located north of Møro and Romsdal in the Norwegian Sea. In the morning the cyclone is located east of Iceland and in the course of the day it moves closer to the coast of Norway (Figure 3.6.1x and 3.6.1z). Before landfall at 16 UTC, a pressure decrease occurs at Haukeliseter (Figure 4.1.1z). During the development of the occluded front, the sea level pressure reaches its lowest point of 985 hPa (Figure 4.1.1z) and increases afterwards during the dissipation of the 2016 Christmas storm.

Since the cyclone was surrounded by colder air (south of the low-pressure system in Figure 3.6.1w), first a drop and then an increase of temperature were observed and forecasted by MEPS (Figure 4.1.1aa). An indication of the occlusion evolution is also visible in the 10 m wind observations and MEPS predictions in Figure 4.1.1ab and ac. On 26 December 2016 at 0 UTC, the low pressure system is east of Iceland (not shown), moving closer into the Norwegian Sea by 12 UTC (Figure 3.6.1w and 3.6.1y). Surface west winds are associated to the cyclone in the Norwegian Sea, and impinging on the West coast of Norway Figure 3.6.1y. The wind measurement and MEPS forecast

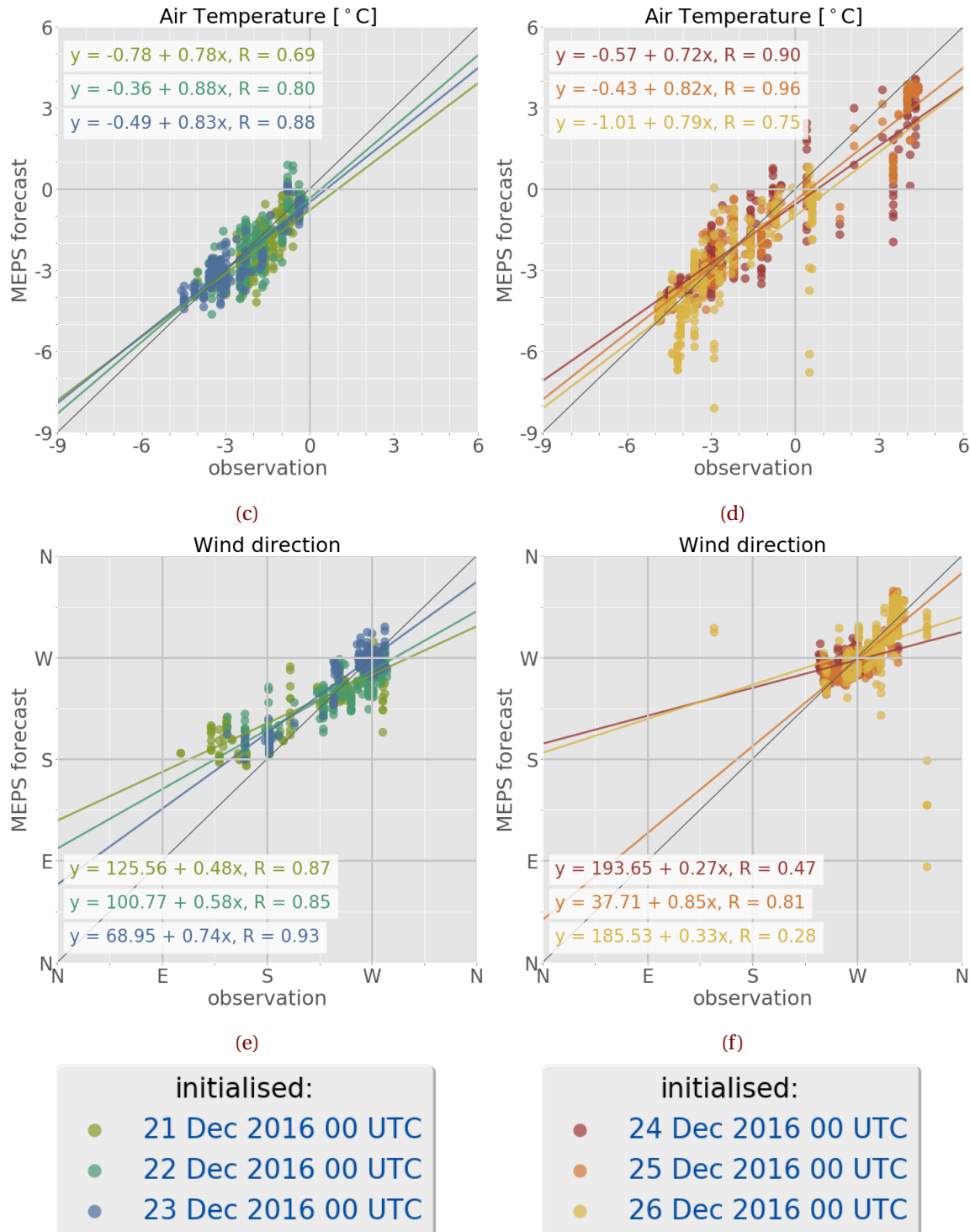


Figure 4.1.2: (Continued from previous page.) Upper panel 2 m air temperature, second panel 10 m wind direction.

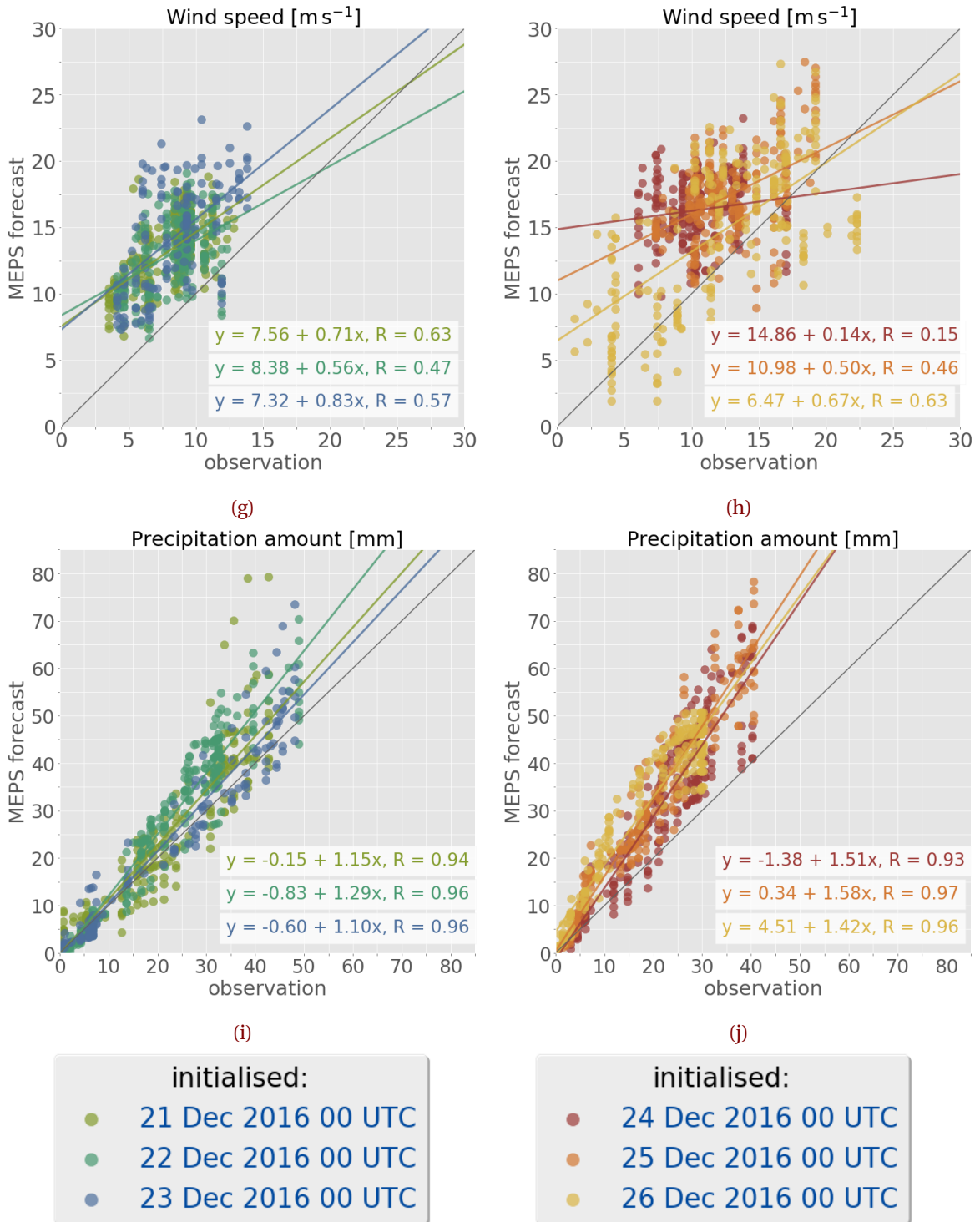


Figure 4.1.2: (Continued from previous page.) Upper panel 10 m wind speed, lower panel surface precipitation amount comparing double fence observations to 48 h MEPS forecasts.



Figure 4.1.3: MASC images of falling water drops observed on 25 December 2016 at 17 UTC from three different angles. Not all parts of the liquid sphere are equally illuminated.

in Figure 4.1.1ab and 4.1.1ac, show a gentle west breeze of up to 17 m s^{-1} at Haukeliseter before 12 UTC. The centre of the occluded front is located over Norway at 18 UTC, and the pronounced surface pressure gradient, in Figure 3.6.1z, indicate an increase in surface wind with a north-west wind direction. During this transition of the occlusion, the wind direction changes to north-west with higher observed wind speeds up to 20 m s^{-1} (Figure 4.1.1ab and 4.1.1ac).

Precipitation is continuing throughout the day, with light to moderate precipitation before the occlusion passage seen in Figure 4.1.1ad. Heavy precipitation related to the occlusion, around 16 UTC, is followed by moderate to light deposition on 26 December 2016.

While on 23 and 26 December 2016 precipitation was associated with a transition respectively landfall of an occlusion, the 25 December 2016 was marked by the transition of a warm sector. The ECMWF analysis shows a ridging of warm air at the dynamic tropopause (Figure 3.6.1r). The cyclone core is south east of Iceland in Figure 3.6.1r with two associated frontal boundaries. While the warm front is approaching the west coast, the cold front is north-west of Great Britain. In Figure 3.6.1t, the tail of the cold front moved into lower latitudes, following the slowdown of front, leading to a stationary frontal boundary. Furthermore, the mid-latitude jet is aligned with the surface frontal boundaries (??), while the Haukeliseter site is located below the the midlatitudal jet (??).

Neither pressure nor wind observations and forecasts in Figure 4.1.1u, w, and x, indicate the evolution of any frontal boundary. The only indication of a transition could be seen in the increase and then decrease of temperature at 11 UTC until 21 UTC (Figure 4.1.1v). In Figure 4.1.1w, a small wind change from west to north-west is observed by the wind mast at 10 UTC, which is not forecasted by MEPS, it rather estimated strong westerly winds.

Particle images taken by the MASC are available on 25 December 2016, during the transition of the warm sector in Figure 4.1.3. Without theses images taken around 17 UTC it would only be possible to verify that liquid precipitation occurred with the optical precipitation detectors at the Haukeliseter site. Together with the increase in surface temperature (Figure 4.1.1v) it can be concluded that the warm sector of the Christmas 2016 event passed by the measurement site.

The comparison between the ECMWF analysis (Section 3.6) and the observations at the measurement site (Figure 4.1.1), led conclude that the ensemble member forecast system MEPS covers the

prediction of large scale phenomena like occlusions and fronts, as well as liquid precipitation at the surface.

The scatter plots for observations and MEPS forecast show good correlation for most variables (Figures 4.1.2a to 4.1.2d, and f). The best agreement for pressure is reached on 26 December 2016 (Figure 4.1.1z), when the Christmas storm hit land and dissipated after the evolution of the occlusion at 16 UTC. [Dahlgren \[2013\]](#) showed an improvement of sea level pressure forecast for AROME, by including large scale boundary conditions for ECMWF into the regional model. The observation-model comparison by [Dahlgren \[2013\]](#) showed a decrease of pressure bias with lead time after 24 h with the use of pressure mixing. Since surface pressure is in good agreement with the observations, it is assumed that the warm front did not pass through Haukeliseter on 25 December 2016 and only the warm sector associated with the 2016 Christmas storm is observed. This shows a quite detailed forecast ability of MEPS, as from the ECMWF analysis, in Figure 3.6.1r, it is not quite clear if the warm front could have passed through. To be sure that the warm front did not pass through Haukeliseter, or whether it is a predictive error of MEPS, surface pressure, temperature and wind should be compared to the nearest grid point of the global forecast model ECMWF to verify this result.

Figure 4.1.2d displays a moderate correlation between observation and the 48 h MEPS ensemble member forecast system. In general, MEPS underestimates the observed 2 m air temperature, but MEPS estimated the surface temperature changes at the correct occurrence for 23, 25, and 26 December 2016.

Figure 4.1.4b shows warm and cold biases for 23 and 26 December 2016, respectively. On 25 December 2016, within the warm sector a cold bias was observed, underestimating the temperature when compared to the observation. The forecasts for 23, 25, and 26 December 2016 show calculated mean absolute error values (Equation (2.7.5)) of up to 0.61 K, 0.77 K and 1.44 K in Figure 4.1.5b. The previous operational deterministic forecast model AROME-MetCoOp showed a cold bias of 2 m temperature for the Norwegian mean, during winter 2013 with the introduction of AROME-Norway and later AROME-MetCoOp [[Müller et al., 2017](#)]. The mean error for the Norwegian model domain of AROME-MetCoOP estimated by [Müller et al. \[2017\]](#) is smaller than 1.8 K for the surface 2 m temperature in December 2014. The new ensemble forecast system MEPS shows a reduction of mean errors for the Christmas 2016 extreme event, when compared to the Norwegian mean of AROME-MetCoOp.

During the Christmas storm 2016, high wind speeds were observed at the Haukeliseter site (Figure 4.1.1n, x and ac). According to [Müller et al. \[2017\]](#) high wind speeds are significantly better simulated for AROME-MetCoOp compared to ECMWF's forecast for the model domain. Wind speed MEPS predictions in Figure 4.1.1n, x, and ac displays still an overestimation of wind speeds throughout the event. Furthermore, the correlation of observations and wind speed in Figure 4.1.2g and h show an overestimation for stronger wind speeds on 24 to 26 December 2016 than for 21 to 23 December 2016. The mean absolute error for wind speed during the Christmas storm is ranging from 3 m s^{-1} to 7 m s^{-1} for 48 h lead time. During the three days of frontal transitions, the highest mean absolute error of 6.5 m s^{-1} occurs for initialisations on 23 December 2016.

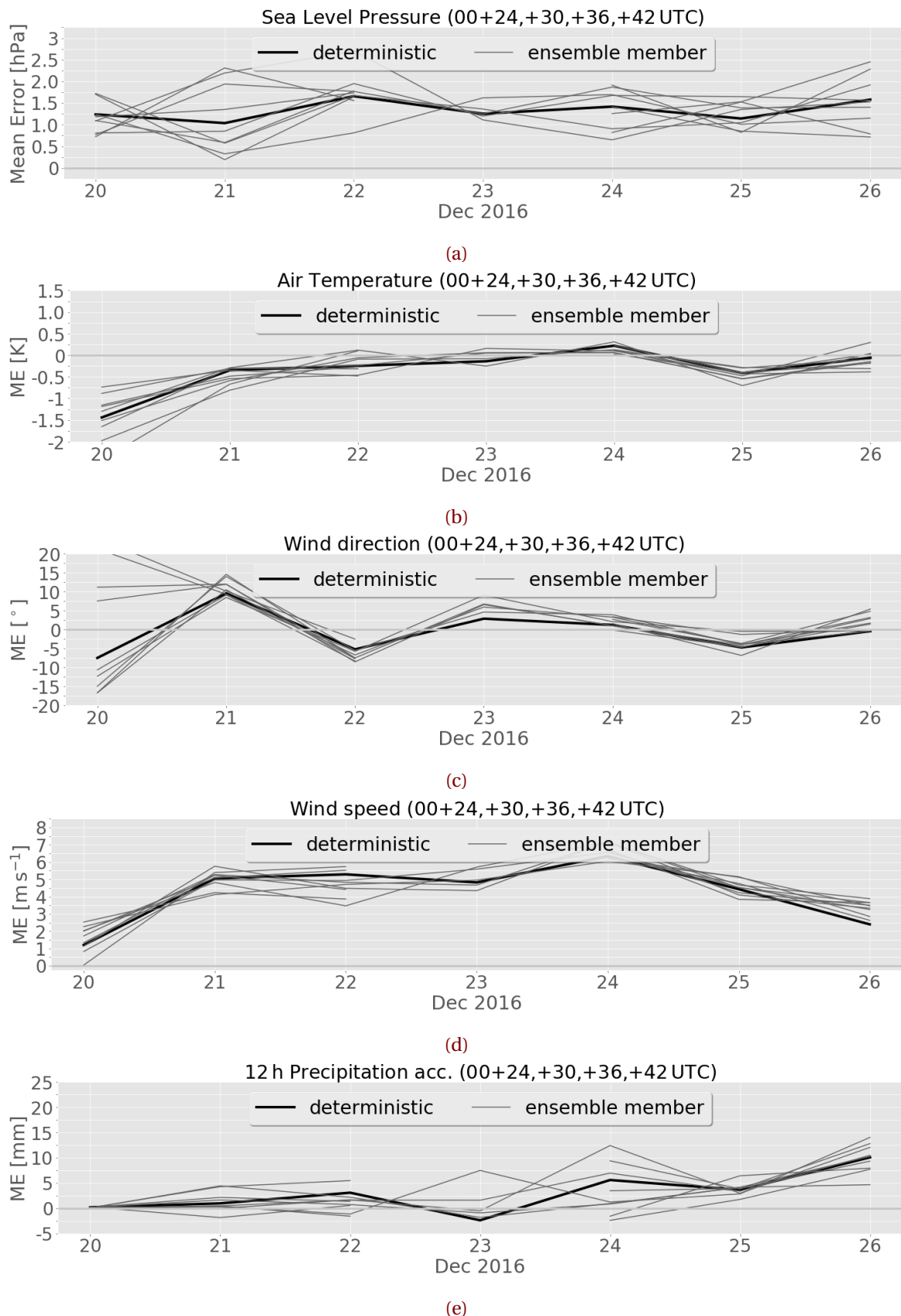


Figure 4.1.4: Mean error (a, b, c, d, e) of surface variables for all ten ensemble members at Haukeliseter, initializations at 0 UTC with lead times from 6 h to 24 h. From top to bottom, sea level pressure (a), 2 m air temperature (b), 10 m wind direction (c), 10 m wind speed (d), precipitation accumulation for 12 h surface accumulation (e).

The inaccuracy for wind speeds is an already known difficulty in the deterministic version of MEPS [Müller et al., 2017]. Müller et al. [2017] presented, that AROME-MetCoOp wind speed prediction generally agreed better with observations for wind speeds between 3 m s^{-1} to 13 m s^{-1} than ECMWF forecasts did, showing the advantage of a high-resolution weather model. Furthermore, with increasing wind speed the forecast accuracy for the Norwegian mean decreased with a mean absolute error below 2 m s^{-1} for 6 h to 24 h lead times, in December 2014 in AROME-MetCoOp. Müller et al. [2017] study case showed a slight underestimation of ECMWF 10 m wind compared to the Norwegian AROME-MetCoOp forecast for February 2015. On 23 December 2016, the mean absolute error is more than three times as high as the monthly averaged value for the Norwegian forecast domain (2 m s^{-1} for 6 h to 24 h forecast time) from Müller et al. [2017]. The larger mean absolute error during the event is firstly related to the comparison of a long term study of Müller et al. [2017], secondly their mean absolute error monthly average for 6 h to 24 h lead times, and third to the location of Haukeliseter.

Haukeliseter is a measurement site exposed to high wind speeds [Wolff et al., 2013, 2015]. The ensemble prediction system MEPS seems to still have issues forecasting the wind speed correctly in mountainous terrain. A detailed insight to the orographical wind influence will be assessed in Section 4.2.5.

Pressure, temperature, and wind changes for the occlusion transition on 26 December 2016 were already forecasted for initialisations on 25 December 2016 (Figure 4.1.1u, v, w, x), only wind speed and precipitation seem not to agree with the observations at Haukeliseter. The same is true for 25 December 2016, when the warm sector passes through Haukeliseter.

Figure 4.1.1e, o, y, and ad illustrate the surface precipitation amount observed and predicted by MEPS for Haukeliseter. MEPS overestimation is shown for precipitation when the cyclone intensifies and gets closer to Norway on 24, 25 and 26 December 2016. The surface observations and MEPS predictions in Figure 4.1.2*i* and *j* show an overestimate for 24, 25 and 26 December 2016, whereas on 21, 22, and 23 December 2016 the surface accumulation is balanced for predictions up to 30 mm. Any reasons for the overestimation of precipitation accumulation on the ground will be further analysed and discussed in Section 4.2.3. I HAVE TO SOMEHOW MERGE THIS IN, BUT HOW? What could be still a weakness that the model overestimates the wind speed? In Müller et al. [2017]: change from ECOCLIMAP1 because the surface roughness was too low and followed high wind speeds? Is this still the case for MEPS? High wind speeds followed also from wrongly addressed 'permanent snow'. Do not use 'orographic drag' in AROME-MetCoOp, could that lead to the too high estimated wind? When 'canopy drag' was changed saw increase in SBL drag which followed a decrease in wind speed. But AROME-MetCoOp is able to forecast high wind speeds, while ECMWF is not.

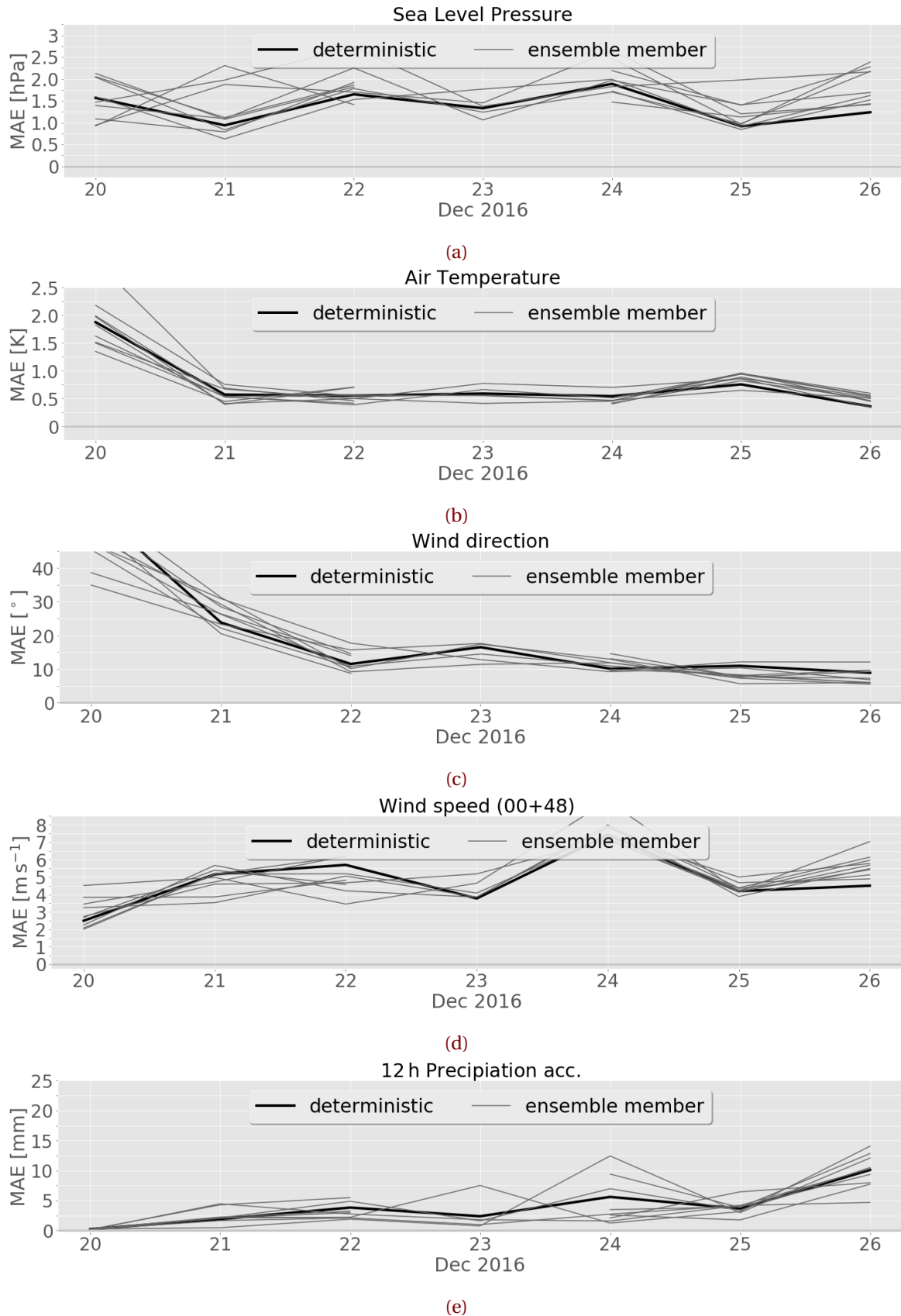


Figure 4.1.5: Mean absolute error (a, b, c, d, e) of surface variables for all ten ensemble members at Haukeliseter, initialisations at 0 UTC, valid for 48 h. From top to bottom, sea level pressure (a), 2 m air temperature (b), 10 m wind direction (c), 10 m wind speed (d), precipitation accumulation for 12 h surface accumulation (e).

Overall, for initialisations on 21 to 23 December 2016 (Figure 4.1.2a, c, e, g) the forecast is best for all variables. The large-scale weather pattern seems to be more predictable as long as the weather situation is not extreme. Figure 4.1.2b, d, f, h suggest as if MEPS has difficulties predicting the intensification and associated pressure decrease of the Christmas 2016 storm at Haukeliseter. The prediction of pressure fits well on all days (Figure 4.1.2a, b) compared to temperature, wind direction, wind speed, and precipitation (Figures 4.1.2c to 4.1.2j). The greatest difficulty has MEPS with the prediction of wind speed during the entire extreme event. The rainfall, however, fit well for 23 December 2016 (Figure 4.1.1o and 4.1.2i), but MEPS has problems predicting the accumulation of surface precipitation amount correctly for the extreme days of the 2016 Christmas storm, 24 to 26 December 2016 (Figure 4.1.1y, ad and Figure 4.1.2j).

Figures 4.1.2a to 4.1.2d have shown good agreement of ensemble members. It is not expected that ensemble members agree they should just give a variability around the observations, that is why ensemble member prediction exists (Section 2.5). Based on the uncertainty in observations the solution space that is possible has to be understood. During extreme events the model is not adjusted to present the extreme event particularly well.

4.2 SNOWFALL

After the analysis of meteorological quantities, the snowfall at Haukeliseter during the Christmas storm will be investigated.

First the results from the optimal estimation retrieval scheme will be examined and compared to the observations of the double fence. After the overestimation of surface accumulation will be analysed, followed by a vertical comparison of snowfall observations and predictions. The sections finishes with the relation between wind and precipitation related to the surrounding topography at Haukeliseter.

4.2.1 SENSITIVITY OF THE OPTIMAL ESTIMATION RETRIEVAL

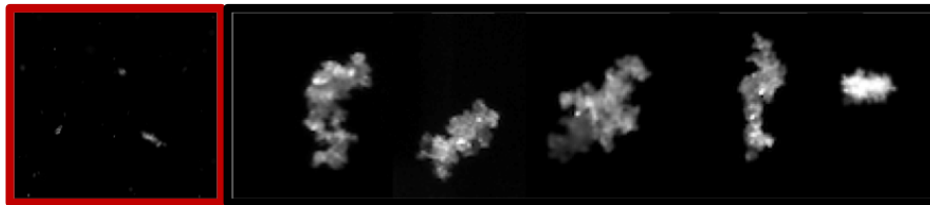


Figure 4.2.1: MASC observations during the Christmas storm 2016. Left (red frame), small ground up blowing snow particles. Five images on the right, rimed particles.

Include some more specific: Which observations, which quantity was used to generate the optimal estimation retrieval? The optimal estimation retrieval scheme for snowfall was applied to the six-day Christmas 2016 storm event. MASC images of snowfall during the event were used to guide the selection of the appropriate particle model and PSD input for the retrieval scheme. In this section, the sensitivity of retrieval results to these inputs is explored. Such an exercise should also allow an identification of those properties that yield the best match with Met-Norway snow gauge measurements at Haukeliseter.

The majority of the MASC images from Haukeliseter contained snow particles that looked like the left image Figure 4.2.1 (red frame). Such images suggest small ground-up blowing snow particles that are consistent with the high winds observed during the event. However, a careful examination of the MASC images also finds the presence of rimed aggregates such as those in the right five images (Figure 4.2.1). Pristine crystals such as plates and columns were not observed during the Christmas 2016 event. As such, the use of two different aggregate particle models developed for the CloudSat mission are further investigate (Figure 4.2.1).

Figure 4.2.2 presents hourly measured snowfall accumulations on 22 December 2016 plotted against retrieved values for the two different aggregate assumptions. The 'B8' aggregate is a low reflectivity per unit mass aggregate that worked well for the cold, dry conditions observed at Barrow as described in Cooper et al. [2017]. The 'B6' aggregate, presented in Appendix A.1, is a high reflectivity per unit mass particle (Section 2.4.1). As such, the 'B6' aggregate would seem more physically consistent with the observed rimed particles (Figure 4.2.1, 5 aggregates to the right) and humid environment found in the coastal mountains at Haukeliseter. The presence of a water or rimed coating on the aggregates aloft would greatly enhance their effective reflectivity.

Indeed, Figure 4.2.2 suggests that the reflective 'B6' aggregate agree much better than the less reflective 'B8' aggregate with the snow gauge. During the Christmas storm 2016 the assumption of the 'B8' aggregate shows overestimation of precipitation amount at the ground compared to the double fence gauge for all six-days.

Table 4.2.1 presents the percentage differences between snow gauge and retrieved estimates found when using these particle model assumptions for 22 December 2016. Use of the 'B6' aggregate agreed within 5 % of the double fence observations (Table 4.2.1) for both 12 h and 24 h surface accumulations. Admittedly, use of the 'B6' aggregate produced slightly too little snowfall relative to the gauges for the remaining days of the event as discussed in Section 4.2.2. The use of the

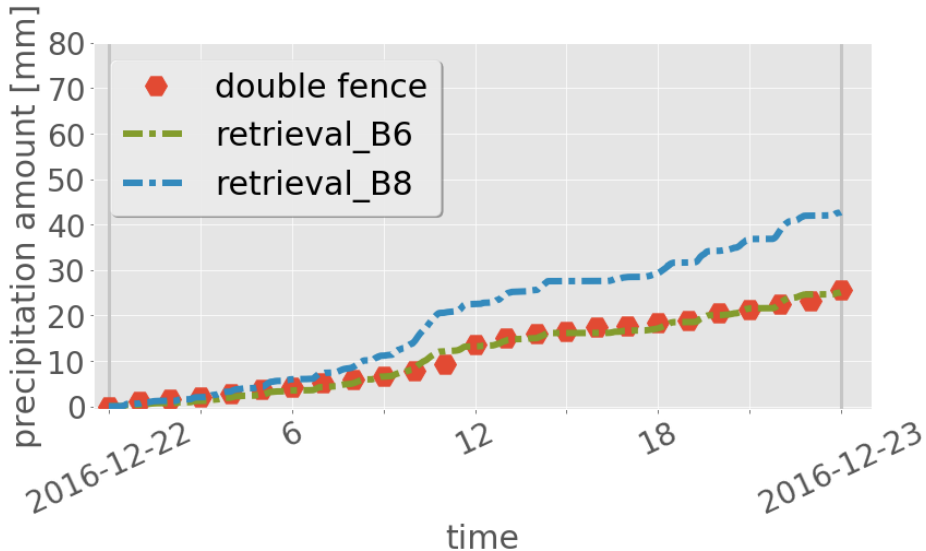


Figure 4.2.2: Hourly double fence snowfall accumulations [mm] plotted against retrieved values for the 22 December 2016 for different retrieval assumptions permutations. Double fence snowfall accumulation, red hexagons, retrieved precipitation amount for the here used study (B6), green, dash-dotted, and for small aggregates (B8), blue dashed.

'B8' aggregate, however, overestimates snowfall by at least 65 % for both the 12 h and 24 h surface accumulations (Table 4.2.1). Since this aggregate had low reflectivity per unit mass, it required significantly more SWC in the forward model calculations (Section 2.4.1) to match MRR reflectivities. The retrieval therefore overestimates snowfall rate for these meteorological conditions at Haukeliseter during the Christmas 2016 storm.

The sensitivity study here has focused on MASC estimates of habit instead of particle size distribution or fall speed. The reason is that MASC and PIP primarily detected blowing snow particles at the surface that likely were much smaller than the particles that the MRR remotely sensed aloft. The use of the PSD measured by the MASC or PIP in the retrieval therefore produced much larger snowfall than those measured by the double fence snow gauges, e.g. on 22 December 2016 (Figure 4.2.2). Essentially, it takes a much greater mass of small particles than large particles to match a given reflectivity. The results during the Christmas 2016 event contrast with those found for low wind speed events at Haukeliseter where the use of MASC habit, PSD, and fall speed observations resulted in retrieved snowfall accumulations very close to Met-Norway double fence gauge observations. Regardless, for this high wind event, the a priori temperature PSD relationship by Wood [2011] and a climatological average fallspeed of 0.85 m s^{-1} [private communication, Schirle, 2018] were employed. S'B6' rimed aggregate assumption resulted in a better agreement than the 'B8' assumption for surface accumulation during the Christmas 2016 storm. Therfore, the difference between the retrieved precipitation amount at the ground and the double fence gauge observations will be further studied in the following section. Conclusion for the rest of my study?

Table 4.2.1: Observations by the double fence gauge (obs.) and retrieved (ret.) snowfall amounts for 22 December 2016 for different particle model assumptions. B6 is the rimed aggregate assumption used in this thesis (Section 2.4.1) and B8 the assumption for small particles as used in the CloudSat optimal estimation snowfall retrieval.

Particle model	12 h accumulation			24 h accumulation		
	Snowfall		Difference	Snowfall		Difference
	obs.	ret.		obs.	ret.	
	[mm]		[%]	[mm]		[%]
B6	13.6	13.2	-3.0	23.1	25.1	-2.1
B8	13.6	22.5	+65.5	23.1	42.7	+66.9

4.2.2 COMPARISON OF SURFACE OBSERVATIONS

To be able to compare the vertical predicted snow water content with the retrieved snow water content a verification of the surface accumulation is made. If the retrieved surface accumulation is confident in comparison to the double fence measurement, then the vertical measurements can be trusted.

The correlation in Figure 4.2.3a demonstrates a good agreement between the 48 h accumulation measured by the double fence and the retrieved surface accumulation. The black line in Figure 4.2.3a presents a linear correlation with a regression coefficient of $R = 0.97$. In general, the retrieved surface snowfall accumulation is underestimated when compared to the double fence measurements, but not to a large degree.

Figure 4.2.3b shows the difference between retrieved accumulation and observed accumulation by the double fence. For the time period 20 to 24 December 2016, Figure 4.2.3b indicates an underestimation of retrieved snow accumulation of less than -5 mm for the first 24 h. Snow accumulation calculated on 23 December 2016 at 0 UTC show after 24 h an underestimation by the retrieval of up to -6.5 mm. On 24 December 2016, larger underestimation after 43 h is related to the observation of liquid precipitation on 25 December 2016 between 12 UTC to 21 UTC. On 25 December 2016 no fair comparison to the double fence measurement can be performed after 12 UTC because of the neglection of liquid precipitation when temperatures exceed 2°C .

For a 12 h accumulation follows for the Christmas storm (21 to 26 December 2016) an average difference of 85.5 % (Table 4.2.2). For longer, 24 h accumulation decreases the average difference to be -4.7 % (excluding values on 25 December 2016 after 12 UTC and on 26 December 2016 after 17 UTC because of attenuation at the MRR). The daily surface snowfall accumulation difference between retrieval and observation in Table 4.2.2 show almost always a well agreement to the double fence. The only well pronounced mismatch is seen on 21 December 2016, where it measures much more than the double fence gauge (+435.8 %).

Similar to this study, Cooper et al. [2017] used a CloudSat snow particle model, PSD and fall speed from MASC observations for five snow events at Barrow, Alaska. The comparison to the

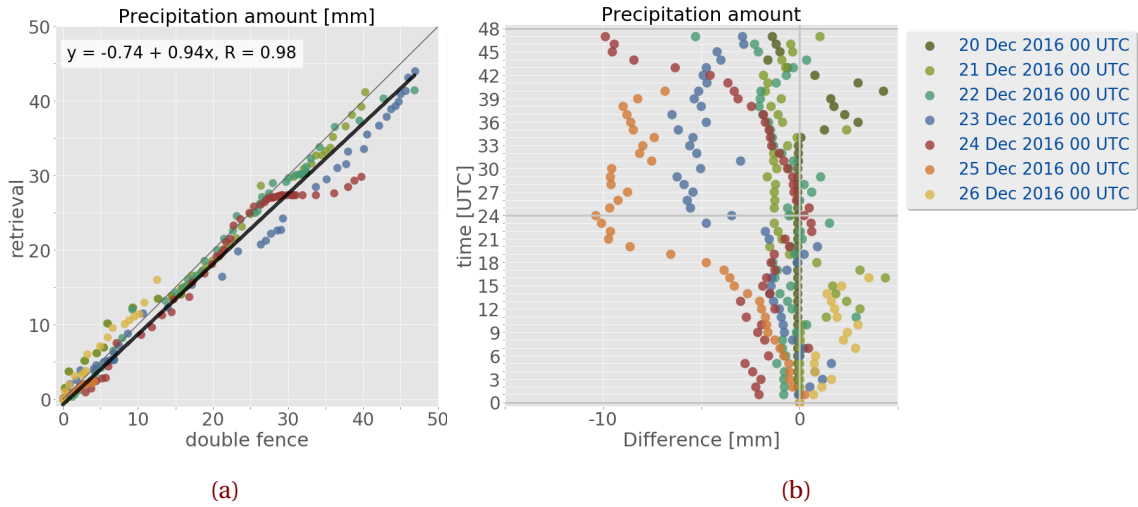


Figure 4.2.3: a: Surface precipitation amount comparison between the double fence observations and the retrieved surface accumulation of precipitation for 48 h. In black the linear correlation between the double fence observations and retrieved surface snow. b: Difference between the retrieved and the observed accumulation by the double fence. The colours represent the different starting days at 0 UTC for the 48 h accumulation.

Table 4.2.2: Comparison of observed (obs.) and retrieved (ret.) snowfall amounts for the Christmas storm 2016. Difference refers to the difference of the retrieved and observed snow accumulation after 12 h and 24 h. The average difference is the value over all six/four days. Excluding values after 12 UTC on 25 December 2016 and after 17 UTC on 26 December 2016.

Day in 2016	12 h accumulation				24 h accumulation			
	Snowfall		Difference	Average difference	Snowfall		Difference	Average difference
	obs.	ret.			obs.	ret.		
	[mm]		[%]	[%]	[mm]		[%]	[%]
20 Dec	0.1	0.0	-97.8		0.1	0.0	-97.8	
21 Dec	0.7	3.8	+435.8		17.1	16.6	-2.7	
22 Dec	13.6	13.2	-3.0		25.6	25.1	-2.1	
23 Dec	6.3	5.2	-16.8		23.3	19.8	-14.9	
24 Dec	14.7	13.4	-8.6		24.8	25.0	+0.8	
25 Dec	4.3	-	-		+15.4	-	-	
26 Dec	8.8	10.6	+20.1		25.1	-	-	

weather station revealed an difference between National Weather Service observations and retrieved accumulations of -18 % for five snow events.

Table 4.2.2 shows the difference for each individual day and the average difference for six and four days, depending on the accumulation of 12 h or 24 h. The choice of the correct PSD model, slope parameters and fall speed in the optimal estimation snowfall retrieval, shows a good agreement with the observations at Haukeliseter for the 2016 Christmas storm in contrast to the 200 % difference when only using the CloudSat snowfall algorithm (Section 2.4). It indicates also a reduction of

the non-uniqueness of snow accumulation is reduced, when using a combination of ground-based observations instead of only Ze-S relationships.

It turns out that there is no relation between high and low precipitation events since the differences vary daily. [Cooper et al. \[2017\]](#) showed also different combinations of PSD assumptions and snow fall speed. For Barrow, best agreements between observations and retrieved snowfall were found by using the CloudSat particle model, slope parameters and snowfall speeds from the MASC. In the here presented study, the best assumption for surface snowfall accumulation was found by using a particle model for rimed aggregates (Section 2.4 and 4.2.1) such as in Figure 4.2.1.

On 20 and 21 December 2016, the difference error is large (-97.8% and 435.8% , respectively). This is probably related to an observation of precipitation at the double fence, even though no precipitation was observed. On 20 December 2016, observation at the double fence might be related to some particles stirred up by wind into the orifice of the gauge. Since no manual observations are done at the Haukeliseter site, is it difficult to say if blowing snow occurred or if it was snowing. This introduces additional errors on the double fence measurements. From the vertical MRR reflectivity, in Section 4.2.4, Figure 4.2.6, it can be seen, that precipitation was not observed on 21 December 2016 before 9 UTC.

Even though it is assumed that the double fence is the correct measurement it still underlies some uncertainties, such as under-catch during high wind speeds [[Wolff, unpublished](#)]. A better way to asses the accuracy of the retrieved surface snowfall accumulation could be to compare the results to measurements inside a bush gauge.

[Wolff, unpublished](#) estimates the under-catchment of double fence gauge compared to bush gauge measurements to 10% , for outside winds of 9 m s^{-1} (Section 2.3.1). If the double fence gauge underestimate snowfall under high wind condition, would follow that the optimal estimation retrieval results are more than 20% too low to the true state.

Anyway, the low average difference value for 24 h accumulation, in Table 4.2.2 during the Christmas 2016 event (-4.7%) follow a much lower average difference between retrieved and observed surface accumulation than at Barrow (36%) and therefore a very good agreement between observed and retrieved snow accumulation during 21 to 24 December 2016. In Section 4.2.4, the vertical SWC will be compared to the forecasted MEPS values for the 2016 Christmas storm. Despite the under-catchment of wind related snow precipitation, the double fence measurement give confidence for the retrieved profiles of snow water content. While snow water content is compared to the MEPS forecast, it should be kept in mind that retrieved snow accumulation is underestimated and therefore the vertical SWC may be too low.

4.2.3 COMPARISON OF SURFACE OBSERVATIONS AND MEPS

Hereafter, MEPS surface precipitation prediction forecast is compared to the double fence gauge observations at Haukeliseter to see if observed surface accumulation was correctly predicted by MEPS.

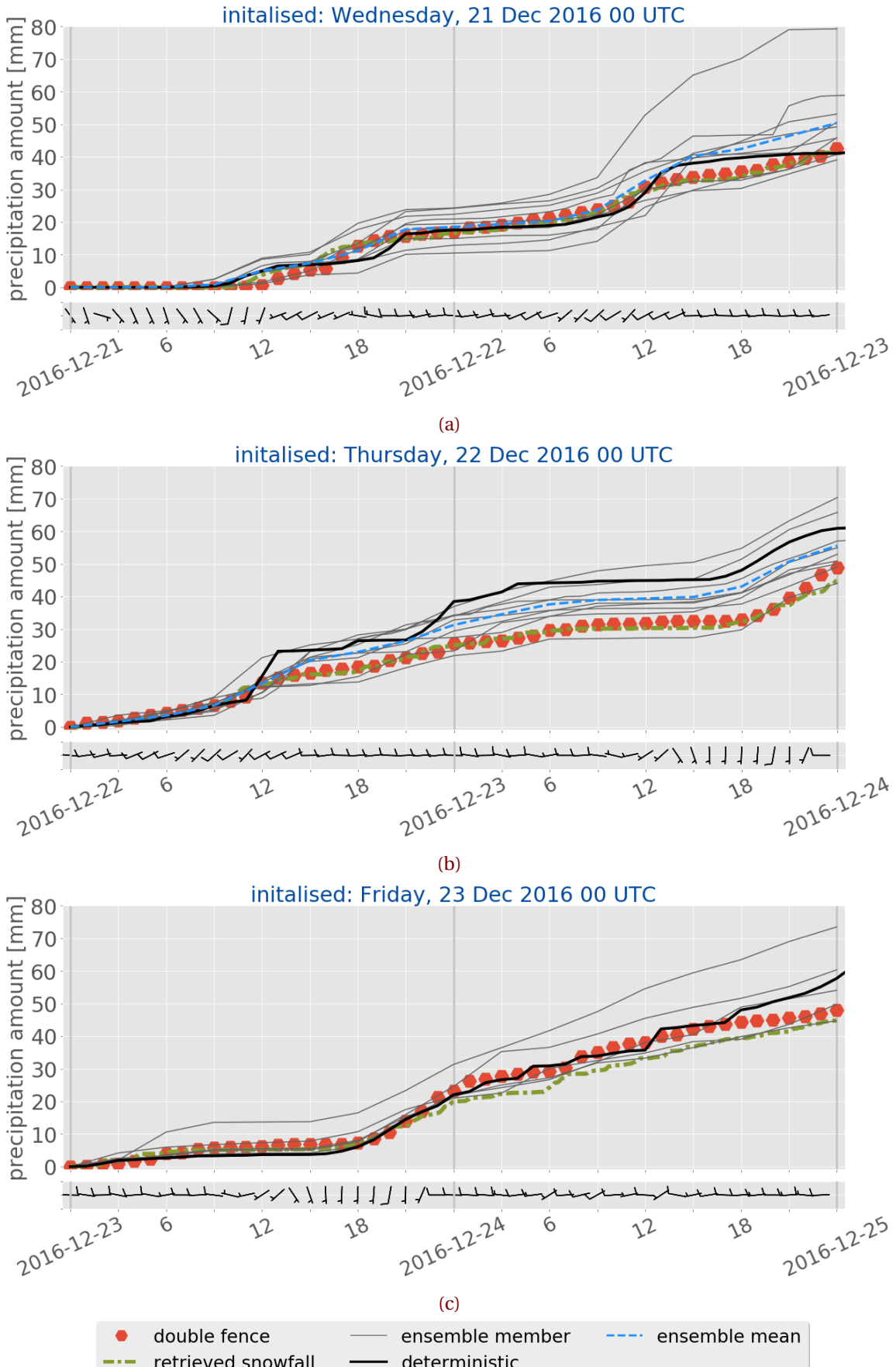


Figure 4.2.4: 48 h surface precipitation accumulation for 21 to 26 December 2016 (a to f). Representing the values from the double fence in red, hexagons; optimal estimation retrieval output at the first noise free level in dash-dotted green; MEPS ensemble member deterministic forecast, initialised at 0 UTC in black and its nine perturbed ensemble members in grey. The ensemble mean of all ten members is shown in dashed blue. Underneath is the associated last hour 10 min average wind from the weather mast at 10 m height. *Continued on next page.*

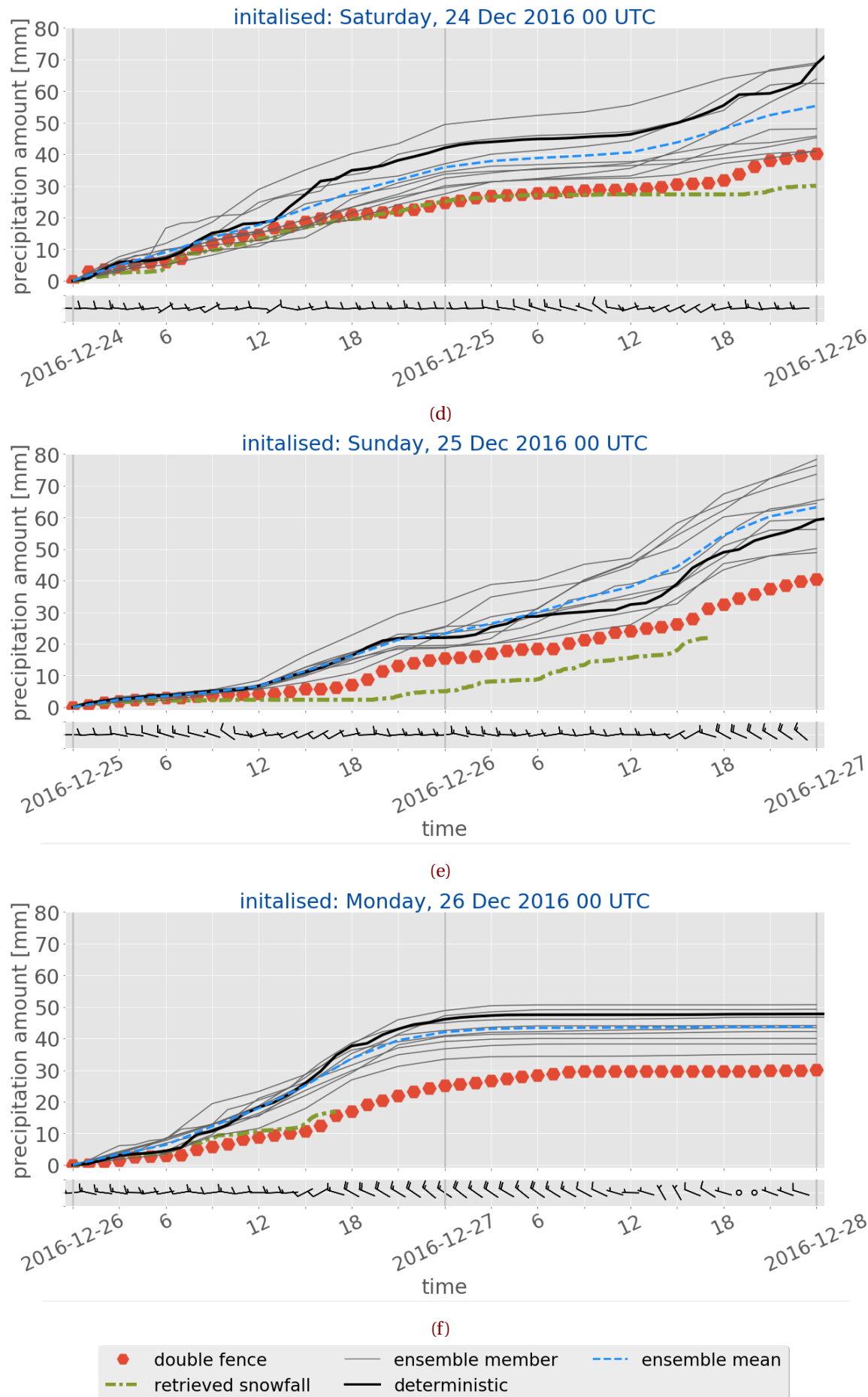


Figure 4.2.4: (Continued from previous page.)

Figure 4.2.4 shows surface accumulation observations at the double fence, retrieved snow accumulation, and MEPS forecast for 48 h. The blue dashed line shows the ensemble mean of all ten members. The ensemble mean of precipitation amount is calculated every three hours, due to the three hourly time resolution of most of the perturbed member (Section 2.7.1). When not all perturbed member forecast data was available from the [Norwegian Meteorological Institute \[2016\]](#), like on 23 December 2016 (Figure 4.2.4c), no ensemble mean is calculated. At the bottom of Figure 4.2.4 the associated 10 min average wind of the last hour from the 10 m weather mast at Haukeliseter is presented. This will help to see if surface accumulation observations by the double fence may be influenced by wind. MEPS surface accumulation does not account for undercatchment by too high wind speeds, and therefore are not presented in Figure 4.2.4.

In general, Figures 4.2.4a to 4.2.4c show a better agreement between double fence precipitation amount observations and forecast for 48 h forecasts initialised on 21 to 23 December 2016 at 0 UTC than for initialisations on 24 to 26 December 2016. The double fence observation lie for 21, 22, and 23 December 2016 within the spread of the ensemble members (Figures 4.2.4a to 4.2.4c), covering the uncertainty within the measurements (Section 2.5). On the other hand, observations between 24 and 26 December 2016 are too low compared to the ensemble spread (Figures 4.2.4d to 4.2.4f). During 24 and 26 December 2016, the low-pressure system intensifies and gets closer to the Norwegian coast, influencing the local weather in Norway (Section 3.6). Figure 4.2.4d to f indicate a larger estimated surface precipitation amount for all ten ensemble members compared to observed values at the measurement site between 24 to 26 December 2016. Furthermore, all ensemble members seem to overestimate the surface accumulation after 18 h on 24 December 2016 and after 12 h on 25 and 26 December 2016.

The correlation for precipitation between 48 h double fence observation and ensemble precipitation forecast is presented in Figure 4.1.2i and j. Showing a better agreement for 21 to 23 December 2016 than initialisation on 24 to 26 December 2016. On 21 to 23 December 2016 the slope of the regression line is relatively close to unity.

Initialisations on 24 December 2016 (Figure 4.2.4d) indicate an overestimation of the deterministic surface snowfall prediction already after 13 h forecast time. The deterministic forecast in solid black in Figure 4.2.4d is much higher and increases faster than the observations and the nine perturbed members. In Figure 4.2.4d at 16 UTC, a difference of approximately 15 mm can be seen when compared to the surface measurements. This difference remains almost constantly over the forecast time.

While the cyclone propagates closer to Norway, the forecast inaccuracy of the surface precipitation increases. Overestimation occurs around 12 UTC on 25 December 2016. This overestimation of the precipitation amount could be associated with the warm sector evolution at Haukeliseter (Section 4.1.1). Afterwards, with increasing lead time MEPS forecasts show the same precipitation evolution as the double fence, but too high. An overestimation of the surface precipitation is also simulated on 26 December 2016. While the surface analysis indicates the passage of an occlusion after 15 UTC (Figure 3.6.1w, 3.6.1y, and Section 4.1.1). The overestimation seems to occur after 12 h lead time in Figure 4.2.4f. The MEPS ensemble seems to predict the occurrence of precipitation

Table 4.2.3: Observations (obs.) and forecasted (MEPS) snowfall amounts for the Christmas storm 2016. Difference refers to the percentage difference between MEPS ensemble members and the double fence observation, averaged over all ensemble member for 12 h and 24 h. The average difference is the value over all days.

Day in 2016	12 h accumulation						24 h accumulation					
	Snowfall		Difference	Average difference	Snowfall		Difference	Average difference				
	obs.	MEPS			obs.	MEPS						
	[mm]	[%]		[%]	[mm]	[%]		[%]				
21 Dec	0.7	5.1	+626.1			17.1	18.5	+8.3				
22 Dec	13.6	13.4	-1.6	+1.3	+134.7	25.6	31.3	+22.2	+10.8	+32.6	+54.4	
23 Dec	6.3	6.6	+4.2			23.3	23.7	+1.8				
24 Dec	14.7	17.7	+20.4			24.8	35.9	+44.8				
25 Dec	4.3	6.7	+55.1	+59.8		15.4	23.3	+50.8				
26 Dec	8.8	17.9	+104.0			25.1	42.1	+67.5				

correctly compared to the double fence, but estimates a too high surface accumulation. Table 4.2.3 shows the difference between the observations and ensemble mean MEPS forecast for 12 h and 24 h accumulation. As seen in Table 4.2.3, the average difference error decreases with longer forecast time. For 21 to 26 December 2016 the average difference error is +134.7 %. For longer lead times, 24 h, the average difference error is reduced to +32.6 %. Generally the forecast accuracy decreases with lead time [Kalnay, 2003]. On 21 December 2016 very large difference error (626.1 %) is shown. This error is related to the small precipitation amount (0.7 mm) observations at Haukeliseter, which is a known difficulty for precipitation forecasts [Müller et al., 2017]. The daily percent difference show to be high for the last three days of the 2016 Christmas extreme event.

The largest overestimation of MEPS forecast for precipitation amount is seen in Table 4.2.3 on 26 December 2016 with +104 % for 12 h. This shows the highest overestimation for the three days (24 to 26 December 2016).

In Figure 4.1.4 show the ensemble member a balanced bias from 21 to 23 December 2016. The bias for 24 to 26 December 2016 is wet, also showing the overestimation of surface accumulation. In Figure 4.1.5e, the mean absolute error is less than 7 mm for 21 to 23 December 2016 and increases with intensification of the storm up to 14 mm on 26 December 2016. The mean absolute error in Figure 4.1.5e for 12 h precipitation is less than 7 mm on 25 December 2016, similar to 21 to 23 December 2016.

Since MEPS performance was better on 21 to 23 December 2016 one might assume that the double fence measurement is influenced by surface winds. Wolff, [unpublished] states that the double fence gauge is influenced by wind, and that the double fence gauge underestimates precipitation accumulation within 10 % for winds up to 9 m s^{-1} . A relation between high wind and double fence observation could be possible. Table 4.2.4 presents the percentage difference between the double fence and MEPS forecasts under the condition that the double fence is affected by wind with a catch-ratio less than 10 %. Here, it also shows an increase in forecast accuracy for precipitation

Table 4.2.4: Same as Table 4.2.3, just for an under-catchment of 10 % difference by the double fence gauge.

Day in 2016	12 h accumulation					24 h accumulation				
	Snowfall		Difference	Average		Snowfall		Difference	Average	
	obs.	MEPS		difference	obs.	MEPS	difference			
	[mm]		[%]		[%]		[mm]		[%]	
21 Dec	0.8	5.1	+553.5		+111.2	19.0	18.5	-2.5	+39.0	+19.3
22 Dec	15.1	13.4	-11.4			28.4	31.3	+9.9		
23 Dec	7.0	6.6	-6.2			25.9	23.7	-8.4		
24 Dec	16.3	17.7	+8.4			27.6	35.9	+30.3		
25 Dec	4.8	6.7	+39.6			17.1	23.3	+35.8		
26 Dec	9.8	17.9	+83.6			27.9	42.1	+50.8		

accumulation over 24 h. The average difference is reduced by 23.5 % for 12 h accumulation. Assuming an accumulation underestimation of 10 % would lead to a reduction of overestimation to 43.8 % for 12 h during 24 to 26 December 2016 (Table 4.2.4). This shows, even though a 10 % under-catchment of the double fence gauge was present, MEPS would overestimate the surface accumulation (12 h: +43.8 %; 24 h: +39 %).

On 24, 25, and 26 December 2016 winds between 5 m s^{-1} and 20 m s^{-1} were observed (Figure 4.1.1n, x, ??). The accumulation after 12 h lead time in Table 4.2.4 indicate if wind may have influenced the catchment of the double fence and effect the result of overestimation. It shows, overestimation would still be present on 25 and 26 December 2016. On the other hand, overestimation would not be present for 24 December 2016 until 12 h accumulation.

Still, an simulation of too much surface accumulation is apparent for 24 h lead time. It seems even though the double fence gauge is influenced by wind, the overestimation of surface accumulation by MEPS is still present.

In order to quantify the statistical uncertainty of the ensemble members a box-whisker plot is provided in Figure 4.2.5. The box-whisker-plots in Figure 4.2.5 show the time evolution of the distribution of the precipitation amount made of ten ensemble members up to 48 h on 24, 25, and 26 December 2016 (Figures 4.2.5a to 4.2.5c). Figure 4.2.5 provides information every 3 h, since some ensemble member do not have forecast values every hour.

All three days with overestimation seem to have different variability between the ensemble member. As expected the forecast uncertainty increases with longer forecast time for precipitation amount. Figure 4.2.5b and c show a smaller ensemble member variability on 25 and 26 December 2016 than on 24 December 2016.

Large variability is already present after 3 h prediction time in Figure 4.2.5a on 24 December 2016. The spread between the ensemble members (shown by the minimum and maximum whiskers) seems to be wide indicating a large uncertainty about the amount of surface accumulation. The ensemble mean (red line) is always higher than the median, suggesting a positively skewed distribution. After 12 h forecast time, the median is closer to the lower 25th percentile, indicating a

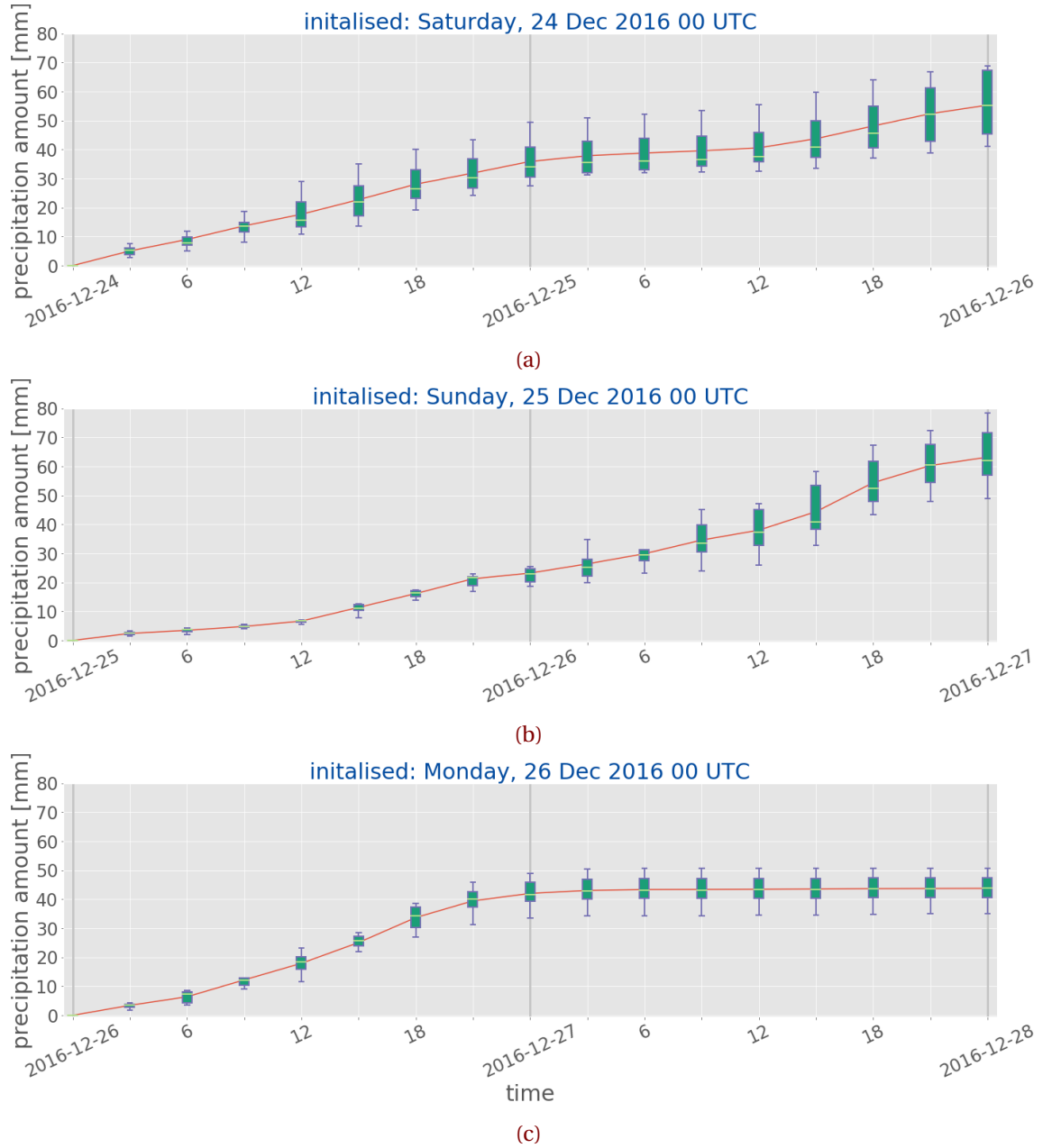


Figure 4.2.5: Box-whisker-plot in order to quantify the statistical uncertainty of the ten ensemble members of MEPS. The red line shows the ensemble mean of all ten members and if the distribution is skewed. The short light green, horizontal line is showing the median, the wide vertical box represent the 25th and 75th percentiles, and minimum and maximum values are indicated by the vertical lines, whiskers.

negative skewness. Also, all upper whiskers in Figure 4.2.5a are longer than the lower ones, which would follow that the ensemble members vary amongst the most positive quartile and that it is very similar for the least positive quartile group.

The variability on 25 December 2016 in Figure 4.2.14 show no large variation between the ensemble members (narrow box-whiskers). This day is also the forecast with the smallest wet bias of 5 mm on the three days with overestimation (Figure 4.1.4e). This may be related to the small variability between the ensemble members in Figure 4.2.5b. The variability in the forecast increases after 15 h prediction time. Median and mean agree well for the entire period of a 48 h lead time. After 39 h

the mean is much higher than the median and closer to the lower 25th percentile in Figure 4.2.5b. It seems, that all ten ensemble members agree well on the prediction and nevertheless MEPS overestimates the surface accumulation.

On 26 December 2016 the highest deviation to the double fence observations is estimated (Table 4.2.4). The precipitation amount forecast is overestimating at 12 UTC in Figure 4.2.4f. Figure 4.2.5c indicates increasing variability after 6 h, but the variability between the ensemble members is not as large as on 24 December 2016 after 12 h lead time. Nevertheless, agree the ensemble member the least about the precipitation amount at 12 UTC. The spread between the ensemble members is wide showing the uncertainty. As Figure 4.2.4f also shows is the double fence observation not within the spread of the ensemble member after 9 h lead time. According to Müller et al. [2017] strong precipitation events are better predicted with AROME-MetCoOp than with ECMWF. In Section 2.2 it was described, that during 21 to 27 December 2016 56.9 % of the total December 2016 accumulation of precipitation were observed. The extreme 2016 Christmas event follows to be a strong precipitation event. The overestimation at the surface could be related to the 10 % under-catchment by the double fence gauge under high wind condition. As Table 4.2.4 indicates the difference between the forecast system and the double fence observations is decreased, but still too much surface accumulation is estimated by MEPS. The difference for 12 h lead time on 25 and 26 December 2016 is however more than 40 %. Only a 10 % under-catchment by the double fence is assumed in this thesis. This value is approximated by Wolff, [unpublished] from measurement sites for wind speed below 9 ms^{-1} . Wolff, [unpublished] states that estimates for higher wind speeds such observed at Haukeliseter do not exist but is believed to be within 20 %. During the event the wind was less than 20 ms^{-1} and the forecast error could be reduced because of the wind related effect of the double fence.

The uncertainty of the surface accumulation might also have been related to the fact that the large-scale situation intensified more than low pressure systems in Norway usually do.

The overestimation on 24 December 2016 can be related to the high precipitation amount in the evening of 23 December 2016. The precipitation amount associated with the transition of the occluded front on 23 December 2016, after 18 UTC, is higher than on previous days (Figure 4.2.4c and Figure 3.6.1n). During 20 to 21 December 2016, the hourly precipitation around 0 UTC is less intense than on 23 December 2016 (Figure 3.6.1n). High accumulation amount over shorter time followed and could have resulted in a larger variability of the MEPS members (Figure 4.2.5). **DOUBLE CHECK THIS:** In the analysis cycle 6 h prior the initialisation of MEPS observations are included inside the model domain. Since the precipitation amount associated with the occlusion passage on 23 December 2016 was quite high, might this have led to the overestimation of surface precipitation amount.

Another possibility is MEPS might have accounted for additional accumulation around 12 UTC on 24 December 2016 than it was observed. This could show the large predicted precipitation amount in Figure 4.2.4d at 13 UTC.

On 25 December 2016 MEPS surface forecasts suggest that MEPS did not expect the occurrence of a warm front (Figures 4.1.1u to 4.1.1x). However, from the surface accumulation prediction it

could be concluded that MEPS expected more precipitation around 12 UTC on 25 December 2016. Maybe MEPS has expected a weak warm-front passage and therefore more precipitation. The fact that the temperature is rising and therefore the phase is changing from snow to liquid precipitation (Figure 4.1.3) may have led to MEPS expecting more liquid precipitation hence MEPS predicted more surface accumulation.

On 26 December 2016 between 15 UTC and 18 UTC, the core of the Christmas 2016 low-pressure system passes over Haukeliseter (Figures 4.1.1z to 4.1.1ac). Overestimation of surface accumulation are seen after 12 UTC in Figure 4.2.4f. It is very likely that overestimation on 26 December 2016 is related to passage of the low pressure system, since ensemble prediction systems are not adjusted to predict perfectly for extreme events.

Observations are used as initial condition in weather forecast systems, such as MEPS. As described in Section 2.5, should the observations be within the spread of the ensemble member prediction. Furthermore, the forecast members should be close together for a short time , which was not the case for 24 to 26 December 2016 after 12 h lead time.

Uncertainties appearing already after 3 h and 6 h on 24 and 26 December 2016 could be associated with a long spin-up time of MEPS. As described in Section 2.5, MEPS precipitation has a spin-up time of 6 h and values before that should not be used as very certain [Køltzow, 2018, private communication]. Even though this is taken into account, Figure 4.2.5 show larger variability for the ensemble members on 24 and 26 December 2016 after 6 h prediction.

As a result of poorer initial conditions the spin-up time could have been longer on 24, 25, and 26 December 2016. The spin-up time can vary due to less or also false observations going into the initialisation [Warner et al., 1997]. Longer spin-up time than the usual 6 h for precipitation can lead to larger variation from early on in Figure 4.2.5a and c than e.g. on 25 December 2016. More variability between the ensemble members does not necessarily mean, that a forecast is bad, it only shows the uncertainty of the initial conditions.

Since the box-whisker-plot in Figure 4.2.5b (25 December 2016) show less variability in the beginning it is assumed that spin-up time issues are less likely, but not totally excluded. It could be related to an error in the initialisation, even though it does not show within the variability at the beginning.

The overestimation of accumulated precipitation during 24 and 26 December 2016 might be related to local horizontal resolution of MEPS at Haukeliseter as well as to the complex development of the low-pressure system north-west of Norway on 24 December 2016.

Generally, ensemble prediction forecast systems are tuned to perform best during usual large-scale weather situations and not to present extreme events particularly well. Still, the studies from Buizza et al. [1999], Petroliagis et al. [1997] show that the ECMWF ensemble prediction can be extremely beneficial for assessing the forecast skill during extreme precipitation events.

Therefore, it is more likely that the overestimation of precipitation amount was more related to the local topography and the strong winds observed during the intensification of the extreme event. As well as the orographic representation in the regional model MEPS. Effects of the topographical

resolution on MEPS at Haukeliseter, will be further discussed in Section 4.2.5.

4.2.4 COMPARISON OF SNOW WATER CONTENT IN THE VERTICAL

Frontal boundary passages were observed at the surface several times throughout the extreme storm in December 2016. MEPS is able to predict the large scale synoptics and related surface changes for initialisation more than 24 h in advance (Section 4.1.1). In winter 2016, three additional instruments were installed to measure the vertical snow water content at Haukeliseter. This unique approach gives the opportunity to compare the forecasts of SWC with frozen precipitation observations in the vertical. As far as the author is aware of there is no study about verification of vertical ensemble member prediction models with observations.

Previous studies such as [Joos and Wernli \[2012\]](#) motivate to make accurate surface measurements more available to improve mesoscale models.

Passages of occluded fronts and a warm sector were observed on 23, 26, and 25 December 2016. Additionally, an overestimation at the ground is shown on 24, 25, and 26 December 2016 for surface precipitation amount (Section 4.2.3, Figure 4.2.4). Figure 4.2.6 shows the reflectivity from the MRR at Haukeliseter for these days. On the 26 December 2016 only values until 17 UTC are displayed, because of the temperature change and hence a precipitation shift led to liquid drops freezing on the MRR dish so that the signal got attenuated.

In Figure 4.2.6 areas with orange and red indicate likely periods with snowfall. More stable flow pattern with high reflectivity values in Figure 4.2.6 indicate the transition of the frontal boundaries on 23, 25, and 26 December 2016. On 24 December 2016 short, disturbed patterns are presented in Figure 4.2.6b. While on 23, 24, and 26 December 2016 the reflectivity did not pass values larger than 28 dBZ, Figure 4.2.6c shows high reflectivity values larger than 30 dBZ (compare for approximation Table 2.3.1). These high values indicate the observation of possible liquid precipitation. Images from the MASC were able to verify observed liquid drops during 12 UTC to 21 UTC (Figure 4.1.3). On 23 December 2016, the surface observations allow to assume that the occluded front passed through between 12 UTC and 21 UTC (Figure 4.1.1k, l, m). The observation of the lower atmosphere at Haukeliseter show high reflectivity and therefore more intense precipitation after 16 UTC (Figure 4.2.6a). After 16 UTC, the wind is from the south, upslope (Figure 4.1.1m, Figure 2.1.1c) which led to a smooth precipitation pattern in Figure 4.2.6a. In the morning of 23 December 2016 high amount of frozen precipitation was observed, but with a more disturbed pattern than in the evening.

Another occlusion passed through on 26 December 2016 shortly before 15 UTC which lasted until 21 UTC (compare surface observations Figure 4.1.1k to o). An uninterrupted precipitation pattern and high reflectivity in Figure 4.2.6d indicate the passage around 15 UTC. The high reflectivity on both days shows the passage of the occlusion and the associated frozen precipitation. Figure 4.1.1w and x indicate strong wind from the west which led to a disturbed precipitation structure in Figure 4.2.6c at 15 UTC on 25 December 2016. The orography influences the surface wind and therefore a possible relation to the precipitation will be further investigated in Section 4.2.5.

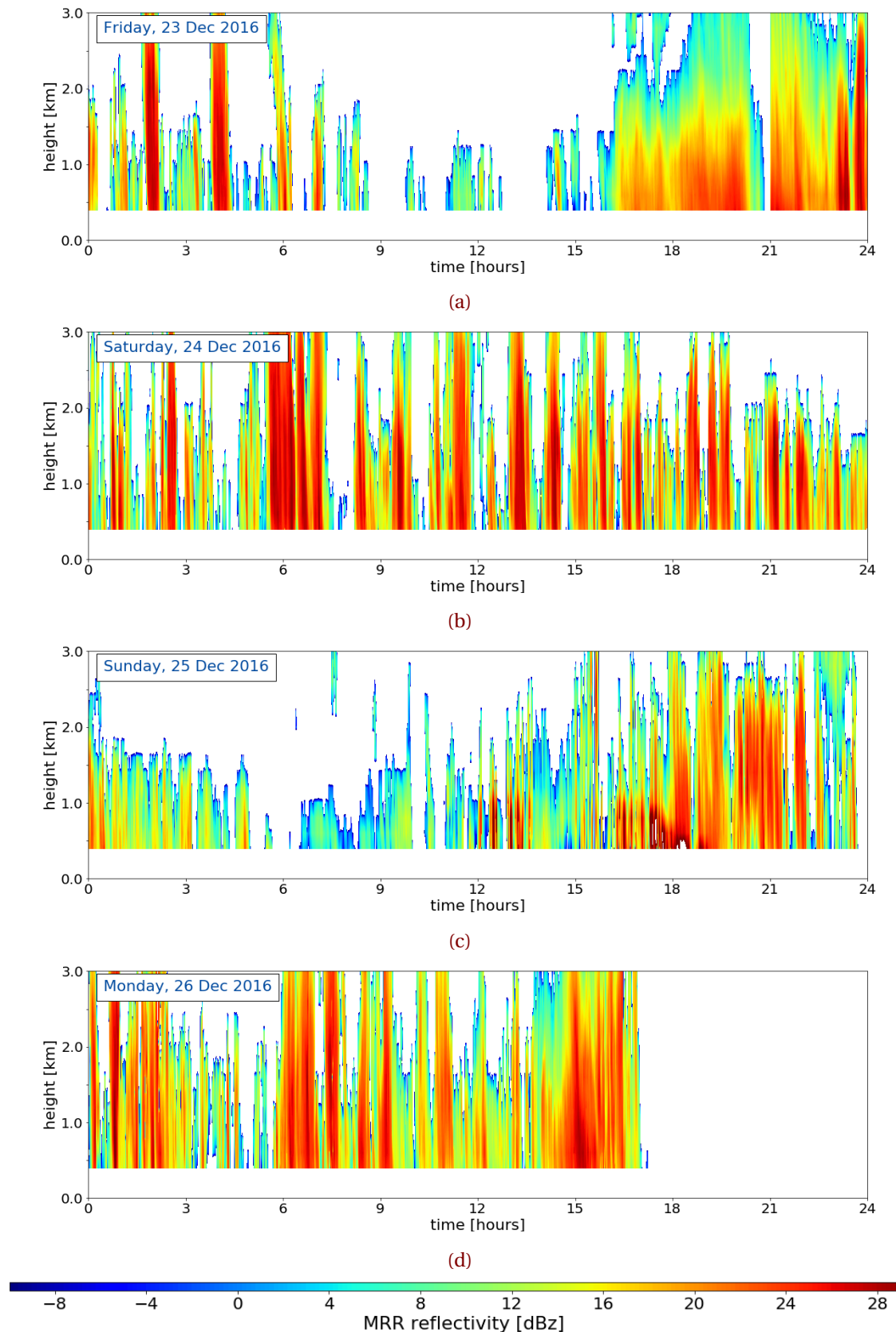


Figure 4.2.6: MRR reflectivity for the days with frontal passage and overestimation at the ground at Haukeliseter. dBZ reflectivity according to the colour bar, with weaker precipitation in blue and more intense precipitation in red. **a:** Friday, 23 December 2016, **b:** Saturday, 24 December 2016, **c:** Sunday, 25 December 2016, and **d:** Monday, 26 December 2016.

Figures 4.2.8 to 4.2.12 presents the reflectivity of the MRR and the snow water content retrieved from the reflectivity as well as the 48 h forecast values. Minutely MRR reflectivity and retrieved snow water content can be seen in Figure 4.2.8a, 4.2.9a, 4.2.11a, and 4.2.12a. Figure 4.2.8b, 4.2.9b, 4.2.11b, 4.2.12b show in the upper panel the hourly averaged values from the retrieved SWC and in the lower panel the ensemble mean of the instantaneous forecast values every hour over all ensemble member. Three hourly averaged retrieved values are then presented in the upper panel of Figure 4.2.8c, 4.2.9c, 4.2.11c, and 4.2.12c, the lower panel are the ensemble mean forecast values every three hours.

On 23 December 2016 an occlusion passes over Haukeliseter between 16 UTC to 23 UTC. The passage of the occlusion on 23 December 2016 is already predicted for initialisations on 22 December 2016 in Figure 4.2.8b, c. The predicted hourly and three hourly snow water content increases with shorter lead time in Figure 4.2.9b and c after 16 UTC. MEPS is able to estimate the snow water content for time resolutions of 3 h in Figure 4.2.8c, c.

In general, the forecasted instantaneous snow water content amount is weaker than the retrieved values for predictions on 23 December 2016. Hourly averages, only using the deterministic forecast and the first ensemble member show no occurrence of the occlusion passage on either day (??). The variation of each initialisation ensemble member is given in Figure B.2.1 for the respective day In Figure B.2.1b the prediction for the occlusion passage is quite weak for all ensemble members No data was available for first perturbed ensemble for initialisations on 23 December 2016. Averaging the the deterministic and first ensemble member forecast leads to little snow water content Figure B.1.1b). A comparison with the other days show the same result, when only the deterministic forecast and first perturbed member is used ??.

On 26 December 2016, retrieved snow water content until the passage of the occlusion is observed (Figures 4.1.1z to 4.1.1ad. The average of all ensemble members (Figure 4.2.12b) as well as the three-hourly instantaneous SWC (Figure 4.2.12c) predict the frontal transition between 15 UTC and 21 UTC. Initialisations already 39 h prior let assume that intense precipitation will occur over a short time (Figure 4.2.11b, c). The variation of all members in Figure B.2.1e and f indicate that almost all perturbed member would have predicted the precipitation around 16 UTC on 26 December 2016, but the ensemble mean weakens the result. Higher SWC is predicted by the deterministic forecast for initialisations on 25 and 26 December 2016 than for any other ensemble member (Figure B.2.1e, f). This deviation might have led to an overestimation of surface accumulation on 26 December 2016, where the deterministic forecast simulates higher values than the perturbed members (Figure 4.2.4f). In Figure B.1.1e and f the amount of snow water content is very weak. Still, the instantaneous values averaged for all ensemble members are much weaker than the retrieved SWC.

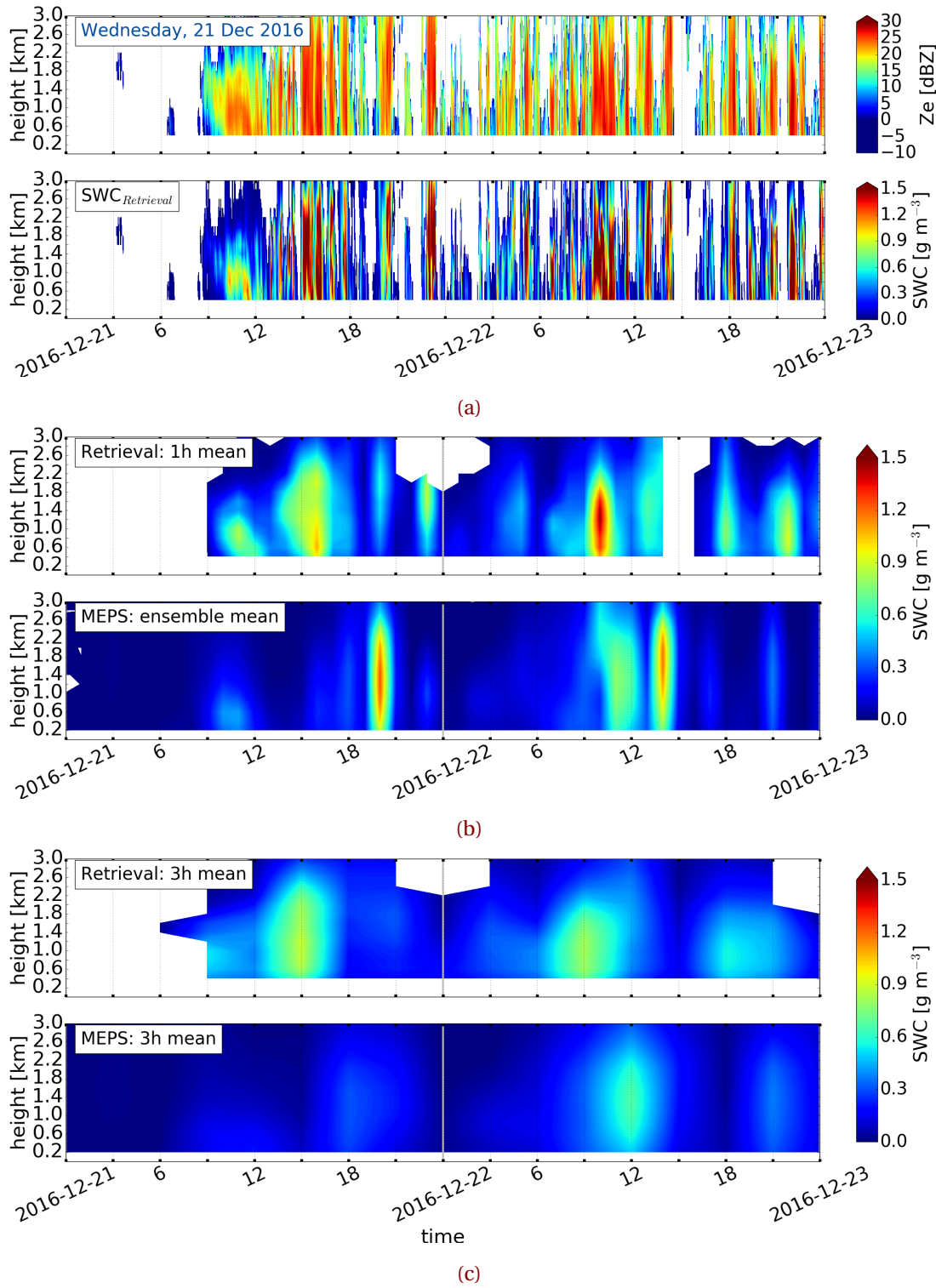


Figure 4.2.7: Initialisation on 21 December 2016 at 0 UTC. From top to bottom: (a) MRR reflectivity for 48 h, minutely retrieved SWC. (b) Hourly averaged retrieved SWC, lower panel instantaneous hourly averaged forecast of all ensemble member SWC, neglecting missing values. (c) Three hourly averaged retrieved SWC, lower panel instantaneous three hourly averaged forecast of all ensemble member SWC.

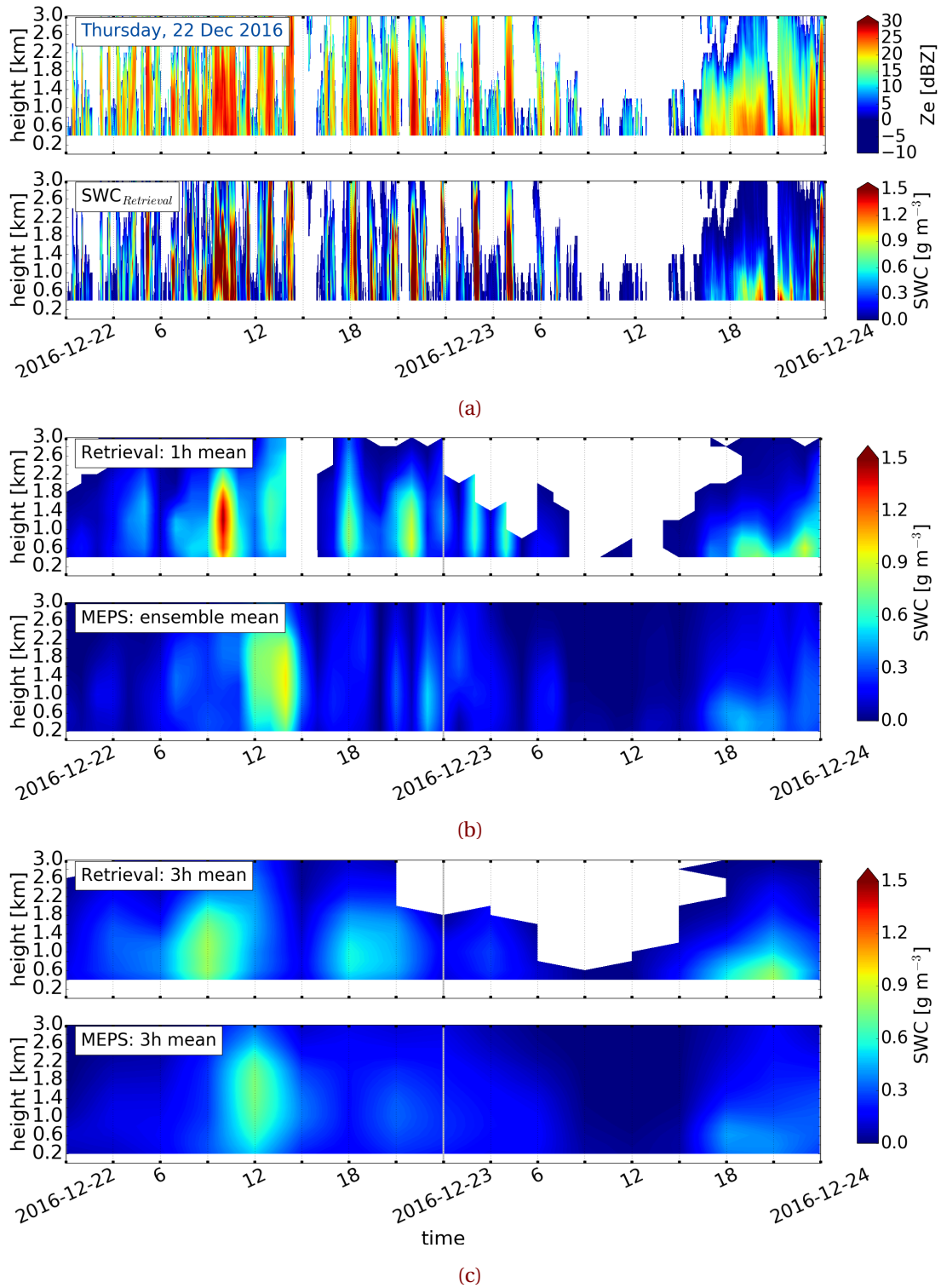


Figure 4.2.8: (As Figure 4.2.7.) Initialisation 22 December 2016 at 0 UTC.

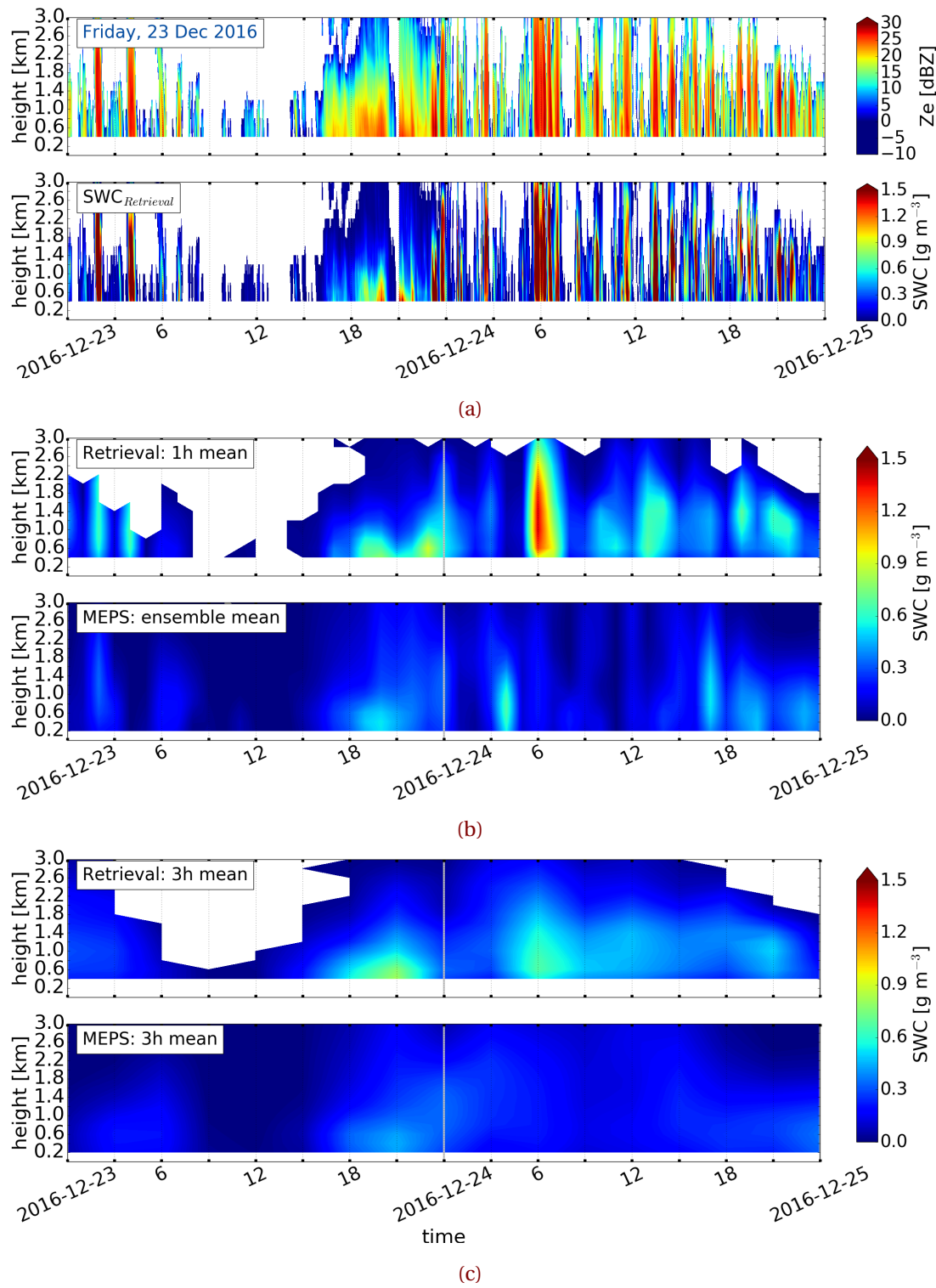


Figure 4.2.9: (As Figure 4.2.7.) Initialisation 23 December 2016 at 0 UTC.

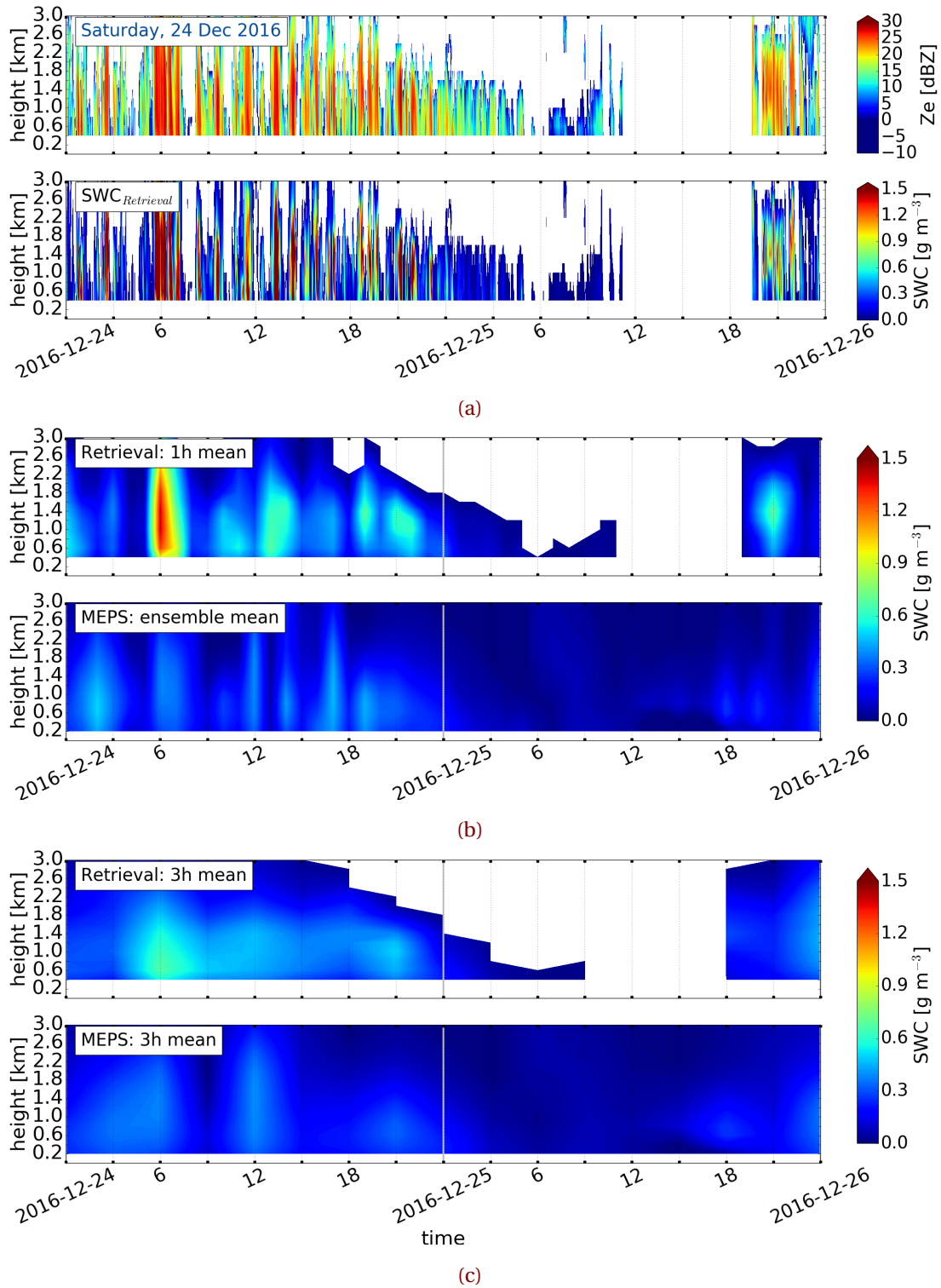


Figure 4.2.10: (As Figure 4.2.7.) Initialisation 24 December 2016 at 0 UTC.

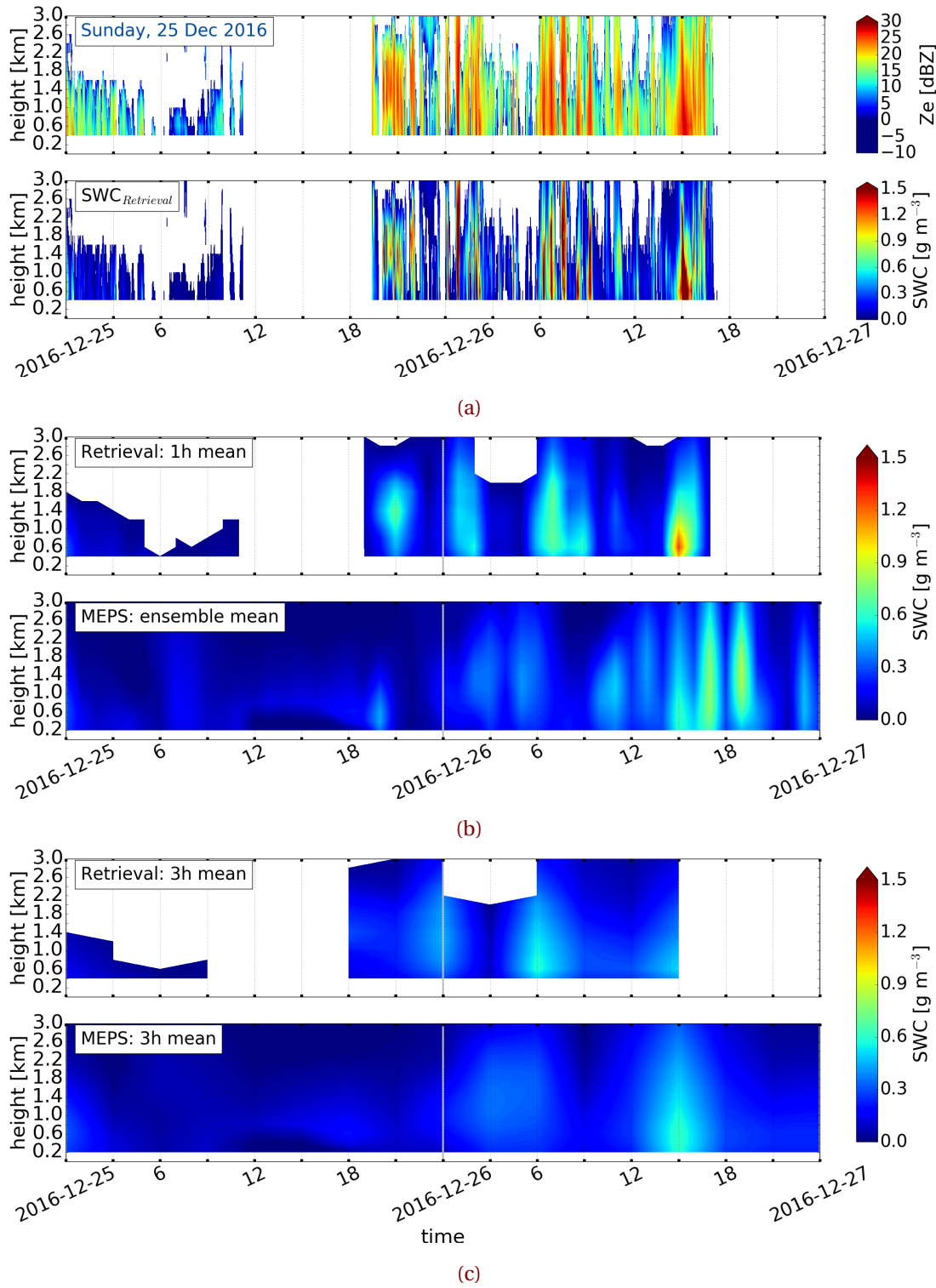


Figure 4.2.11: (As Figure 4.2.7.) Initialisation 25 December 2016 at 0 UTC.

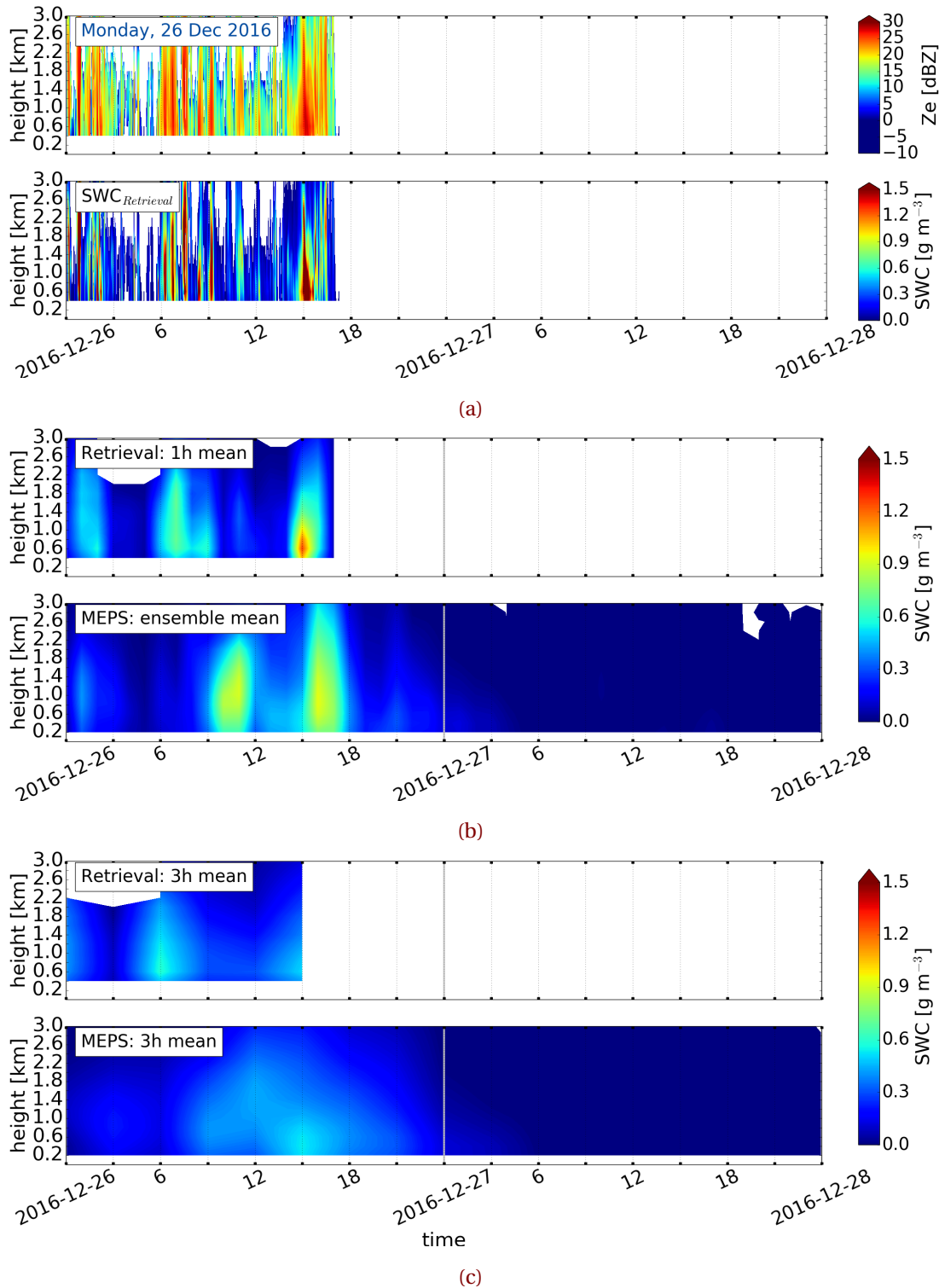


Figure 4.2.12: (As Figure 4.2.7.) Initialisation 26 December 2016 at 0 UTC.

In the observations on 25 December 2016, patterns of possible liquid precipitation (Figure 4.1.3) related to high temperatures (Figure 4.1.1v) and high reflectivity (Figure 4.2.6c) are shown, between 12 UTC to 21 UTC. High reflectivity is present around 18 UTC with layer thickness up to 1.2 km (Figure 4.2.6c). To see if liquid precipitation is predicted, the atmospheric cloud condensed water content and rainfall amount in model levels is summed (Figure 4.2.13). Figure 4.2.13a and b show

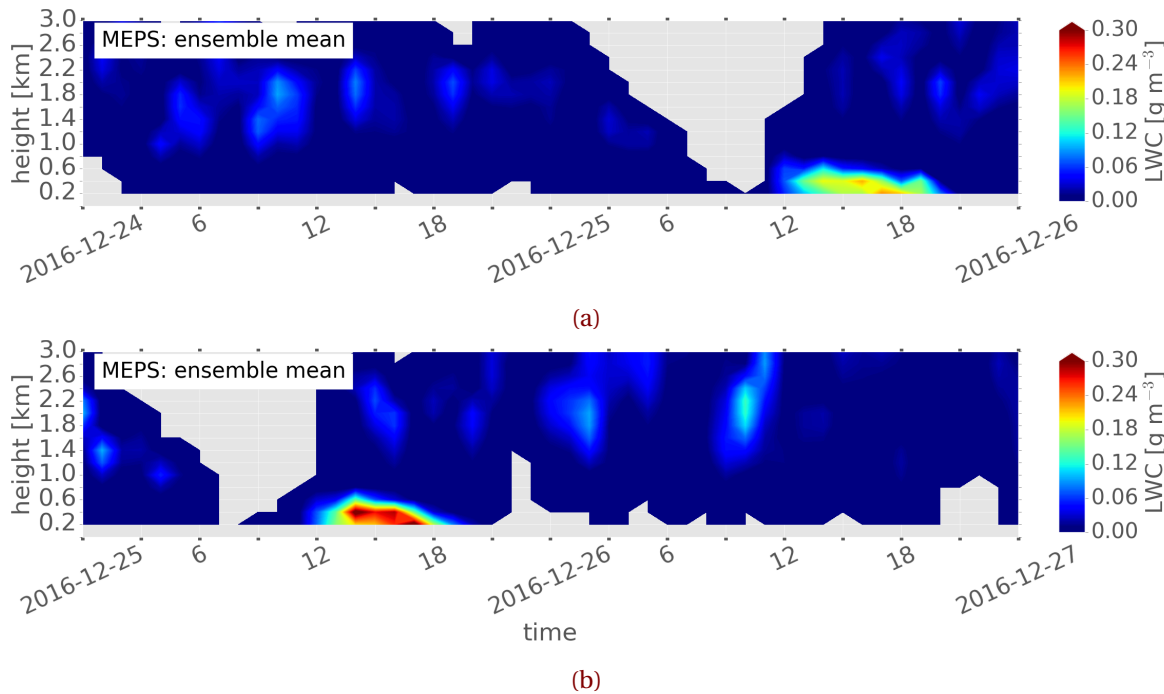


Figure 4.2.13: 200m hourly averaged LWC forecast from MEPS with all ensemble members, neglecting missing values. Initialised on 24 December 2016 and 25 December 2016 at 0 UTC. Liquid water content according to the colorbar.

liquid water content for initialisations on 24 December 2016 and 25 December 2016, respectively. Positive surface temperatures are forecasted between 12 UTC and 21 UTC (Figure 4.1.1v). Initialisations more than 24 h prior (24 December 2016) show already the occurrence of the liquid precipitation layer (Figure 4.2.13a). Figure 4.2.13a and b show also a narrow liquid layer thickness up to 800 m for initialisations on 24 and 25 December 2016.

In Norwegian mountainous terrain this is an important forecast ability, since precipitation change can lead to a high risk for people. The avalanche danger increases with the precipitation change especially during high wind speeds [Hansen et al., 2014]. Since MEPS forecasts the liquid layer correctly in thickness and duration it seems to be a good interaction between the surface model temperature and the temperature assimilation. This follows a high accuracy of MEPS and the positive impact of using a high resolution convective scheme model.

For the first glance MEPS snow water content forecast operates well when compared to observed snow water content, even though weaker ensemble mean prediction occur compared to the observations. One possibility to quantify the variability of all ensemble member is by calculating the coefficient of variation (CV) for SWC, described in Section 2.7.1. Figures 4.2.14a to 4.2.14d show the coefficient of variation for SWC and gives the possibility to compare the SWC for different days with each other.

The grey line in Figure 4.2.14 presents the ensemble mean of the hourly predicted SWC values. The darker the shading in Figure 4.2.14 the smaller the variation of the SWC relative to the mean.

MEPS data does not exist for all ten ensemble members on 23 December 2016. No coefficient of variation is calculated for this day, since only six perturbed members were available. Therefore,

Table 4.2.5: Interpretation of the coefficient of variation for SWC.

Size of CV [%]	Interpretation
	variability
0 to <25	negligible
25 to <50	low
50 to <75	moderate
75 to <100	high
100 to ∞	very high

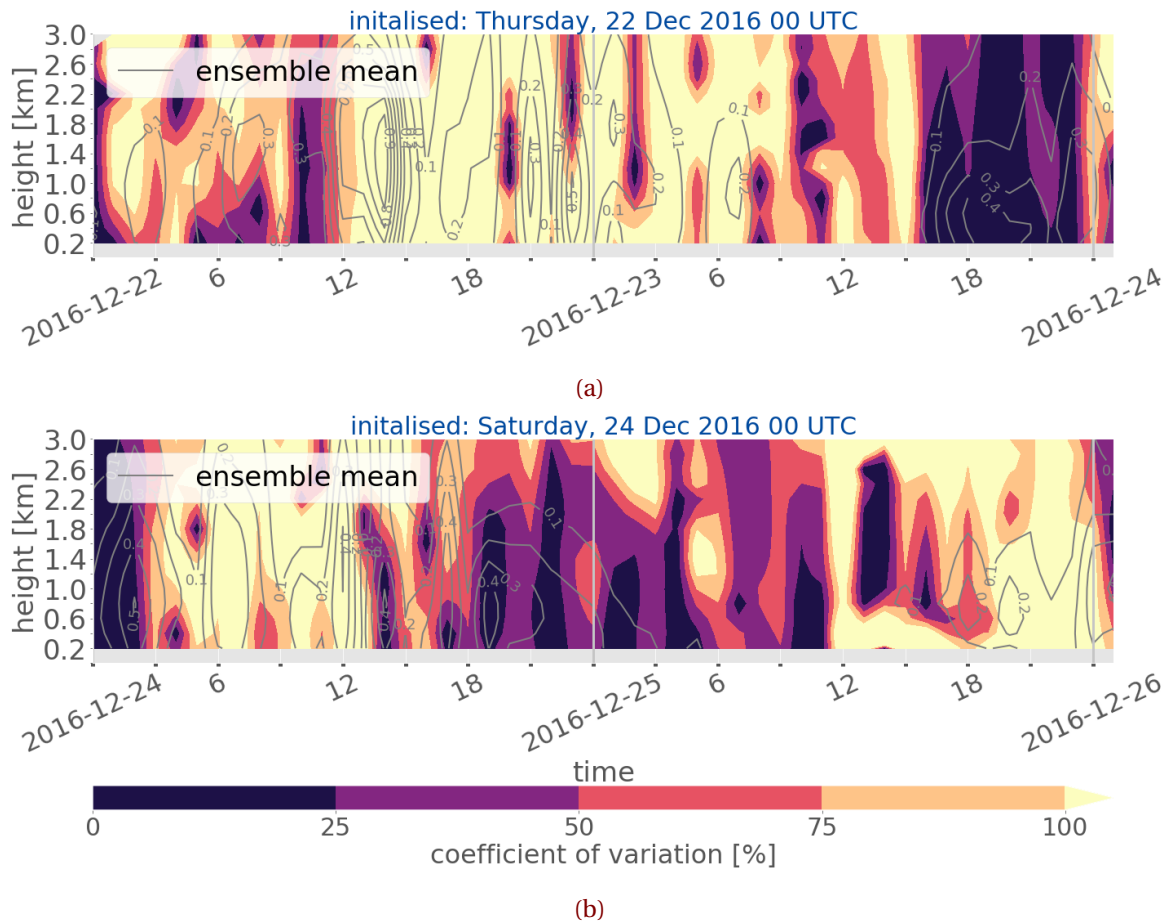


Figure 4.2.14: SWC variation of the ten ensemble members of MEPS. The lighter the colour according to the colour bar the higher the variation between the perturbed ensemble members. In grey the ensemble mean of all ten members. For initialisations on 22 and 24 December 2016. *Continued on next page.*

the initialisation on 22 December 2016 is used to validate the forecast. The interpretation of the coefficient of variation for SWC is presented in Table 4.2.5.

All ensemble members agree well with the occurrence of the up-slope storm on 23 December 2016 after 15 UTC (Figure B.2.1b). For prediction initialised on 22 December 2016 the verification in Figure 4.2.14a shows little variability below 50 % and show a good agreement on the occurrence of snow precipitation. All ten ensemble members forecast the up-slope to occur after 16 UTC,

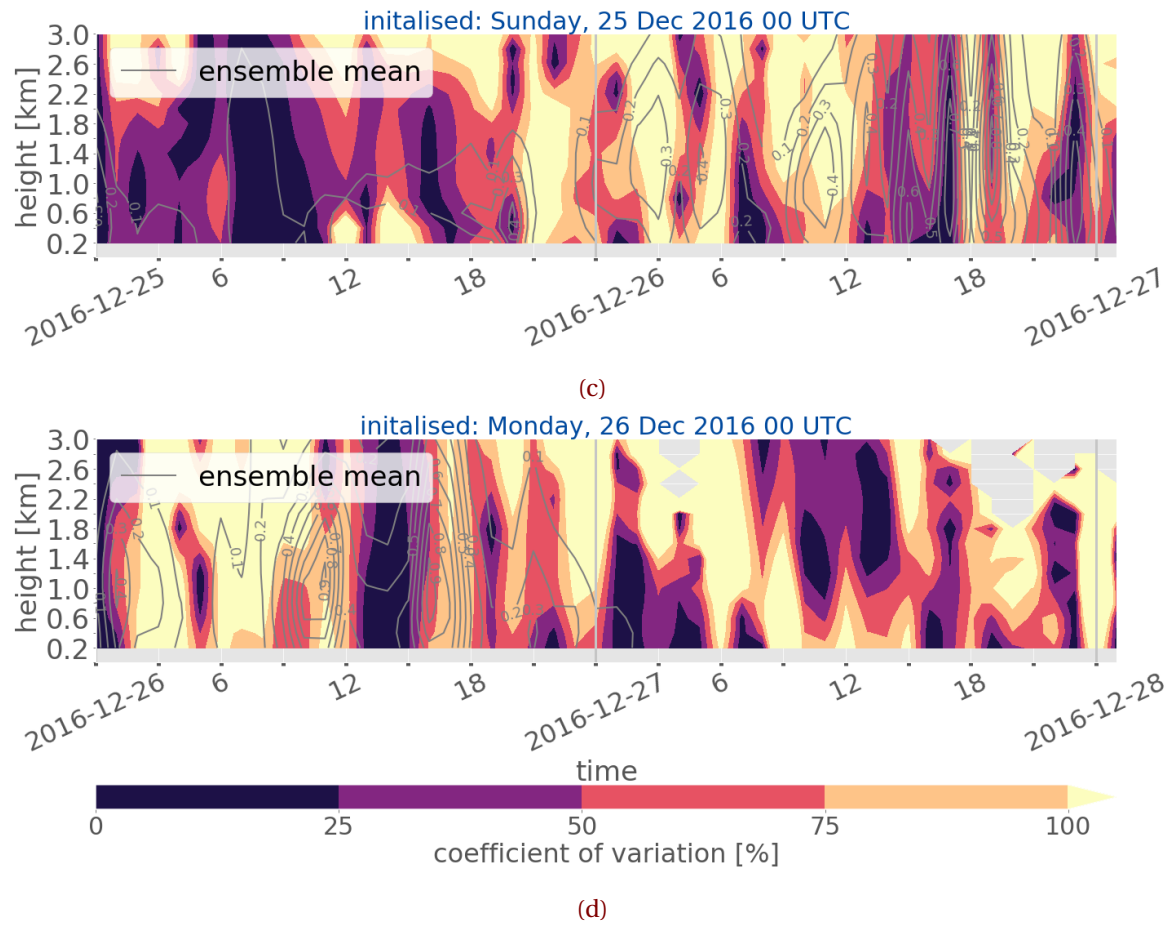


Figure 4.2.14: (Continued from previous page.) Initialisation 25 and 26 December 2016.

compare Figure B.2.1b and c. The comparison of only six ensemble members in Figure B.2.1c, let assume that the variability between all ensemble members during the up-slope storm is low, but not as certain as for an initialisation on 22 December 2016 at 0 UTC. The deterministic forecast (EM0) and ensemble member one in Figure B.2.1b indicate peaks of high SWC before 8 UTC. The retrieved SWC on 23 December 2016 had two peaks, one at around 2 UTC and another at 4 UTC. The deterministic forecast, initialised on 22 December 2016 predicted a peak at 2 UTC, 6 UTC and 8 UTC, where the first perturbed ensemble member (EM1) has a strong SWC at 7 UTC. Overall seems a combination of the deterministic and first ensemble member of the 22 December 2016 initialisation to be a good forecast when comparing to the retrieved SWC in Figure 4.2.8a, b, ??, ???. A larger variability between the ensemble members is shown for the evolution of the occlusion on 26 December 2016 in Figure 4.2.14d. In general, the 25 December 2016 was a very weak snow storm with strong liquid precipitation observed between 12 UTC and 18 UTC. Initialisations on 25 December 2016 (Figure 4.2.14c) present a lower variability for the transition after 15 UTC on 26 December 2016 than initialisations less than 24 h prior. Therefore, an increase of variability after shorter time is given rather than long lead time (48 h). Figures 4.2.10a to 4.2.10c and Figures 4.2.11a to 4.2.11c give a low value of predicted SWC in the course of a day. As Figure 4.2.14b indicates is the forecast accuracy very high up to 1.8 km until noon, this is when liquid precipitation was measured. The depth of the liquid layer was up to 0.8 km in Figure 4.2.13a and 4.2.13b. The vari-

ation coefficient (Figure 4.2.14b and 4.2.14c) has a large disagreement below 0.8 km, but above the variability is between the members not existing or low. Initialisation on 24 December 2016 show weak snow water content peak in Figure 4.2.10b and c at 18 UTC, which had a moderate variability (Table 4.2.5, Figure 4.2.14b). Afterwards it is very high. Initialisation on 25 December 2016 the forecast variability is low until noon (Figure 4.2.14c). While liquid precipitation was monitored the variability in the lower layer is first very high and shortly before 18 UTC not existing. A high agreement for the SWC peak at 20 UTC up to 0.8 km exists in Figure 4.2.14c and decreases to be moderate above.

Figure 4.2.11b and c would suggest a continues pulsing of the storm. The two peaks around 18 UTC (Figure 4.2.11b) are predicted with a negligible and moderate variability in ???. The SWC peaks at around 3 UTC and 5 UTC show a very high variability. Figure B.2.1e displays that four out of ten ensemble members would agree with the peaked event around 5 UTC. Whereas the peak at 3 UTC is dominated by the strong predicted SWC of the deterministic forecast, which follows the high variation in Figure 4.2.14c. Initialisation on 26 December 2016 follow that the SWC peak at 1 UTC is related to a moderate variability of the ensemble members. Low forecast accuracy is shown for the SWC between 9 UTC to 12 UTC and the one between 15 UTC to 18 UTC has a low to moderate variability between the members. When looking at Figure B.2.1f might this disagreement be related to the colourful variation of the vertical predicted SWC. There seems to be no agreement between the different members about the incidence of the SWC peaks. The high conflict for the CV before noon is most likely related to the high SWC of the deterministic SWC.

Again, this is not a fair comparison since hourly instantaneous values are used and there might be a time delay of half an hour about the development of boundaries which would follow it is not seen in the model forecast.

One question to answer in this work is, if the operational model MEPS simulates large scale correctly. As discussed here and in Section 4.1.1 it seems that the model is able to resolve the development of large scale and its associated precipitation. Even with the intensification of the Christmas 2016 storm MEPS seem to be able to predict extreme events for vertical snowfall such as occlusions and liquid precipitation related to warm fronts. MEPS might have some issues predicting surface precipitation amount and wind speed.

MEPS also distinguishes realistically between liquid and solid precipitation in strength and duration for the lower most atmosphere in mountainous terrain in Norway like Haukeliseter. This can be a major challenge since a change in temperature and associated precipitation transformation can lead to high risk in the Norwegian mountains, especially during winter.

The here presented results are a first look, trying to compare a mesoscale ensemble member forecast system (MEPS) with vertical in-situ measurement for snowfall.

The next section will go into detail, how the local orography at Haukeliseter may influence frozen precipitation, and how MEPS's representation of the topography may affect it.

4.2.5 DISCUSSION

The Haukeliseter site is suspended to high wind speeds during the winter. The previous results in Section 4.1.1, 4.2.3, 4.2.4 have shown, that wind plays an important role for the precipitation at Haukeliseter. The mountain plateau is surrounded by higher mountains to the west and more open to the south east (Figure 4.2.15a). This orography seems to influence the vertical precipitation pattern. The correlation between wind speed observations and forecast show an overestimation of predicted wind speed throughout the event (Figure 4.1.1d, n, x and ac). Müller et al. [2017] already mentioned the weakness of too strong wind prediction in AROME-MetCoOp, the previous operational deterministic version of MEPS.

Figure 4.2.15b shows the MEPS resolution and its 2.5 km grid cells around the Haukeliseter site. The complex terrain and its representation in MEPS might have followed the overestimation of accumulation. In this thesis the closest grid point to the Haukeliseter measurement site is used. Alternatively, the use of an average of the grid points surrounding the Haukeliseter site could lead to a solution that is closer to the truth and must be evaluated further.

On 21 and 23 December 2016 wind directions from the south-east and south were observed, respectively. As earlier discussed in Section 4.1.1 and 4.2.4 the wind change is associated with the occlusion passage on 23 December 2016 (Figure 3.6.1j and 3.6.1l). The wind direction on 21 December 2016 in Figure 4.1.1c change was also related to the large scale synoptic flow but is not associated to a frontal boundary. A comparison with the large scale weather analysis from ECMWF shows, that the large scale surface wind is from the south-west at 6 UTC on 21 December 2016 (not shown) and has changed to west at 12 UTC (Figure 3.6.1d). The observations at the Haukeliseter site show between 6 UTC and 12 UTC wind from south-east, while the predicted wind direction is from south in Figure 4.1.1c. The local wind direction influenced the precipitation pattern in the vertical on 21 and 23 December 2016, in the matter that a more consistent storm structure was observed and predicted between 9 UTC to 12 UTC (Figures 4.2.7a to 4.2.7c).

Both days show a more consistent storm structure with not as intense snow water content than for storm patterns from the west such as on 24 December 2016 (Figures 4.2.10a to 4.2.10c). Figure 4.2.15a presents the local topography around Haukeliseter and Figure 4.2.15b shows the topography resolved by MEPS. MEPS is able to cover some of the complex structure around the site (Figure 4.2.15b), with the higher mountain to the west and the valley to the south-east (Figure 4.2.15a). The forecast model seems to forecast the wind direction overall well, only on 21 December 2016 before 10 UTC is a south-west instead of a south-east wind predicted. It displays that even if the large scale wind is from the south-west the local wind is rather from the south or south-east (Figure 3.6.1d).

Figure 4.1.2f shows a good correlation for west winds, but on the other side, southerly winds seem to be troublesome to predict for MEPS. Figure 4.1.2e indicates an unbalance for south-westerly winds. While south-easterly winds (along the valley) are observed at Haukeliseter predicts MEPS the 10 m wind to be south-westerly.

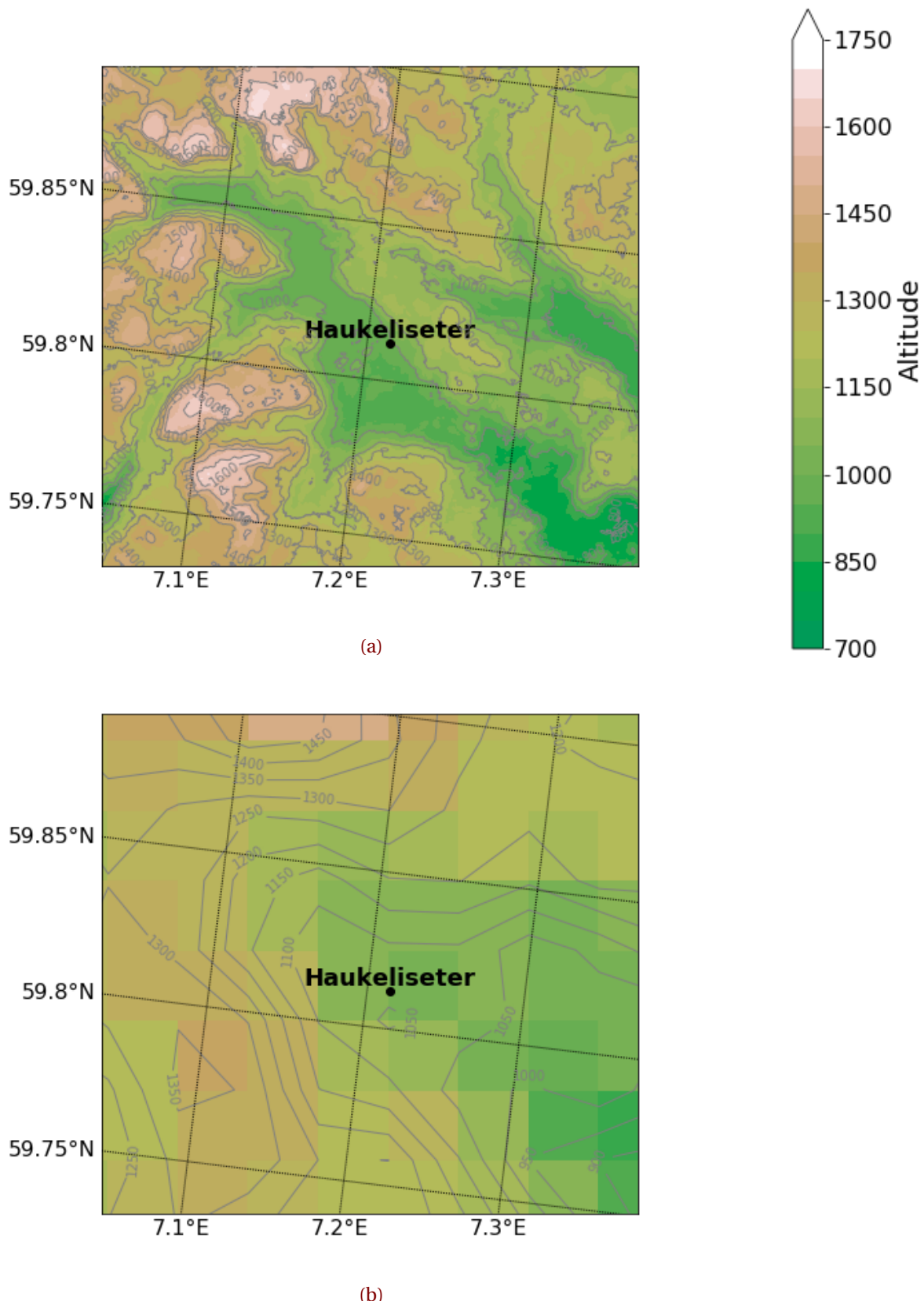


Figure 4.2.15: Topography around Haukeliseter. In **a** the DTM 10 Terrain Model (UTM33) from [Geonorge \[2018\]](#). Contours and shading according to the colorbar. **b:** Representation of the topography around the measurement site Haukeliseter in MEPS. Contours and shading present the elevation of the grid cells.

Figure 4.2.15 shows the comparison between the orography and the resolved topography by MEPS. Observed south-easterly winds are forced along the valley, directed in south-east. MEPS resolves it in the way, that the wind is south-westerly. Figure 4.2.15b displays a high mountain to the west of the station and a small one to the south. 10 m wind predicted by MEPS is predicted to blow between these two elevations.

As Figure 4.2.7b indicates is the model able to cover almost the exact timing of the up-slope storm pattern. The variability of each ensemble member is presented in Figure B.2.1a. It shows that almost all ensemble member agree on the occurrence of the storm pattern during 9 UTC to 12 UTC.

Wind from the west and therefore over high mountains (1500 m) always follow a pulsing with more intense vertical precipitation e.g. on 24 December 2016, Figure 4.2.10a and 4.2.11a). This effect might be related to wave breaking at the mountain and result into a pulsing precipitation pattern. More precipitation events need to be studied to understand this effect around the Haukeliseter site. MEPS does not cover all pulses related to west wind during the course of a day. This is related to the short occurrence of the pulses as well as to the time resolution of the forecast values. Since the prediction values exist only every hour the model might miss some of the high pulses 30 min before or after the frozen precipitation.

One outcome of the presented study is that MEPS is able to resolve the local topography and predicts the wind direction correctly. The variability between the ensemble members is smaller for precipitation related to south-easterly winds (Figure 4.2.14a, c, d). It did not cover the south-east wind direction on 21 December 2016 (Figure 4.1.1c), which must be related to the local topography. It seems more intuitive for the model to force large scale south-westerly flow into south direction rather than the observed wind direction along the south-easterly directed valley. As seen in Figure 4.2.15 the wind must go along the 7.2° longitude, since a higher (1500 m to 1650 m) elevation is to the west and a 1350 m high mountain to the east. True prediction of wind direction leads to the correct estimation of frozen precipitation patterns, such as up-slope (south-easterly wind) and pulsing (west wind).

Section 4.2.3 describes the overestimation of surface snow accumulation during the intensification of the extreme storm. MEPS forecast in Figure 4.2.4d, e, and f show more ground accumulation than it is observed for 24 to 26 December 2016. One approach was to see, if the wind might have had an influence on the surface measurement of the double fence, which did not show to be true, even if 10 % under-catch by the double fence gauge is assumed (Table 4.2.4). A comparison of the hourly values of MEPS, show neither on 24 nor on 25 nor 26 December 2016 high vertical snow amount compared to the estimated SWC (Figure 4.2.10b, 4.2.11b, and b). Figure B.2.1 shows values of very intense instantaneous snow water content for individual ensemble members, but no prominent sign of overestimation when the surface miscalculation was present.

During 24 to 26 December 2016 the wind was constantly from the west with higher wind speeds

observed than during 21 to 23 December 2016 (Figure 4.1.1). Figure 4.1.2e and f indicate a better correlation for the forecasted and observed wind directions when precipitation overestimation occurred (24 to 26 December 2016). During 24 and 26 December 2016, observed wind speeds were higher up to 18 m s^{-1} than on the previous days. As Figure 4.1.2g and h present is the correlation between observation and forecasts lower for high wind speeds. The high wind speeds from the west followed a pulsing storm pattern with changing intense and less intense snowfall (e.g. 22 and 24 December 2016, Figures 4.2.8a to 4.2.8c, a, b, c). MEPS is able to forecast the pulsing pattern for initialisations longer than 24 h prior. Since the model estimates the wind direction correctly for west wind and local mountain affects it follows that there seems to be an interaction issue between frozen precipitation and the surface accumulation. Hourly vertical instantaneous values could have led to a misinterpretation of the here presented results. Furthermore, this study presents only a first look for a comparison between observations up to 3 km of precipitation to MEPS forecast for an extreme event.

The ensemble variability in Figure 4.2.14 show that the ensemble members are divided about the existence of the exact precipitation pulsing.

While the wind direction of MEPS has a good agreement, at least for west wind, shows the wind speed larger values over all days (Figures 4.1.2e to 4.1.2h). Although MEPS includes ten perturbed ensemble members the insufficiency of AROME-MetCoOp too high wind prediction in extreme situations is not resolved. As Müller et al. [2017] mentioned are higher wind speeds in general better forecasted in AROME-MetCoOp than in ECMWF, which is an advantage for small scale forecast models. Especially in Norway, where the topography changes from sea to mountains.

CHAPTER 5: SUMMARY AND OUTLOOK

In this thesis, a case study of an extreme event for snowfall occurring on 21 to 26 December 2016 has been explored. The extreme weather event 'Urd' affected large parts of Eastern, Southern, and Western Norway. During this period the first low-pressure system developed east of Iceland, and the second cyclone evolved in the western Atlantic. Temperature changes related to the cold and warm fronts, and warm sectors followed observed precipitation changes from snow to liquid at Haukeliseter.

A sensitivity study of retrieved snow accumulation for different a-priori assumptions was carried out. Snowfall comparisons between double fence gauge observations and MEPS forecast of precipitation amounts have been investigated at the WMO measurement site Haukeliseter. Meteorological parameters have been evaluated to see if large scale phenomena such as occlusion passages were observed and predicted by MEPS. Furthermore, a vertical comparison between retrieved profiles of snow water content is compared to 48 h forecasts of MEPS. Wind related topographical influence on precipitation and the horizontal resolution of MEPS were examined.

Double fence gauge measurements are considered as one of the best surface measurements for snowfall. During winter 2016/2017 additional instruments such as a MRR, MASC and PIP were installed at Haukeliseter. A state of the art optimal estimation snowfall retrieval allowed to compare surface observations to vertically retrieved snowfall amounts. Assumptions of a particle model for rimed aggregates, climatological particle size distributions and fall speeds followed the best estimate for surface snowfall accumulation compared to the use of the CloudSat PSD estimate at Haukeliseter. The difference between retrieved snowfall amount and double fence was not larger than -5% for 12 h and 24 h snowfall accumulation. The small difference between observation and estimated snowfall shows the importance to choose a priori assumptions correctly to achieve reasonable surface estimates of precipitation amount at the ground.

AROME-MetCoOp was operational until November 2016 when it got substituted by the ensemble prediction weather forecast system at the Norwegian Meteorological Institute. The change from a deterministic forecast to an ensemble prediction system will help to take into account measurement uncertainties. Since MEPS has just become operational, an unique opportunity is given to do first comparisons between observations at the WMO station Haukeliseter, the additional installed instruments, and the weather forecast model for the Christmas storm. The closest model grid point to the measurement site Haukeliseter was chosen to answer the research question if MEPS is able to predict large-scale phenomena such as occlusions related to an extreme event. It turns out that the regional forecast model MEPS is capable of predicting changes associated to frontal passages and occlusions. Pressure, temperature, and wind changes associated with transitions of fronts

were predicted 24 h and 48 h in advance. The correlation between surface observations at the site and the weather forecast model were best for sea level pressure prediction. The mean absolute error for 2 m temperature was never larger than 1 K, but a warm temperature bias occurred on 24 December 2016. **Include in results? Or double check** During the extreme Christmas storm in 2016, overestimation of wind speed and precipitation accumulation at the surface were predicted by MEPS.

In the meteorological analysis an overestimation of surface precipitation accumulation up to 60 % shows during the intensification of the Christmas 2016 event, hence in detail analysed. The average difference between precipitation amount at the surface decreases with increasing lead time for 21 to 26 December 2016. The 12 h precipitation accumulation had a mean absolute error up to 15 mm which is more than eight times larger than the Norwegian mean for AROME-MetCoOp of December 2014.

Forecasted surface precipitation accumulation comparison of the wind influenced under-catchment by the double fence of 10 % showed a smaller difference error. Nevertheless, the surface accumulation was overestimated by more than 40 %. Reasons for the prediction of too much precipitation accumulation at the ground could be initialisation errors as well as the use of one grid point instead of using a variable average of surrounding grid points. The results show that MEPS is not able to predict the precipitation correctly during the Christmas 2016 extreme event.

The vertical snowfall measurements can be trusted after it was shown that the retrieved estimated snowfall at the surface is in good agreement with those observed at the double fence gauge.

The one and three hourly ensemble means of MEPS displayed the ability to predict more consistent, up-slope snow storm patterns. For this type of storm the ensemble variability for initialisations 24 h and 48 h prior storm occurrence was low. MEPS ensemble members were uncertain about the appearance of snowfall pulsing patterns related to westerlies. Greater variability between the ensemble members for pulsing storm patterns is probably related to the temporal resolution of MEPS ensemble forecast data and the short appearance of the pulses of around 30 min.

In general, the estimated snow water content from MRR profiles is greater than the instantaneous average prediction of snowfall. The deterministic and first ensemble member (1 h resolution) predicted high snow water content on some days during the 2016 Christmas storm.

On 25 December 2016, MASC images could verify the presence of liquid precipitation during the passage of a warm sector at Haukeliseter. MEPS was able to estimate the episode of liquid precipitation 24 h and 48 h in advance. Vertical comparison between reflectivity profiles and modelled liquid water content did show the prediction of liquid precipitation, both in time and layer thickness. This is an important advantage of a regional weather forecast model, as the change from snowfall to liquid precipitation poses a great risk in Norwegian mountains.

Although MEPS has a horizontal resolution of 2.5km, the representation of the mountainous terrain in Norway might still be an issue. MEPS is able to resolve some of the major orographic patterns, such as high mountains to the west and the south-east of Haukeliseter. Westerlies and their associated pulsing precipitation pattern were correctly predicted by MEPS but the ensemble members showed a large variability about the existence of this storm patterns. Forecasts for westerlies during

24 and 26 December 2016 showed a good correlation. In contrast, observed south-east winds were often predicted to be south-westerly wind (not along the mountain valley, south-east) during 21 and 23 December 2016. Nevertheless, MEPS is able to relate southerly winds with up-slope patterns of precipitation.

This study demonstrates the complex interaction of analysing snowfall extreme events with observations, and regional model prediction. The here presented results are a first look for only one extreme storm at one station and further studies have to be done.

5.1 OUTLOOK

Only a few studies have addressed similar approaches like the comparison of vertical snowfall prediction to observations, and thus comparison with other work is difficult. Hence, the presented results motivate to deal more with the subject of vertical snowfall observations and its comparison to regional weather forecast models.

First and foremost it is important to investigate more extreme snowfall events during winter at Haukeliseter, whether deviations between surface accumulation and estimated precipitation amount from vertical observations keep as small. Furthermore, these results should be compared to different stations in Norway with similar polar tundra climate, to find if a-priori assumptions can be generalised for the same local climate.

More study cases will also help to get a better estimate about the performance of MEPS for snowfall prediction during extreme storm events during winter. The mean absolute error for the 12 h accumulation of precipitation revealed large variability depending on the initialisation time of MEPS and the low cyclone getting more extreme. The presented increase in mean absolute error with intensification might be low compared to other cases.

The previous chapters have indicated that the regional model MEPS is able to predict larger scale phenomena. This might be related to the outer boundary condition ECMWF or the Christmas 2016 extreme event was more predictable for large scale phenomena. In general, surface parameters such as sea level pressure and temperature were predicted well in MEPS. only wind speed and precipitation accumulation showed overestimation in MEPS predictions. Wind speed forecasts were higher than observed wind speed. Related to the representation of the orography in MEPS the general overestimation of wind speed could already be apparent in the deterministic version AROME-MetCoOp.

Sensitivity studies for the outer boundary could help to understand how the influence of ECMWF forecast on the MEPS predictions for local meteorological effects. ECMWF as boundary condition might not have reached its background climate state when MEPS was initiated during the event. This could also have contributed to the overestimation of wind speed and surface accumulation. A comparison between ECMWF forecast and MEPS will verify if this might be the case. Re-analysis data can help to show the uncertainty in the initial and boundary conditions. A re-run with analysis data from ECMWF could possibly improve the original forecast. It will be interesting to initiate

MEPS with new boundary conditions from ECMWF. Even though meteorological observations are transmitted to ECMWF at the meteorological observation times, not all observations will be communicated in time for the initialisation. An initialisation now with all available observations inside ECMWF will help to see an influence on the overestimation of wind and precipitation accumulation.

Another approach could be to perturb the deterministic forecast in another way. Different perturbations might lead to a better correlation between observation and MEPS forecast at the ground. Furthermore, the choice of using the closest grid point to Haukeliseter might not have been the best approach. Using four nearby grid points instead of only one could help to verify if overestimations of MEPS forecasts would still be present compared to observations.

Even though MEPS performed well in the vertical by relating the wind to the storm structure correctly, it will be interesting to investigate the presented results with a higher time resolution to resolve for the short pulses. Since MEPS overestimates the surface accumulation and the vertical SWC of ensemble means show to be in general smaller than the estimated snow water content, the afore mentioned solution helps to investigate the overestimation of snowfall at the surface and the relationship between the vertical forecast and surface prediction model.

The local effect of pulsing patterns related to westerlies should be examined. To understand if e.g. wave breaking occurs at the mountain to the west or if it is an effect of local surface fronts.

It is important to have correct measurements such as the double fence gauge or the MRR-PSD retrieval approaches. The double fence gauge observations should be investigated further to understand the wind related under-catchment of surface precipitation amount. Correct measurements will help to improve initial conditions for weather forecast models, so initialisations can start at a more true state. Furthermore accurate observations will help to get a greater understanding of vertical snowfall structure. Investigating in more detail microphysical processes within mesoscale storms with vertical measurements of snowfall for extreme events can be a grand improvement for weather and climate prediction.

Include the following:

With the forecast output more than 24 h prior can risk notice be send out to the population and rescue teams can prepare in advance. Furthermore, roads and train tracks can be closed to increase the safety.

LIST OF ABBREVIATIONS

ACC	Accretion
AGG	Aggregation
AR	Atmospheric River
AROME	Applications of Research to Operations at Mesoscale
AUT	Autoconversion
BER	Bergeron-Findeisen process
C3VP	Canadian CloudSat-CALIPSO Validation Project
CFR	Contact Freezing of Raindrops
CPR	Cloud Profiling Radar
CV	Coefficient of Variation
CVM	Conversion-melting
DDA	Discrete Dipole Approximation
DEP	Deposition
DRY	Dry processes
DT	Dynamic Tropopause
ECMWF	European Centre for Medium-Range Weather Forecasts
EPS	Ensemble Prediction System
FMI	Finnish Meteorological Institute
HEN	Heterogeneous Nucleation
HON	Homogeneous Nucleation
IVT	Integrated Vapour Transport
LWC	Liquid Water Content

MASC	Multi-Angular Snowfall Camera
MEPS	MetCoOp Ensemble Prediction System
Meso-NH	Mesoscale Non-Hydrostatic model
Met-Norway	Norwegian Meteorological Institute
MetCoOp	Meteorological Co-operation on Operational NWP
MLT	Melting
MRR	Micro Rain Radar
MSLP	Mean Sea Level Pressure
NSF	National Science Foundation
NWP	Numerical Weather Prediction
PIP	Precipitation Imaging Package
PSD	Particle Size distribution
RIM	Riming
SMHI	Swedish Meteorological and Hydrological Institute
SWC	Snow Water Content
SWP	Snow Water Path
WCB	Warm Conveyor Belt
WET	Wet processes
WMO	World Meteorological Organization

REFERENCES

- Azad, R. and Sorteberg, A. Extreme daily precipitation in coastal western Norway and the link to atmospheric rivers. *Journal of Geophysical Research: Atmospheres*, 122(4):2080–2095, January 2017. ISSN 2169-8996. doi: 10.1002/2016JD025615. URL <https://agupubs.onlinelibrary.wiley.com/doi/abs/10.1002/2016JD025615>.
- Barnett, T. P., Adam, J. C., and Lettenmaier, D. P. Potential impacts of a warming climate on water availability in snow-dominated regions. *Nature*, 438(7066):303–309, November 2005. ISSN 1476-4687. doi: 10.1038/nature04141. URL <https://www.nature.com/articles/nature04141>.
- Buizza, R., Hollingsworth, A., Lalaurette, F., and Ghelli, A. Probabilistic Predictions of Precipitation Using the ECMWF Ensemble Prediction System. *Wea. Forecasting*, 14(2):168–189, April 1999. ISSN 0882-8156. doi: 10.1175/1520-0434(1999)014<0168:PPOPUT>2.0.CO;2. URL <https://journals.ametsoc.org/doi/full/10.1175/1520-0434%281999%29014%3C0168%3APP0PUT%3E2.0.CO%3B2>.
- Caniaux, G., Redelsperger, J.-L., and Lafore, J.-P. A Numerical Study of the Stratiform Region of a Fast-Moving Squall Line. Part I: General Description and Water and Heat Budgets. *J. Atmos. Sci.*, 51(14):2046–2074, July 1994. ISSN 0022-4928. doi: 10.1175/1520-0469(1994)051<2046:ANSOTS>2.0.CO;2. URL [https://journals.ametsoc.org/doi/abs/10.1175/1520-0469\(1994\)051%3C2046:ANSOTS%3E2.0.CO;2](https://journals.ametsoc.org/doi/abs/10.1175/1520-0469(1994)051%3C2046:ANSOTS%3E2.0.CO;2).
- Christensen, M. W., Behrangi, A., L'ecuyer, T. S., Wood, N. B., Lebsack, M. D., and Stephens, G. L. Arctic Observation and Reanalysis Integrated System: A New Data Product for Validation and Climate Study. *Bull. Amer. Meteor. Soc.*, 97(6):907–916, January 2016. ISSN 0003-0007. doi: 10.1175/BAMS-D-14-00273.1. URL <https://journals.ametsoc.org/doi/10.1175/BAMS-D-14-00273.1>.
- Cooper, S. J., Wood, N. B., and L'Ecuyer, T. S. A variational technique to estimate snowfall rate from coincident radar, snowflake, and fall-speed observations. *Atmos. Meas. Tech.*, 10(7):2557–2571, July 2017. ISSN 1867-8548. doi: 10.5194/amt-10-2557-2017. URL <https://www.atmos-meas-tech.net/10/2557/2017/>.
- Dahlgren, P. A Comparison Of Two Large Scale Blending Methods. page 16, 2013. URL <http://metcoop.org/memo/2013/02-2013-METCOOP-MEMO.PDF>.
- Dando, P. Introducing the octahedral reduced Gaussian grid, June 2016. URL <https://software.ecmwf.int/wiki/display/FCST/Gaussian+grids>.
- Doviak, R. J. and Zrnic, D. S. *Doppler Radar and Weather Observations*. Courier Corporation, 1993. ISBN 978-0-486-45060-5. Google-Books-ID: ispLkPX9n2UC.

- eklma. Norwegian Meteorological Institute, 2016. URL http://sharki.oslo.dnmi.no/portal/page?_pageid=73,39035,73_39049&_dad=portal&_schema=PORTAL.
- Færaas, A., Rommetveit, A., Duesund, J., and Senel, E. «Urd» har nådd orkan styrke – flytter seg mot Østlandet, December 2016. URL http://www.yr.no/artikkelen/_urd_-har-nadd-orkan-styrke--flytter-seg-mot-ostlandet-1.13292245.
- Farestveit, E. 80.000 mista radioen under ekstremvêret, December 2016. URL <https://www.nrk.no/hordaland/80.000-mista-radioen-under-ekstremveret-1.13294980>.
- Field, C. B., Barros, V. R., Dokken, D. J., Mach, K. J., Mastrandrea, M. D., Bilir, T. E., Chatterjee, M., Ebi, K. L., Estrada, Y. O., Genova, R. C., Girma, B., Kissel, E. S., Levy, A. N., MacCracken, S., Mastrandrea, P. R., and White, L. L. Summary for policymakers. In: Climate Change 2014: Impacts, Adaptation, and Vulnerability. Part A: Global and Sectoral Aspects. Contribution of Working Group II to the Fifth Assessment Report of the Intergovernmental Panel on Climate Change. Cambridge: Cambridge University Press, page 34, 2014.
- Garrett, T. J., Fallgatter, C., Shkurko, K., and Howlett, D. Fall speed measurement and high-resolution multi-angle photography of hydrometeors in free fall. *Atmos. Meas. Tech.*, 5(11):2625–2633, November 2012. ISSN 1867-8548. doi: 10.5194/amt-5-2625-2012. URL <https://www.atmos-meas-tech.net/5/2625/2012/>.
- Geonor Inc. T-200b All Weather Precipitation – Rain Gauge, 2015. URL <http://geonor.com/live/products/weather-instruments/t-200b-weather-precipitation-rain-gauge/>.
- Geonorge. DTM 10 Terrengmodell (UTM33) - Kartverket - Kartkatalogen, May 2018. URL <https://kartkatalog.geonorge.no/metadata/uuid/dddbb667-1303-4ac5-8640-7ec04c0e3918>.
- Goodison, B. E., Louie, P. Y. T., and Yang, D. WMO Solid Precipitation Measurement Intercomparison: Final Report. Instruments and Observing Methods Rep. 67, WMO/TD-No. 872,. World Meteorological Organization, Geneva, Switzerland, page 318, 1998.
- Gowan, T. M., Steenburgh, W. J., and Schwartz, C. S. Validation of Mountain Precipitation Forecasts from the Convection-Permitting NCAR Ensemble and Operational Forecast Systems over the Western United States. *Wea. Forecasting*, 33(3):739–765, June 2018. ISSN 0882-8156, 1520-0434. doi: 10.1175/WAF-D-17-0144.1. URL <http://journals.ametsoc.org/doi/10.1175/WAF-D-17-0144.1>.
- Hansen, B. B., Isaksen, K., Benestad, R. E., Kohler, J., Pedersen, Ø. Ø., Loe, L. E., Coulson, S. J., Larsen, J. O., and Varpe, Ø. Warmer and wetter winters: characteristics and implications of an extreme weather event in the High Arctic. *Environ. Res. Lett.*, 9(11):114021, 2014. ISSN 1748-9326. doi: 10.1088/1748-9326/9/11/114021. URL <http://stacks.iop.org/1748-9326/9/i=11/a=114021>.
- Homleid, M. and Tveter, F. T. Verification of operational weather prediction models september to november 2015. *METInfo Rep.*, 16:2016, 2016. URL https://www.met.no/publikasjoner/met-info/met-info-2016/_attachment/download/b0463915-cba0-42ac-8539-4233ae2bf01c:3d71565a27f88085373199a33ab8569151c144e9/MET-info-22-2016.pdf.
- Hudak, D., Barker, H., Rodriguez, P., and Donovan, D. The Canadian CloudSat Validation Project.

- 4th ERAD, September 2006. URL <http://www.crahi.upc.edu/ERAD2006/proceedingsMask/00165.pdf>. Barcelona, Spain.
- Hurrell, J. W. Decadal Trends in the North Atlantic Oscillation: Regional Temperatures and Precipitation. *Science*, 269(5224):676–679, August 1995. ISSN 0036-8075, 1095-9203. doi: [10.1126/science.269.5224.676](https://doi.org/10.1126/science.269.5224.676). URL <http://science.sciencemag.org/content/269/5224/676>.
- Joos, H. and Wernli, H. Influence of microphysical processes on the potential vorticity development in a warm conveyor belt: a case-study with the limited-area model COSMO. *Q. J. Royal Meteorol. Soc.*, 138(663):407–418, January 2012. ISSN 00359009. doi: [10.1002/qj.934](https://doi.org/10.1002/qj.934). URL <http://doi.wiley.com/10.1002/qj.934>.
- Kalnay, E. *Atmospheric modeling, data assimilation and predictability*. Cambridge University Press, Cambridge, 2003. ISBN 978-0-521-79179-3.
- Kartverket. Norgeskart, November 2018. URL http://www.norgeskart.no/?_ga=2.7509489.291164698.1524482471-1352211079.1517515119#!?project=seeiendom&layers=1002,1015&zoom=4&lat=7197864.00&lon=396722.00.
- Kochendorfer, J., Nitu, R., Wolff, M., Mekis, E., Rasmussen, R., Baker, B., Earle, M. E., Reverdin, A., Wong, K., Smith, C. D., Yang, D., Roulet, Y.-A., Buisan, S., Laine, T., Lee, G., Aceituno, J. L. C., Alastraú, J., Isaksen, K., Meyers, T., Brækkan, R., Landolt, S., Jachcik, A., and Poikonen, A. Analysis of single-Alter-shielded and unshielded measurements of mixed and solid precipitation from WMO-SPICE. *Hydrol. Earth Syst. Sci.*, 21(7):3525–3542, July 2017. ISSN 1607-7938. doi: [10.5194/hess-21-3525-2017](https://doi.org/10.5194/hess-21-3525-2017). URL <https://www.hydrol-earth-syst-sci.net/21/3525/2017/>.
- Køltzow, M. A. Ø. Spin-up time of MEPS. Private Communication, 2018.
- Kulie, M. S. and Bennartz, R. Utilizing Spaceborne Radars to Retrieve Dry Snowfall. *J. Appl. Meteor. Climatol.*, 48(12):2564–2580, January 2009. ISSN 1558-8424. doi: [10.1175/2009JAMC2193.1](https://doi.org/10.1175/2009JAMC2193.1). URL <http://journals.ametsoc.org/doi/abs/10.1175/2009JAMC2193.1>.
- Kulie, M. S., Milani, L., Wood, N. B., Tushaus, S. A., Bennartz, R., and L'Ecuyer, T. S. A Shallow Cumuliform Snowfall Census Using Spaceborne Radar. *J. Hydrometeor.*, 17(4):1261–1279, February 2016. ISSN 1525-755X. doi: [10.1175/JHM-D-15-0123.1](https://doi.org/10.1175/JHM-D-15-0123.1). URL <https://journals.ametsoc.org/doi/abs/10.1175/JHM-D-15-0123.1>.
- Køltzow, M. A. MetCoOp EPS - A convection permitting ensemble prediction system, October 2017.
- L'Ecuyer, T. S. AOS 441 - Satellite and Radar Meteorology. January 2017. URL <https://lecuyer.aos.wisc.edu/aos441>.
- Liu G. Deriving snow cloud characteristics from CloudSat observations. *J. Geophys. Res. Atmos.*, 113(D8), September 2008. ISSN 0148-0227. doi: [10.1029/2007JD009766](https://doi.org/10.1029/2007JD009766). URL <https://agupubs.onlinelibrary.wiley.com/doi/abs/10.1029/2007JD009766>.
- Lorenz, E. N. Atmospheric Predictability as Revealed by Naturally Occurring Analogues. *J. Atmos. Sci.*, 26(4):636–646, July 1969. ISSN 0022-4928. doi: [10.1175/1520-](https://doi.org/10.1175/1520-)

- 0469(1969)26<636:APARBN>2.0.CO;2. URL <https://journals.ametsoc.org/doi/abs/10.1175/1520-0469%281969%2926%3C636%3AAPARBN%3E2.0.CO%3B2>.
- Markowski, P. and Richardson, Y. *Mesoscale Meteorology in Midlatitudes*. John Wiley & Sons, September 2011. ISBN 978-1-119-96667-8. Google-Books-ID: MDeYosfLLEYC.
- Martin, J. E. *Mid-Latitude Atmospheric Dynamics: A First Course*. Wiley, May 2006. ISBN 978-0-470-86466-1.
- McCumber, M., Tao, W.-K., Simpson, J., Penc, R., and Soong, S.-T. Comparison of Ice-Phase Microphysical Parameterization Schemes Using Numerical Simulations of Tropical Convection. *J. Appl. Meteor.*, 30(7):985–1004, July 1991. ISSN 0894-8763. doi: [10.1175/1520-0450-30.7.985](https://doi.org/10.1175/1520-0450-30.7.985). URL <https://journals.ametsoc.org/doi/abs/10.1175/1520-0450-30.7.985>.
- Meehl, G. A., Karl, T., Easterling, D. R., Changnon, S., Pielke, R., Changnon, D., Evans, J., Groisman, P. Y., Knutson, T. R., Kunkel, K. E., Mearns, L. O., Parmesan, C., Pulwarty, R., Root, T., Sylves, R. T., Whetton, P., and Zwiers, F. An Introduction to Trends in Extreme Weather and Climate Events: Observations, Socioeconomic Impacts, Terrestrial Ecological Impacts, and Model Projections. *Bull. Amer. Meteor. Soc.*, 81(3):413–416, March 2000. ISSN 0003-0007. doi: [10.1175/1520-0477\(2000\)081<0413:AITTIE>2.3.CO;2](https://doi.org/10.1175/1520-0477(2000)081<0413:AITTIE>2.3.CO;2). URL [https://journals.ametsoc.org/doi/abs/10.1175/1520-0477\(2000\)081%3C0413:AITTIE%3E2.3.CO;2](https://journals.ametsoc.org/doi/abs/10.1175/1520-0477(2000)081%3C0413:AITTIE%3E2.3.CO;2).
- MetCoOp Wiki. Description of MEPS, December 2017. URL <https://metcoop.smhi.se/dokuwiki/nwp/metcoop/>.
- METEK, M. M. G. Micro Rain Radar MRR-2, October 2010. URL <http://metek.de/wp-content/uploads/2014/05/Metek-Micro-Rain-Radar-MRR-2-Datasheet.pdf>.
- Meteo France. The Meso-NH Atmospheric Simulation System: Scientific Documentation, Part III: Physics, January 2009.
- Meteorologene. "Her kommer #Urd! Selve Lavtrykksenteret treffer Møre og Romsdal, men den sterkeste vinden kommer sør for Stad. #SørNorge" 26 December 2016, 9:34am, 2016. URL <https://twitter.com/Meteorologene>.
- Moore, R. Large-scale dynamics inducing atmospheric rivers and extreme precipitation over norway. unpublished.
- Müller, M., Homleid, M., Ivarsson, K.-I., Køltzow, M. A. Ø., Lindskog, M., Midtbø, K. H., Andrae, U., Aspelien, T., Berggren, L., Bjørge, D., Dahlgren, P., Kristiansen, J., Randriamampianina, R., Ridal, M., and Vignes, O. AROME-MetCoOp: A Nordic Convective-Scale Operational Weather Prediction Model. *Wea. Forecasting*, 32(2):609–627, January 2017. ISSN 0882-8156. doi: [10.1175/WAF-D-16-0099.1](https://doi.org/10.1175/WAF-D-16-0099.1). URL <https://journals.ametsoc.org/doi/abs/10.1175/WAF-D-16-0099.1>.
- Newman, A. J., Kucera, P. A., and Bliven, L. F. Presenting the Snowflake Video Imager (SVI). *J. Atmos. Oceanic Technol.*, 26(2):167–179, February 2009. ISSN 0739-0572. doi: [10.1175/2008JTECH1148.1](https://doi.org/10.1175/2008JTECH1148.1). URL <https://journals.ametsoc.org/doi/abs/10.1175/2008JTECH1148.1>.
- Nielsen-Gammon, J. W. A Visualization of the Global Dynamic Tropopause. *Bull. Amer. Meteor. Soc.*, 82(6):1151–1168, June 2001. ISSN 0003-0007. doi: [10.1175/1520-0469%282001%2982%3A%3D%3E2.0.CO%3B2](https://doi.org/10.1175/1520-0469%282001%2982%3A%3D%3E2.0.CO%3B2).

- 0477(2001)082<1151:AVOTGD>2.3.CO;2. URL [https://journals.ametsoc.org/doi/abs/10.1175/1520-0477\(2001\)082%3C1151:AVOTGD%3E2.3.CO;2](https://journals.ametsoc.org/doi/abs/10.1175/1520-0477(2001)082%3C1151:AVOTGD%3E2.3.CO;2).
- Noh, Y.-J., Liu, G., Seo, E.-K., Wang, J. R., and Aonashi, K. Development of a snowfall retrieval algorithm at high microwave frequencies. *J. Geophys. Res.*, 111(D22), November 2006. ISSN 2156-2202. doi: 10.1029/2005JD006826. URL <https://agupubs.onlinelibrary.wiley.com/doi/abs/10.1029/2005JD006826>.
- Norin, L., Devasthale, A., L'Ecuyer, T. S., Wood, N. B., and Smalley, M. Intercomparison of snowfall estimates derived from the CloudSat Cloud Profiling Radar and the ground-based weather radar network over Sweden. *Atmos. Meas. Tech.*, 8(12):5009–5021, December 2015. ISSN 1867-8548. doi: 10.5194/amt-8-5009-2015. URL <https://www.atmos-meas-tech.net/8/5009/2015/>.
- Norwegian Meteorological Institute. MET Norway Thredds Service, 2016. URL <http://thredds.met.no/thredds/catalog/meps25epsarchive/catalog.html>.
- Olsen, A.-M. and Granerød, M. Ekstremværrapport. Hendelse: Urd 26. desember met. info. no. 18/2017 ISSN X METEOROLOGI Bergen, - PDF, September 2017. URL <http://docplayer.me/48734203-Ekstremvaerrapport-hendelse-urd-26-desember-met-info-no-18-2017-issn-x-meteorologi-bergen.html>.
- Palerme, C., Kay, J. E., Genthon, C., L'Ecuyer, T., Wood, N. B., and Claud, C. How much snow falls on the Antarctic ice sheet? *The Cryosphere*, 8(4):1577–1587, August 2014. ISSN 1994-0424. doi: 10.5194/tc-8-1577-2014. URL <https://www.the-cryosphere.net/8/1577/2014/>.
- Palerme, C., Genthon, C., Claud, C., Kay, J. E., Wood, N. B., and L'Ecuyer, T. Evaluation of current and projected Antarctic precipitation in CMIP5 models. *Clim. Dyn.*, 48(1-2):225–239, January 2017. ISSN 0930-7575, 1432-0894. doi: 10.1007/s00382-016-3071-1. URL <https://link.springer.com/article/10.1007/s00382-016-3071-1>.
- Pedersen, K. and Rommetveit, A. Hva er et «ekstremvær»?, November 2013. URL http://www.yr.no/artikkel/hva-er-et-_ekstremvaer__-1.7890946.
- Peel, M. C., Finlayson, B. L., and McMahon, T. A. Updated world map of the Köppen-Geiger climate classification. *Hydrology and Earth System Sciences Discussions*, 4(2):439–473, March 2007. URL <https://hal.archives-ouvertes.fr/hal-00298818>.
- Petroliagis, T., Buizza, R., Lanzinger, A., and Palmer, T. N. Potential use of the ECMWF Ensemble Prediction System in cases of extreme weather events. *Meteorological Applications*, 4(1):69–84, March 1997. ISSN 1469-8080, 1350-4827. URL <https://www.cambridge.org/core/journals/meteorological-applications/article/potential-use-of-the-ecmwf-ensemble-prediction-system-in-cases-of-extreme-weather-events/C63050704CB35CD43BC4E5998A390DDC>.
- Pinty, J.-P. and Jabouille, P. A mixed-phased cloud parameterization for use in a mesoscale non-hydrostatic model: Simulations of a squall line and of orographic precipitation. pages 217–220. Amer. Meteor. Soc., 1998.
- Rinehart, R. E. *Radar for Meteorologists: Or You, Too, Can be a Radar Meteorologist*. Rinehart Publications, 2010. ISBN 978-0-9658002-3-5. Google-Books-ID: VqatcQAACAAJ.

- Rutz, J. J., Steenburgh, W. J., and Ralph, F. M. Climatological Characteristics of Atmospheric Rivers and Their Inland Penetration over the Western United States. *Mon. Wea. Rev.*, 142(2):905–921, January 2014. ISSN 0027-0644. doi: 10.1175/MWR-D-13-00168.1. URL <http://journals.ametsoc.org/doi/abs/10.1175/MWR-D-13-00168.1>.
- Ruud, S., Carr Ekroll, H., Bakke Foss, A., Torgersen, H. O., and Annar Holm, P. To tonn tungt skilt blåste ned da ekstremværet traff Oslo og Østlandet i natt, December 2016. URL <https://www.aftenposten.no/article/ap-2z6wy.html>.
- Schirle, C. Characterization of snowfall at high latitudes using an optimal estimation-based retrieval algorithm. Private Communication, 2018.
- Shi, W., L'Heureux, M., and Halpert, M. Climate Diagnostics Bulletin - December 2016, Near Real-Time Ocean/Atmosphere: Monitoring, Assessments, and Prediction. Technical report, Climate Prediction Center, 2016. URL http://origin.cpc.ncep.noaa.gov/products/CDB/CDB_Archive_pdf/PDF/CDB.dec2016_color.pdf.
- Skofronick-Jackson, G. M., Kim, M.-J., Weinman, J. A., and Chang, D.-E. A physical model to determine snowfall over land by microwave radiometry. *IEEE Geosci. Remote Sens. Lett.*, 42(5): 1047–1058, May 2004. ISSN 0196-2892. doi: 10.1109/TGRS.2004.825585.
- Stephens, G. L. *Remote Sensing of the Lower Atmosphere: An Introduction*. Oxford University Press, 1994. ISBN 978-0-19-508188-6. Google-Books-ID: 2FcRAQAAIAAJ.
- Stocker, T. F., Qin, D., Plattner, G.-K., Tignor, M. M. B., Allen, S. K., Boschung, J., Nauels, A., Xia, Y., Bex, V., and Midgley, P. M. Working Group I Contribution to the Fifth Assessment Report of the Intergovernmental Panel on Climate Change. *Cambridge: Cambridge University Press*, page 14, 2013.
- Sun, J. Convective-scale assimilation of radar data: progress and challenges. *Quarterly Journal of the Royal Meteorological Society*, 131(613):3439–3463, 2005. ISSN 1477-870X. doi: 10.1256/qj.05.149. URL <https://rmets.onlinelibrary.wiley.com/doi/abs/10.1256/qj.05.149>.
- Uvo, C. B. Analysis and regionalization of northern European winter precipitation based on its relationship with the North Atlantic oscillation. *International Journal of Climatology*, 23(10):1185–1194, July 2003. ISSN 1097-0088. doi: 10.1002/joc.930. URL <https://rmets.onlinelibrary.wiley.com/doi/abs/10.1002/joc.930>.
- Warner, T. T., Peterson, R. A., and Treadon, R. E. A Tutorial on Lateral Boundary Conditions as a Basic and Potentially Serious Limitation to Regional Numerical Weather Prediction. *Bull. Amer. Meteor. Soc.*, 78(11):2599–2618, November 1997. ISSN 0003-0007. doi: 10.1175/1520-0477(1997)078<2599:ATOLBC>2.0.CO;2. URL [https://journals.ametsoc.org/doi/abs/10.1175/1520-0477\(1997\)078%3C2599:ATOLBC%3E2.0.CO%3B2](https://journals.ametsoc.org/doi/abs/10.1175/1520-0477(1997)078%3C2599:ATOLBC%3E2.0.CO%3B2).
- Wolff, M. A. WMO Solid Precipitation Intercomparison Experiment (WMO-SPICE), Ch. 4.2.4 Precipitation measurements in areas with high winds and/or complex terrain. unpublished.
- Wolff, M. A., Brækkan, R., Isaksen, K., and Ruud, E. A new testsite for wind correction of precipitation measurements at a mountain plateau in southern Norway. In *Proceedings of WMO Technical Conference on Meteorological and Environmental Instruments and Methods of Observation (TECO-2010). Instruments and Observing Methods Report*, 2010.

- Wolff, M. A., Isaksen, K., Brækkan, R., Alfnæs, E., Petersen-Øverleir, A., and Ruud, E. Measurements of wind-induced loss of solid precipitation: description of a Norwegian field study. *Hydrol. Res.*, 44(1):35–43, February 2013. ISSN 0029-1277, 2224-7955. doi: 10.2166/nh.2012.166. URL <http://hr.iwaponline.com/content/44/1/35>.
- Wolff, M. A., Isaksen, K., Petersen-Øverleir, A., Ødemark, K., Reitan, T., and Brækkan, R. Derivation of a new continuous adjustment function for correcting wind-induced loss of solid precipitation: results of a Norwegian field study. *Hydrol. Earth Syst. Sci.*, 19(2):951–967, February 2015. ISSN 1607-7938. doi: 10.5194/hess-19-951-2015. URL <https://www.hydrol-earth-syst-sci.net/19/951/2015/>.
- Wood, N. B. *Estimation of snow microphysical properties with application to millimeter-wavelength radar retrievals for snowfall rate.* Ph.D., Colorado State University, 2011. URL https://dspace.library.colostate.edu/bitstream/handle/10217/48170/Wood_colostate_0053A_10476.pdf?sequence=1&isAllowed=y.
- Wood, N. B., L'Ecuyer, T. S., Vane, D. G., Stephens, G. L., and Partain, P. Level 2c snow profile process description and interface control document. Technical Report, 2013. URL http://www.cloudsat.cira.colostate.edu/sites/default/files/products/files/2C-SNOW-PROFILE_PDICD.P_R04.20130210.pdf.
- Wood, N. B., L'Ecuyer, T. S., Heymsfield, A. J., and Stephens, G. L. Microphysical Constraints on Millimeter-Wavelength Scattering Properties of Snow Particles. *J. Appl. Meteor. Climatol.*, 54(4):909–931, January 2015. ISSN 1558-8424. doi: 10.1175/JAMC-D-14-0137.1. URL <http://journals.ametsoc.org/doi/10.1175/JAMC-D-14-0137.1>.

APPENDIX B: FORECASTED SNOW WATER CONTENT

B.1 HOURLY AVERAGES ENSEMBLE MEMBER ZERO AND ONE

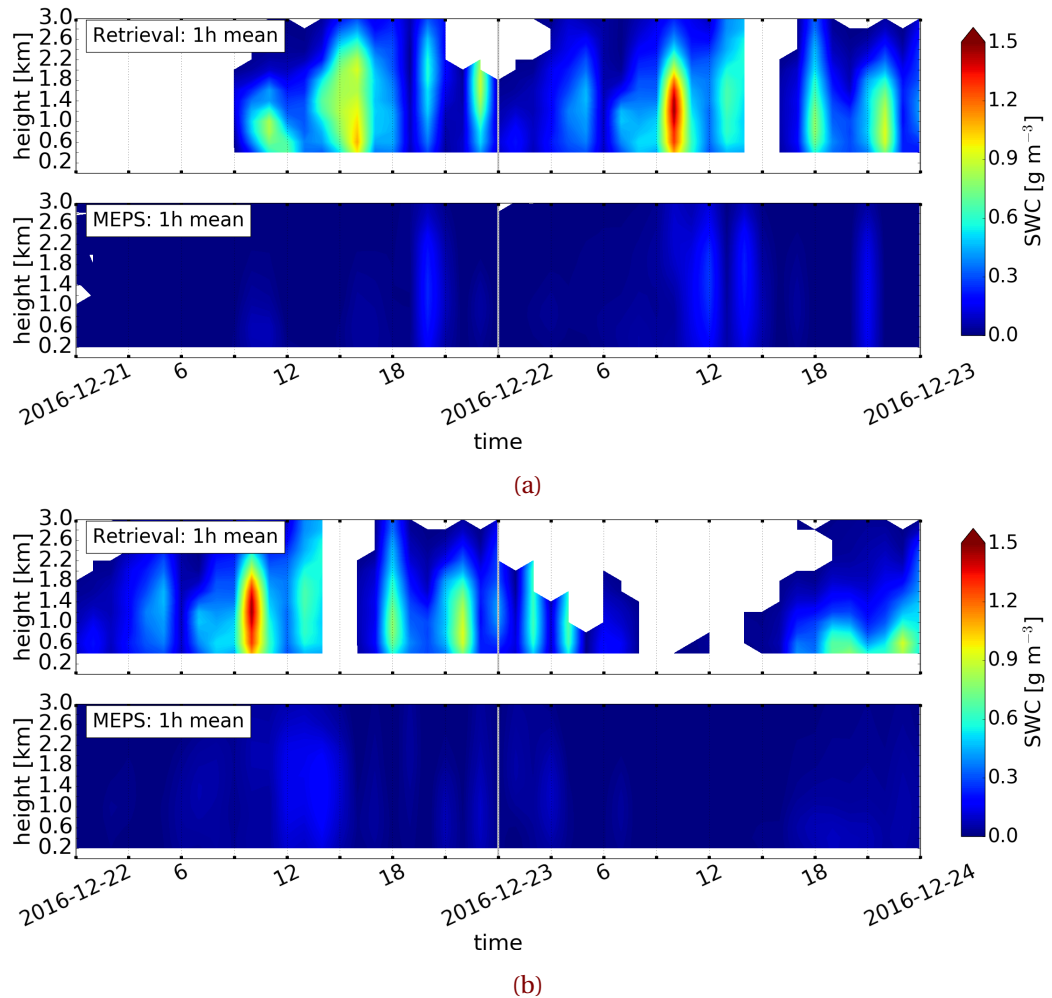


Figure B.1.1: Upper panel: hourly averaged retrieved SWC, lower panel instantaneous hourly averaged SWC forecast of deterministic and first ensemble member. Initialised 21 December 2016 and 22 December 2016 at 0 UTC.

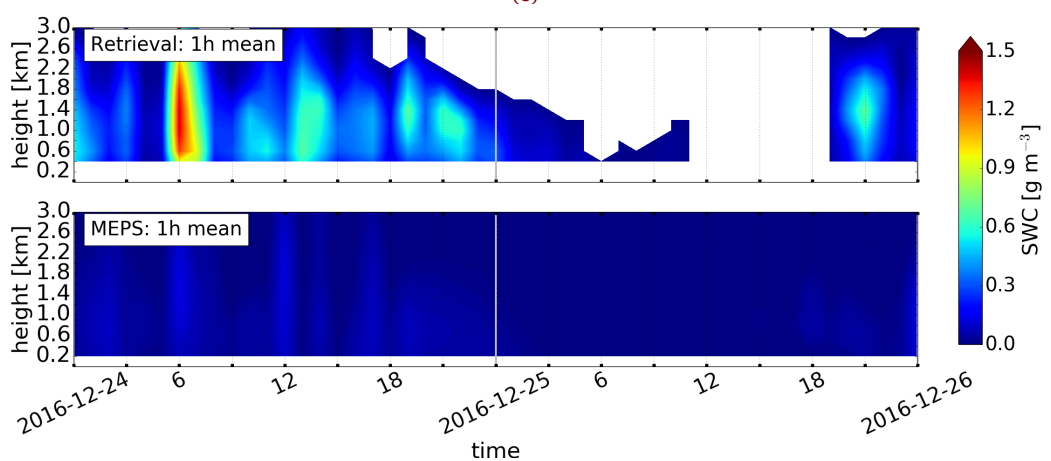
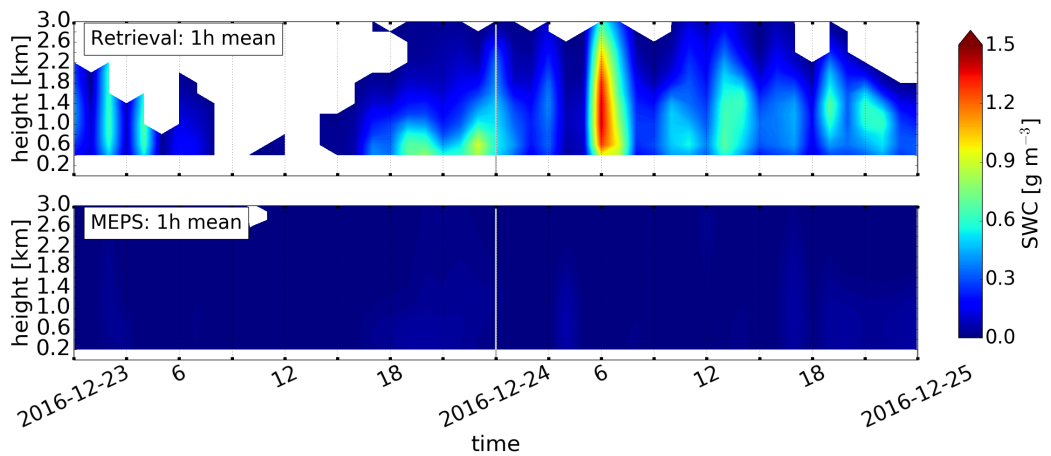


Figure B.1.1: (Continued from previous page.) Initialised 23 December 2016 and 24 December 2016 at 0 UTC.

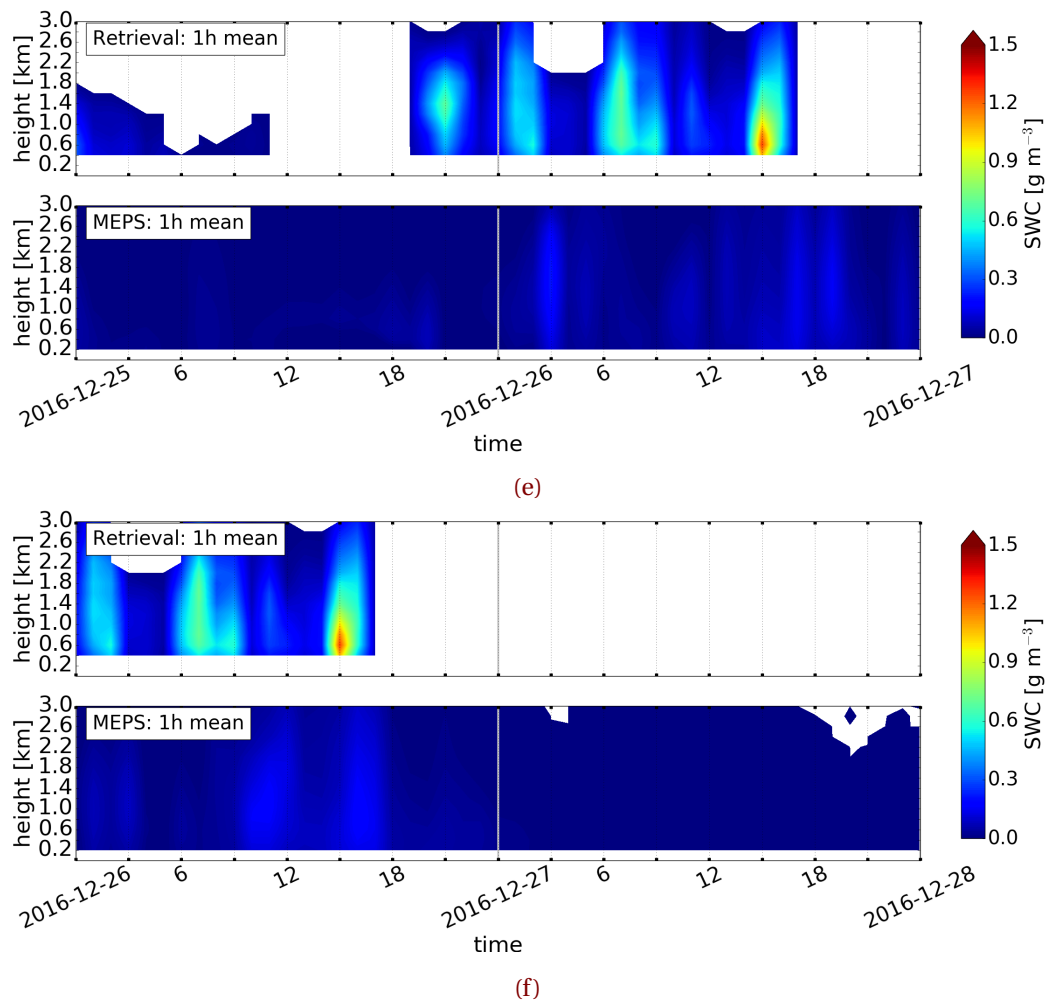
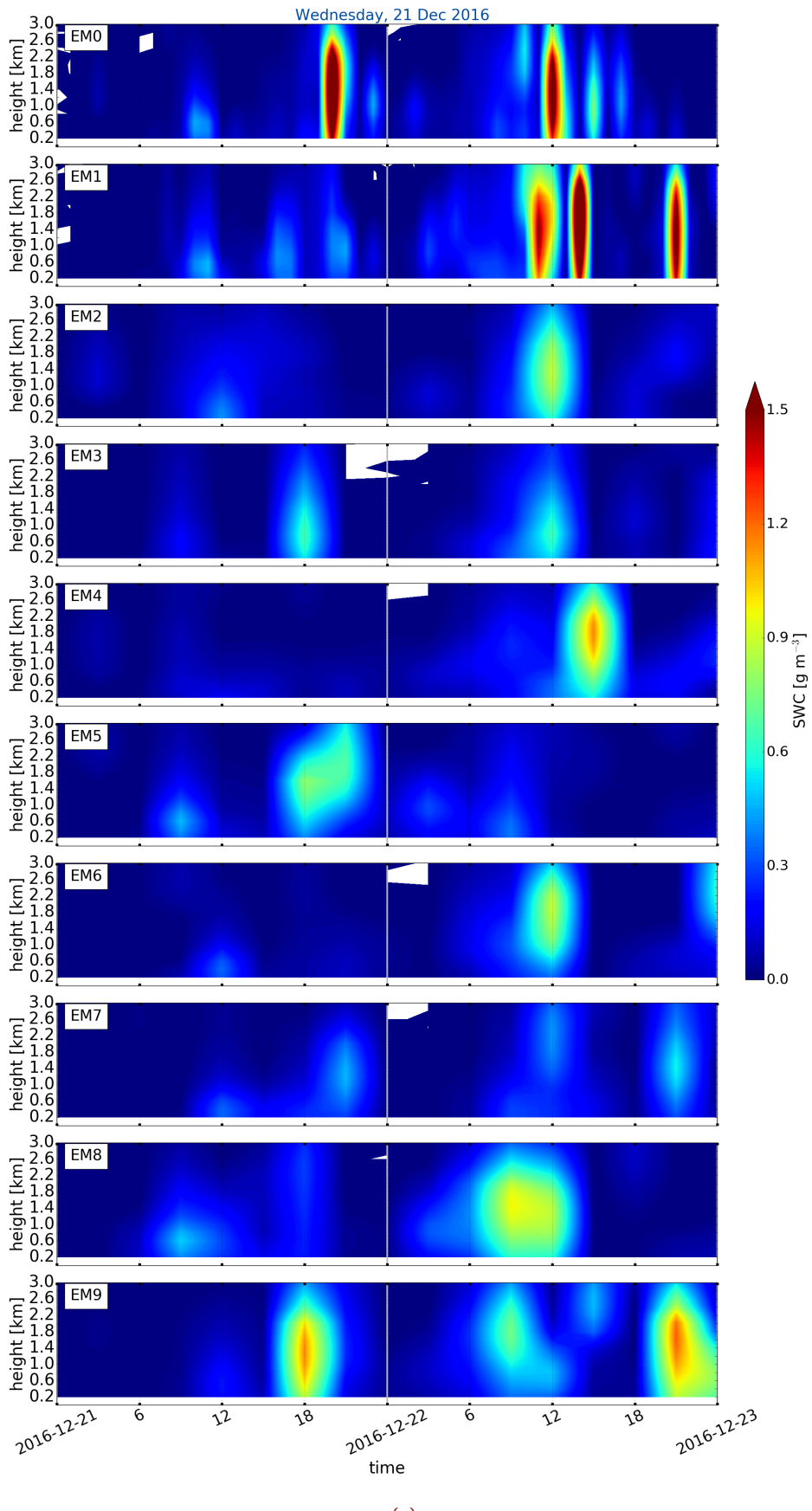


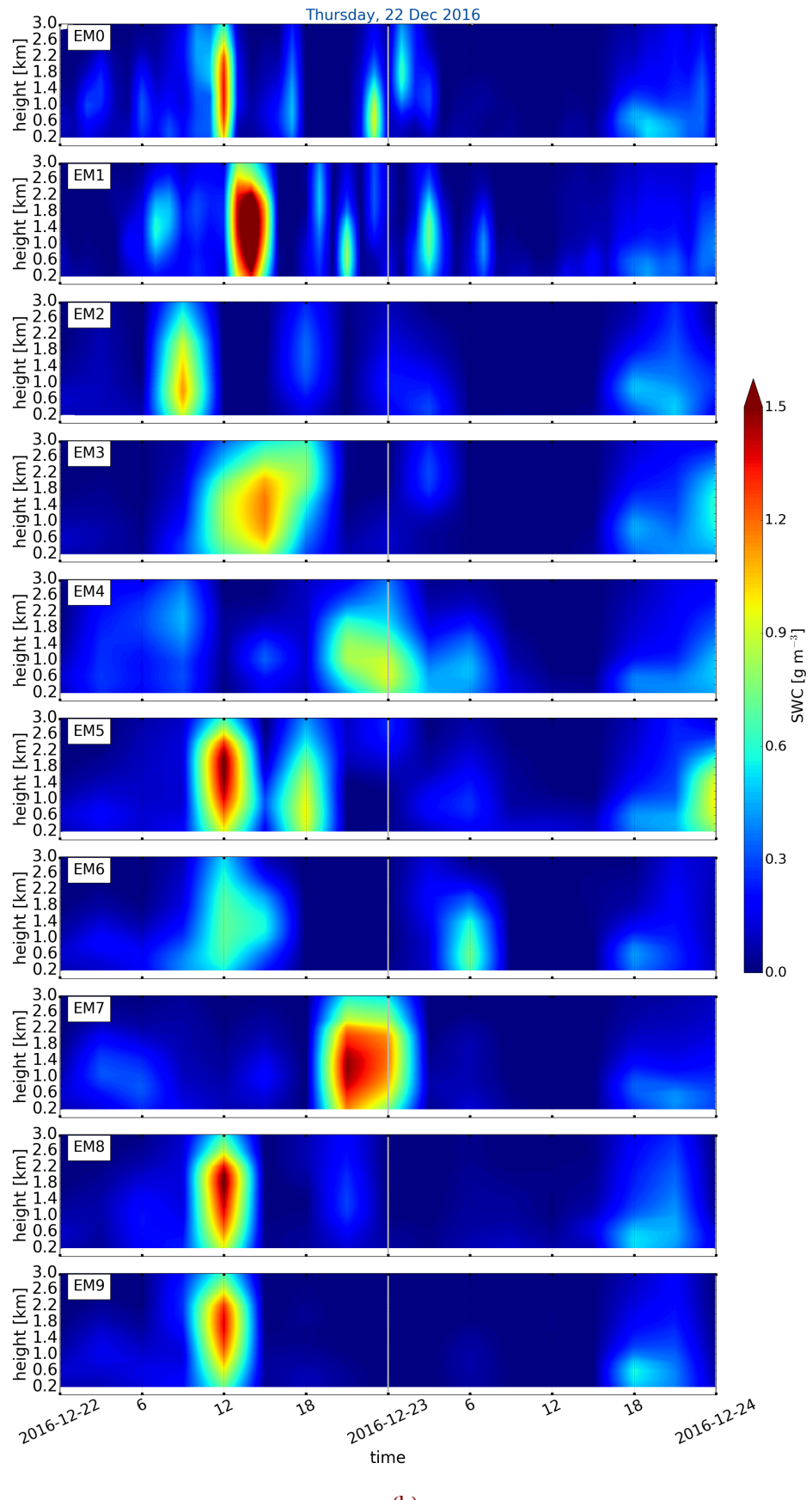
Figure B.1.1: (Continued from previous page.) Initialised 25 December 2016 and 26 December 2016 at 0 UTC.

B.2 VERTICAL SNOW WATER CONTENT - ALL ENSEMBLE MEMBERS



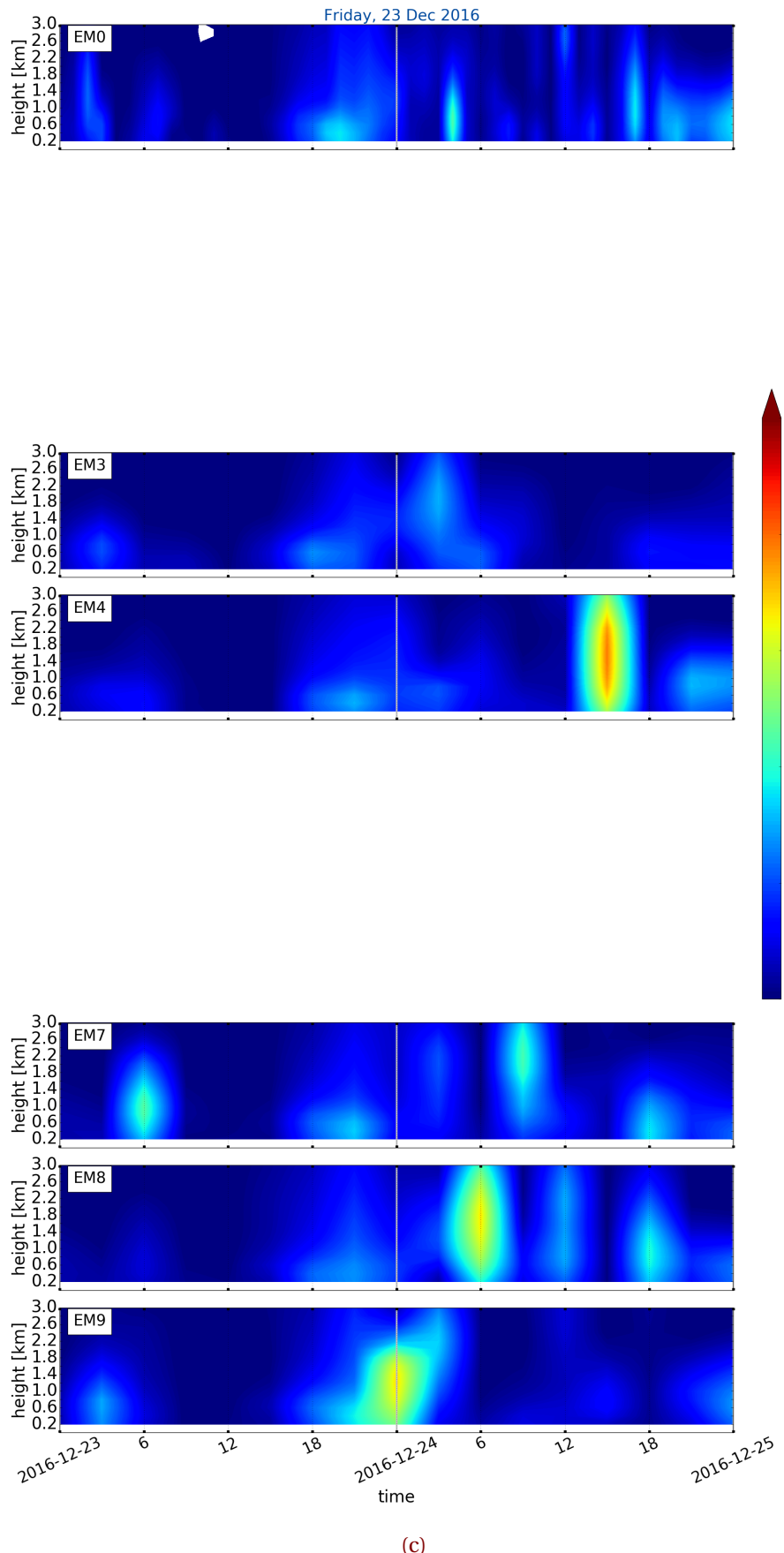
(a)

Figure B.2.1: Vertical SWC of each individual ensemble member from 0 to 9 forecast for 48 h. Initialised 21 December 2016 at 0 UTC.



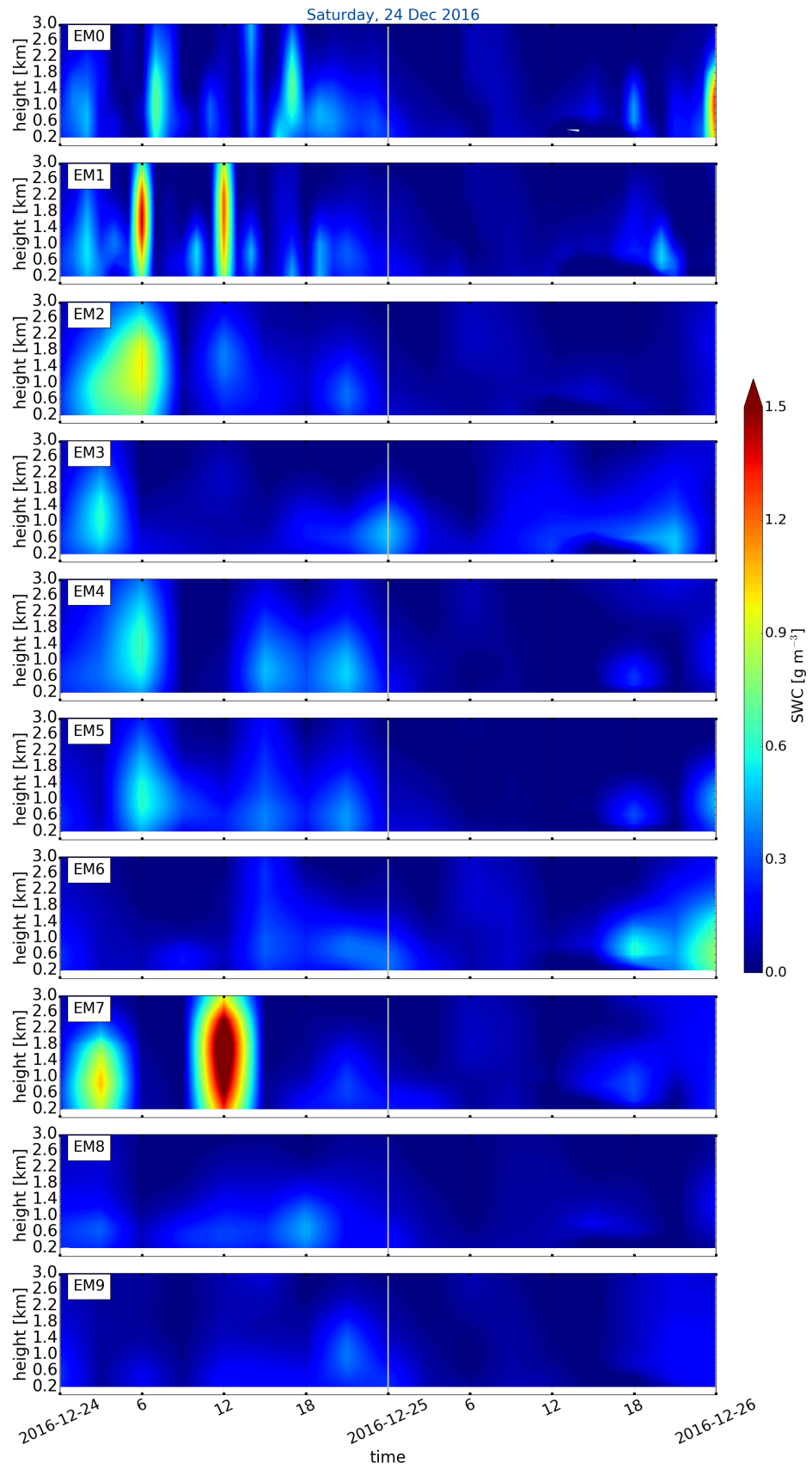
(b)

Figure B.2.1: (Continued from previous page.) Initialised 22 December 2016 at 0 UTC.



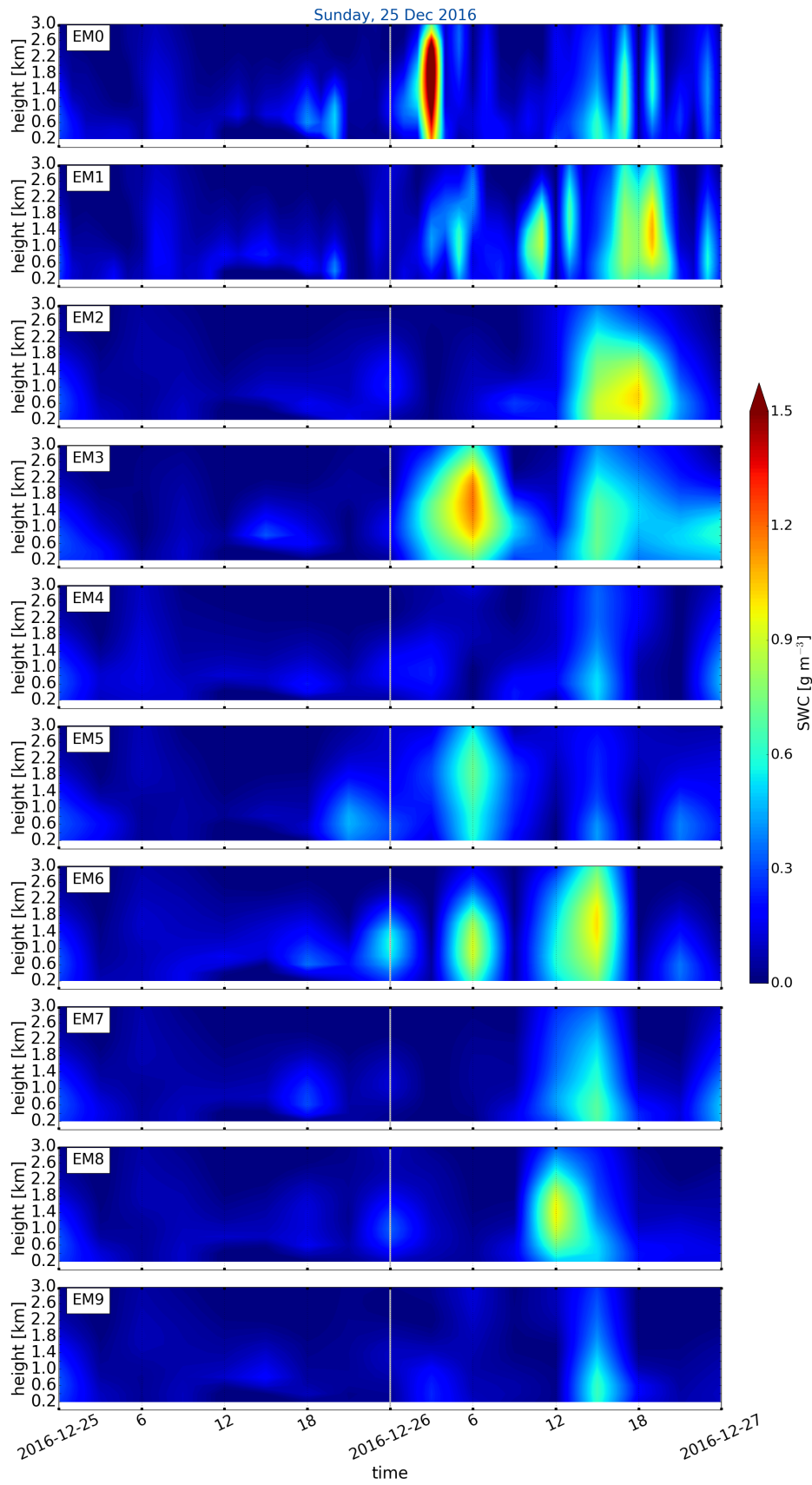
(c)

Figure B.2.1: (Continued from previous page.) Initialised 23 December 2016 at 0 UTC.



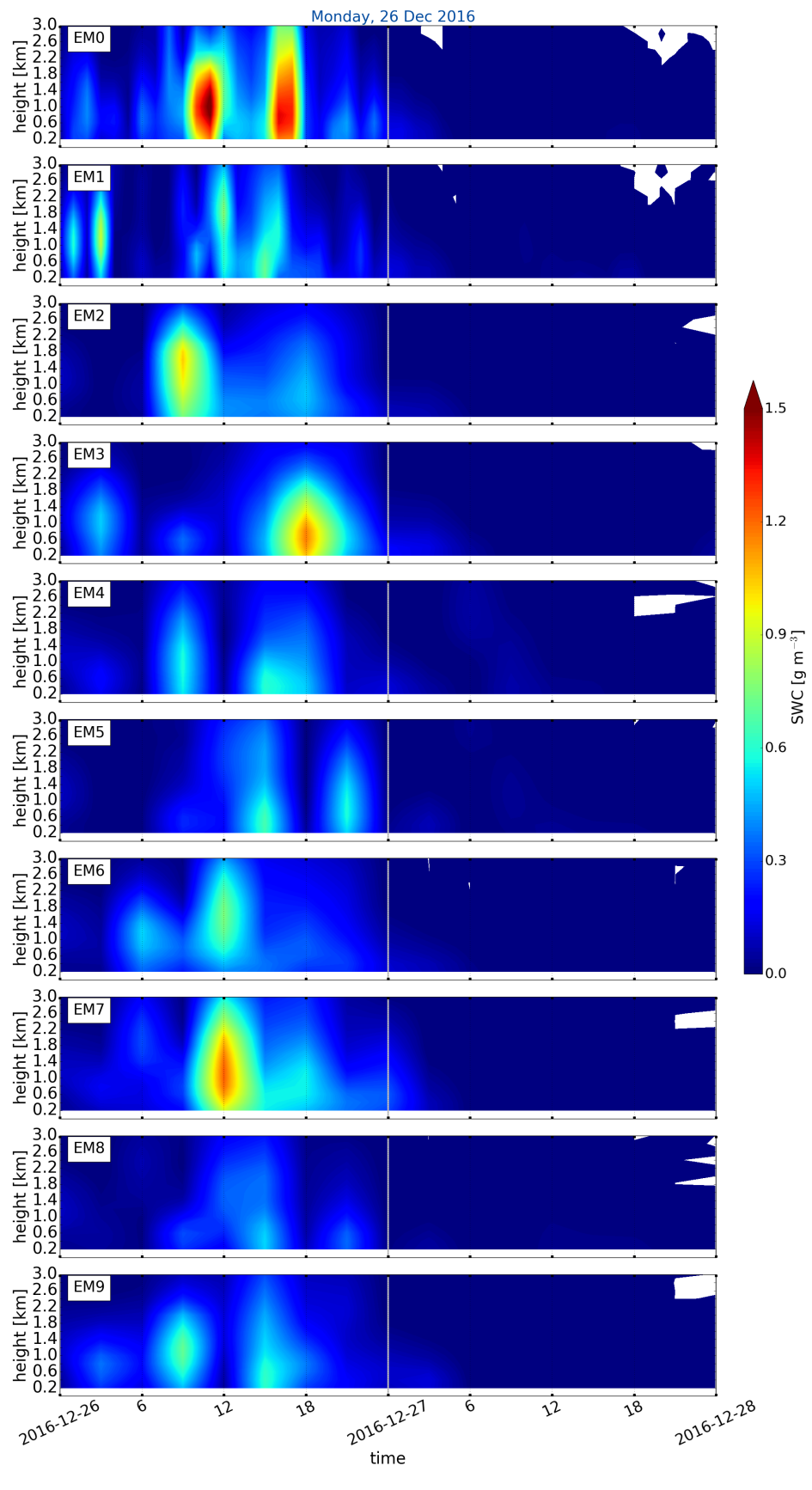
(d)

Figure B.2.1: (Continued from previous page.) Initialised 24 December 2016 at 0 UTC.



(e)

Figure B.2.1: (Continued from previous page.) Initialised 25 December 2016 at 0 UTC.



(f)

Figure B.2.1: (Continued from previous page.) Initialised 26 December 2016 at 0 UTC.

